

Electronic Thesis and Dissertation Repository

6-20-2016 12:00 AM

Parkin Misfolding, Dysfunction, and Degradation in Parkinson's Disease

Alexander S. McCarton
The University of Western Ontario

Supervisor
Dr. Gary Shaw
The University of Western Ontario

Graduate Program in Biochemistry
A thesis submitted in partial fulfillment of the requirements for the degree in Master of Science
© Alexander S. McCarton 2016

Follow this and additional works at: <https://ir.lib.uwo.ca/etd>



Part of the [Biochemistry Commons](#)

Recommended Citation

McCarton, Alexander S., "Parkin Misfolding, Dysfunction, and Degradation in Parkinson's Disease" (2016).
Electronic Thesis and Dissertation Repository. 3799.
<https://ir.lib.uwo.ca/etd/3799>

This Dissertation/Thesis is brought to you for free and open access by Scholarship@Western. It has been accepted for inclusion in Electronic Thesis and Dissertation Repository by an authorized administrator of Scholarship@Western. For more information, please contact wlsadmin@uwo.ca.

Abstract

Mutations in the gene encoding parkin (*PARK2*) result in familial early onset forms of Parkinson's disease (PD) as a result of loss of E3 ubiquitin ligase function. Protein misfolding is a common molecular feature of most neurodegenerative diseases, including PD. To test whether parkin misfolding also plays a role in the more common spontaneous PD, we established and functionally characterized a parkin yeast model. We found that oxidative and protein folding stress, parkin point mutations and truncations, and parkin's interaction with the PD-associated kinase PINK1 profoundly alter parkin's subcellular localization and toxicity. Notably, these conditions also induce parkin fragmentation, degradation, and potential misfolding, all of which may contribute to PD pathogenesis. Future research presents great potential to establish parkin misfolding as a promising new therapeutic target for PD.

Keywords

Neurodegenerative diseases, Parkinson's disease, PD, AR-JP, parkin, *PARK2*, oxidative stress, reactive oxygen species, ROS, UPS, protein quality control, protein folding, protein misfolding, degradation, aggregation, PINK1, *PARK6*, yeast model.

Acknowledgments

First and foremost, I would like to thank Martin and Gary for their continued support, encouragement, and guidance throughout my studies here at Western. While working with Martin on a daily basis, he has taught me countless invaluable lessons that have not only made me a more critical and capable scientist, but have also profoundly shaped both my personal and professional lives. Although I didn't see Gary every day, he was just a short walk away and was always available to show me that an answer is far more satisfying to discover on your own than to simply have it handed to you. Whether it was at the bench while performing one of the countless number of mini preps I completed over the years, in a formal meeting, or while sharing stories at the Grad Club over a pint on Frosty Friday, they have imparted so much knowledge and wisdom onto me that I will not soon forget. I truly believe that I have grown and matured as an individual over the past three years working with these brilliant scientific minds and I can only begin to describe the great deal of thanks I owe them for this amazing opportunity.

During my studies, I have met and grown to know so many wonderful people that I would also like to thank. To the other members of my sometimes overwhelmingly large supervisory and advisory committee, Jane Rylett and Chris Brandl, thank you for helping to build and direct my research. To the members of the many labs I have worked in, I would also like to give thanks. Sonja, you were certainly the first unforgettable individual that I got to work with side by side and you will forever be my lab sister. Anne Brickenden, thank you for showing me that crazy horse ladies can also be a heck of a lot of fun. To the members of the Duennwald lab: Lilian Lin, Vy Ngo, and the many undergraduate students, thank you for the opportunity to teach you and also learn along with you. To the members of the Shaw Lab: Kathy Barber, Jake Aguirre, Tara Condos, Valentina Taiakina, Karen Dunkerley, Yuning Wang, and former members Don Spratt and Brian Dempsey, thank you for making me feel at home whenever I came to visit. Thank you to everyone else in the biochemistry, pathology, and anatomy and cell biology departments.

Another big thank you to my family, friends, and the athletes I've had the privilege of competing alongside. To my loving parents, John and Claudia, thank you for supporting me through my many years of school and listening to me talk science even if you had no clue what I was saying. To my siblings, Joshua, Amanda, and Alysha, and niece Myla, you will forever remind me that the support and love of your family will get you through absolutely anything. To all my friends, thank you for making the scarce opportunities that I got away from the lab joyous and full of excitement. Finally, Michele, thank you for being by my side through thick and thin and always being a beautiful smiling face to come home to after a long day, even if I had to stop and grab seeds or energy drinks on the way.

To everyone who made this possible, and will continue to support me through my future endeavors in medicine, thank you, for making me the man I am today.

Abbreviations

25Q – non-expanded huntingtin protein
72Q – polyQ-expanded huntingtin protein
AD – Alzheimer’s disease
ALS – Amyotrophic Lateral Sclerosis
AMP – ampicillin
APP – amyloid precursor protein
AR-JP – Autosomal Recessive Juvenile Parkinsonism
AZC – azetidine-2-carboxylic acid
BCA – bicinchoninic acid
BSA – bovine serum albumin
CCCP – carbonyl cyanide m-chlorophenyl hydrazine
DMEM – Dulbecco's Modified Eagle Medium
DMSO – dimethyl sulfoxide
DTT – dithiothreitol
EDTA - ethylenediaminetetraacetic acid
ER – endoplasmic reticulum
FBS – fetal bovine serum
GOF – gain of function
H₂O₂ – hydrogen peroxide
HClO – hypochlorous acid
HD – Huntington’s disease
HECT – homologous to the E6-AP carboxyl terminus
HEK – human embryonic kidney
HSP – heat shock proteins
Htt – huntingtin
IPOD – insoluble protein deposit
JUNQ – juxtaneuclear quality-control compartment
KD – kinase dead
Keap1 – kelch-like ECH-associated protein 1
LB – luria bertani
LOF – loss of function
MPP⁺ – 1-methyl-4-phenylpyridinium
MTS – mitochondrial targeting sequence
NEM – N-ethylmaleimide
NMR – nuclear magnetic resonance
NO – nitric oxide
Nrf2 – nuclear factor (erythroid-derived 2)-like 2
O₂•⁻ – superoxide

OH● – hydroxide radicals
OMP – outer mitochondrial protein
PCR – polymerase chain reaction
PD – Parkinson's disease
PINK1 – PTEN-induced putative kinase protein 1
PMSF – phenylmethanesulfonyl fluoride
polyQ – polyglutamine
RBR – RING1-BRcat-Rcat (formerly known as RING1-inBetweenRING-RING2)
RING – Really Interesting New Gene
ROS – reactive oxygen species
SD – selective dextrose
SDD AGE – semi denaturing detergent agarose gel electrophoresis
SDS – sodium dodecyl sulphate
SDS PAGE – SDS polyacrylamide gel electrophoresis
SGal/Raff – Selective Galactose/Raffinose
-SH – free thiols
-SO₂H – sulfinic acid
-SO₃H – sulfonic acid
SOD1 – manganese superoxide dismutase
-SOH – sulfenic acid
Ubl – ubiquitin-like
UPS – ubiquitin proteasome system
WT – wild-type
YFP – yellow fluorescent protein
YPD – yeast peptone dextrose

Table of Contents

Abstract.....	i
Acknowledgments.....	ii
Abbreviations.....	iii
Table of Contents.....	v
List of Tables.....	ix
List of Figures.....	x
List of Appendices.....	xii
Chapter One: Introduction.....	1
1.1 Protein Quality Control.....	1
1.1.1 Oxidative Stress.....	2
1.1.2 Protein Quality Control Machinery.....	4
1.2 Neurodegenerative Disease.....	9
1.2.1 Alzheimer’s Disease.....	10
1.2.2 Huntington’s Disease.....	11
1.2.3 Amyotrophic Lateral Sclerosis.....	12
1.3 Parkinson’s Disease.....	13
1.3.1 Parkin – An E3 Ubiquitin Ligase.....	14
1.3.2 Parkin’s Role in Mitophagy.....	19
1.4 Yeast Models.....	22
1.4.1 Yeast Models of Neurodegeneration.....	23
1.5 Rationale, Hypothesis, Objectives, and Significance.....	26
1.5.1 Rationale.....	26
1.5.2 General Hypothesis.....	26

1.5.3	Objectives	27
1.5.4	Significance.....	28
Chapter Two: Materials and Methods.....		29
2.1	Materials	29
2.1.1	Escherichia coli Strains.....	29
2.1.2	Bacterial Media.....	29
2.1.3	Saccharomyces cerevisiae Strains.....	29
2.1.4	Yeast Media	30
2.1.5	Mammalian Cell Lines.....	30
2.1.6	Cell Culture Media.....	30
2.1.7	Sources of DNA used for Cloning	31
2.1.8	Chemicals.....	31
2.1.9	Antibodies	32
2.2	Methods.....	33
2.2.1	Cloning.....	33
2.2.2	Yeast Culturing Techniques.....	38
2.2.3	Growth Assays	40
2.2.4	Fluorescent Microscopy.....	41
2.2.5	Cell Lysis	41
2.2.6	Western Blotting	42
2.2.7	SYTOX® Green Cell Death Assay	43
2.2.8	Semi Denaturing Detergent Agarose Gel Electrophoresis.....	44
2.2.9	Cell Culture.....	45
2.2.10	Chemical Stress Treatment	46
2.2.11	Viability Assay.....	46

2.2.12 Immunofluorescence Microscopy.....	47
2.2.13 Shutoff.....	47
Chapter Three: Results.....	49
3.1 Parkin Sequence Analysis.....	49
3.2 The Parkin Yeast Model	52
3.3 Genetic Modulators of Parkin Toxicity and Localization.....	56
3.4 Oxidative Stress and Parkin Accumulation	62
3.5 Subcellular Localization of Parkin Truncations and Point Mutations	71
3.6 PINK1 Modulates Parkin Localization, Toxicity, and Stability	84
3.6.1 Co-expression of PINK1 and Parkin in Yeast	85
3.6.2 Co-expression of PINK1 and Parkin in Mammalian Cells.....	101
3.7 Parkin Proteolysis and Degradation in Yeast.....	107
Chapter Four: Discussion.....	115
4.1 Introduction – Parkin in PD	115
4.2 Summary of Findings and Significance	116
4.2.1 Sequence Analysis	116
4.2.2 Parkin Yeast Model.....	117
4.2.3 Genetic Interactions of Parkin	118
4.2.4 Oxidative Damage to Parkin.....	123
4.2.5 Parkin Mutants and Truncations Alter Parkin Localization	126
4.2.6 PINK1 Modulates Parkin Localization and Toxicity.....	128
4.2.7 Parkin Turnover and Degradation.....	138
4.3 Experimental Limitations.....	139
4.3.1 Modelling Parkinson’s Disease in Yeast	139
4.4 Future Directions	141

4.5 Significance.....	143
References.....	144
Appendices.....	159

List of Tables

Table 1-1. PARK family of genes involved in inherited Parkinson’s disease.....	14
Table 2-1. Antibodies used in this study.....	32
Table 2-2. Custom designed primers used to generate constructs for use in Gateway® cloning.....	34
Table 2-3. List of constructs and expression vectors used in this study.	37
Table 3-1. List of yeast deletions and corresponding gene function used to screen for parkin genetic interactions.	60

List of Figures

Figure 1-1. Cellular protein quality control	7
Figure 1-2. The ubiquitin proteasome system (UPS)	8
Figure 1-3. Mutations and deletions in the PARK2 gene causing Parkinson's disease	15
Figure 1-4. Parkin is an E3 ubiquitin ligase involved in the UPS	16
Figure 1-5. Activation of parkin mediated mitophagy of damaged mitochondria by PINK1	21
Figure 1-6. Parkin truncation variants and point mutants	25
Figure 3-1. Parkin sequence alignment	51
Figure 3-2. Establishment of the parkin yeast model	55
Figure 3-3. Pilot screen for genetic modulators of parkin toxicity and localization	59
Figure 3-4. Parkin is oxidatively modified in vivo	63
Figure 3-5. Stress treatment alters parkin localization in yeast	66
Figure 3-6. Stress treatment does not alter oxidative modification of parkin in yeast	67
Figure 3-7. Parkin is unaffected by stress treatment in HeLa cells	70
Figure 3-8. Truncations cause subcellular accumulation of parkin without altering growth in yeast	74
Figure 3-9. Parkin 141C truncation is expressed at higher levels than wild type parkin in yeast	76
Figure 3-10. Parkin point mutants are non-toxic but alter parkin localization and expression levels in yeast	79

Figure 3-11. Point mutations change parkin levels in yeast	80
Figure 3-12. Parkin point mutants and truncations have altered expression and cellular localization in Hela cells	83
Figure 3-13. Co-expression of parkin and PINK1 causes toxicity in yeast	87
Figure 3-14. Co-expression of parkin and PINK1 causes yeast cell death	89
Figure 3-15. PINK1 causes parkin accumulation in yeast	92
Figure 3-16. PINK1 induced parkin aggregates are not amyloid-like	94
Figure 3-17. PINK1/parkin toxicity is rescued by parkin point mutation	97
Figure 3-18. PINK1 mildly affects localization of mutant forms of parkin in yeast	99
Figure 3-19. Parkin levels are decreased upon co-expression with PINK1 in yeast	100
Figure 3-20. Co-expression of PINK1/parkin in HeLa cells	103
Figure 3-21. PINK1 and parkin co-expression in mammalian cells is non-toxic	106
Figure 3-22. Parkin is degraded into distinct proteolytic fragments in vivo	108
Figure 3-23. Inhibiting the 26S proteasome increases parkin stability in yeast	111
Figure 3-24. Parkin stability is mildly increased by MG132 in Hela cells	114
Figure 4-1. Parkin genetic interaction network	122
Figure 4-2. Model of PINK1-mediated increase of parkin ubiquitination activity in yeast causing toxicity	132

List of Appendices

Appendix 1. Discussion of technical limitations.....	158
Appendix 2. Comprehensive parkin sequence alignment.....	163
Appendix 3. Non-specific immunofluorescence signal in HeLa cells with parkin antibodies.....	174
Appendix 4. Supplementary figure data.....	175
Appendix 5. Growth curve of non-toxic protein expression in yeast.....	183

Chapter One: Introduction

Neurodegenerative diseases are a broad spectrum of disorders with a wide variety of symptoms and clinical presentations that are all caused by degeneration or death of neuronal cells. The most common neurodegenerative disorders include Alzheimer's disease (AD), which can be attributed to the majority of dementia cases, Huntington's disease (HD), a heritable disease that results in loss of cognitive function and sporadic jerky movements, and Parkinson's disease (PD), which is the second most common cause of neurodegeneration resulting in loss of motor control. In general, neuronal cell death occurs in the brain, but these diseases can also affect motor neurons in the periphery as seen in Amyotrophic Lateral Sclerosis (ALS). Unlike many other cell types, neurons are post-mitotic during life and cannot regenerate, thus making these conditions permanent and mostly incurable. Neurodegenerative diseases are usually late onset, as they are often associated with aging that leads to the gradual accumulation of toxic molecules, for example, reactive oxygen species (ROS) within neurons that damage cellular components over time. Human cells, including neurons, contain multiple cellular pathways that act to prevent accumulation of cytotoxic proteins. These processes can be generally classified as protein quality control machinery.

1.1 Protein Quality Control

In order to maintain cellular homeostasis and overall cell health, protein quality control machinery must ensure accurate protein production, maintenance, and turnover. One of the main causes of cell damage is the accumulation of damaged or misfolded

proteins, which are often toxic to the cell. Protein damage or protein misfolding can occur in response to many factors, particularly oxidative stress.

1.1.1 Oxidative Stress

ROS play a vital role in maintaining normal cellular processes, including cell growth, immune response, and the synthesis of biological molecules (1,2). However, ROS are also associated with aging and many diseases, including cancer and neurodegenerative disorders. They are highly reactive and thus have the potential to cause major cellular damage to proteins, nucleic acids, and lipids. In healthy cells, there is a balance of pro- and anti-oxidants that maintain healthy levels of ROS, but an imbalance of these reagents can lead to excessive accumulation of ROS, which is often seen in aging. Mitochondria are one of the major sources of ROS because superoxide anions ($O_2^{\bullet-}$) are a natural byproduct of cellular respiration (3). Normally, superoxide anions are reduced to hydrogen peroxide (H_2O_2) by manganese superoxide dismutase (SOD1) which can be further reduced to water and oxygen by catalase (4), but the failure of SOD1 or catalase can lead to the accumulation of $O_2^{\bullet-}$ or H_2O_2 , respectively. Because of its single unpaired electron, superoxide is highly reactive and can generate other ROS including hydroxide radicals (OH^{\bullet}) and hypochlorous acid (HClO). The accumulation of excessive amounts of ROS can damage cellular proteins by causing them to lose proper function. This often leads to misfolding as a result of changes in the protein's hydrophobic properties, consequently leading to protein aggregation (5). Due to the gradual accumulation of ROS over time, oxidative stress has been strongly implicated in many age related diseases, including neurodegeneration (6).

Oxidative damage to proteins occurs when amino acids of proteins are post-translationally modified by ROS. There are many ways ROS can modify proteins, and the most common type of modification is to the thiol group of cysteine residues which are highly sensitive to oxidative damage (7). While they are coded for much less frequently than other amino acids (8), cysteines play an important role in maintaining protein structure and function. When the thiol groups of two cysteines are in close proximity, it is possible for them to form a disulfide bond whereby two free thiol groups form a covalent bond with one another (7). This process can occur between two cysteines within the same protein (intramolecular) or between cysteines of two separate proteins (intermolecular). These interactions are required for proper tertiary or quaternary protein structure, respectively. Due to their polar nature, cysteines are also capable of coordinating metal ions within proteins that are also required for maintaining proper three-dimensional structure, which involves the free thiol side chain.

Under normal cellular conditions, cysteines can freely revert between their free thiol and disulfide forms, but the presence of excessive amounts of ROS can forcibly convert these residues from one form to another, preventing proper function. This often results in the formation of aberrant disulfide bonds within or between proteins, which disrupts their three-dimensional conformation. Additionally, ROS are capable of converting thiols to sulfur based acids, which are incapable of performing either of the normal functions of cysteines. In the presence of low amounts of ROS, free thiols (-SH) can be converted to sulfenic acid (-SOH), which can be reverted back to a free thiol and resume normal function when ROS levels are reduced (7). Alternatively, if ROS levels are much higher, -SOH is converted sulfenic acid (-SO₂H) and subsequently, sulfonic acid

(-SO₃H), both of which occur irreversibly. In this situation, the proteins are damaged beyond repair and are typically targeted for degradation (7).

1.1.2 Protein Quality Control Machinery

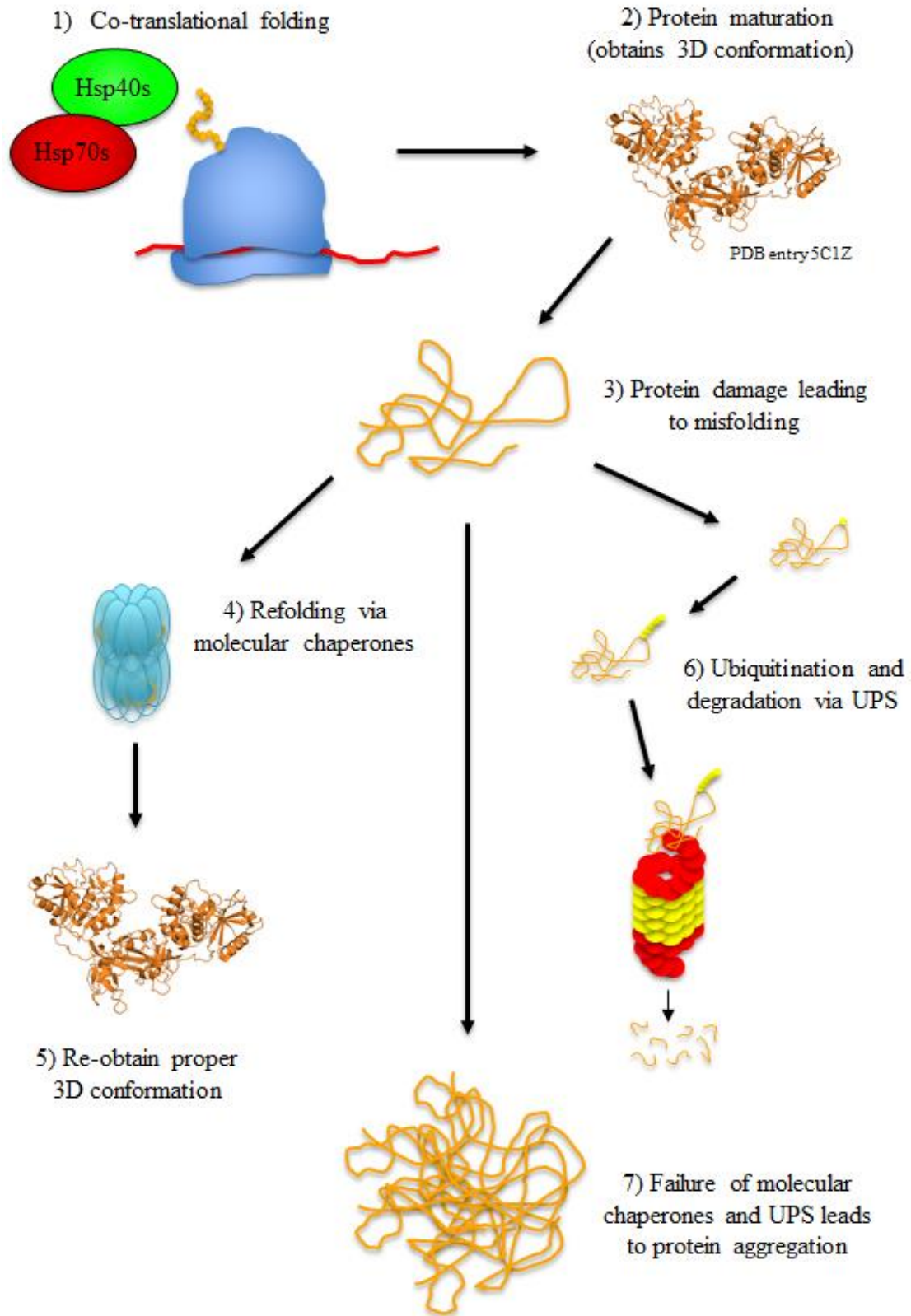
As mentioned above, protein structure and function are closely linked. When proteins are unable to form their native confirmation (misfold), which can occur naturally as a result of mutation or in response to protein damage, they often lose their ability to function properly and have an increased propensity to aggregate. The processing of damaged or misfolded proteins is essential in maintaining protein homeostasis, and the failure of this process can result in cellular dysfunction or cell death, which is associated with many diseases. Cells have two major systems for eliminating damaged and misfolded proteins (**Figure 1-1**):

1) The molecular chaperone machinery. Most proteins require the assistance of molecular chaperones during and after translation to attain their accurate three-dimensional structure (9, 10). This process either occurs in the cytosol or proteins can be directed to the endoplasmic reticulum, mitochondria, or other cellular organelles, for further processing (11, 12). By changing the immediate local chemical and physical environment surrounding misfolded proteins, chaperones promote refolding, thus facilitating proper folding and reducing the accumulation of damaged proteins. Not surprisingly, dysfunction of the molecular chaperone machinery has been strongly implicated in multiple neurodegenerative disorders (13) and has also been identified as a target for therapeutic intervention (10, 15, 16).

2) The ubiquitin proteasome system (UPS). UPS is the second system that is essential for protein homeostasis, which is shown in **Figure 1-2**. The addition of ubiquitin

to a substrate protein (ubiquitination) plays a large role in protein regulation by altering cellular localization, effecting interactions with other proteins, and with particular relevance to this study, targeting damaged proteins for degradation. The UPS acts to transfer ubiquitin successively through E1, E2, and E3 enzymes to build mono- or poly-ubiquitin chains on substrate proteins (17). Following ubiquitination, substrate proteins are directed to the 26S proteasome where they are degraded. Humans contain nine genes encoding E1 ubiquitin activating enzymes, two of which are involved in ubiquitin conjugation in the UPS (18–20), about 40 genes for E2 ubiquitin conjugating enzymes, and over 600 genes for E3 ubiquitin ligases (21). Each class of enzyme contains structural similarities that are required to facilitate ubiquitin transfer, but they also have differences that affect their regulation and it is this diversity that differentiates substrate recognition. Dysregulation of the UPS is a highly studied field and research has shown its involvement in cancer (22, 23), cardiovascular disease (24, 25), and neurodegenerative diseases (26, 27).

Figure 1-1. Cellular protein quality control. 1) Following transcription, mRNA is directed to the ribosome for translation which often required co-translational assistance from molecular chaperones like HSP40s and HSP70s. 2) Fully translated proteins mature and obtain their proper functional three-dimensional conformation. 3) The buildup of damaging molecules over time as a result of aging, environmental exposure, or cellular dysfunction causes protein damage leading to misfolding whereby the protein can no longer function properly. 4-5) Molecular chaperones can recognize damaged proteins and assist in their refolding which will cause them to re-attain their proper three-dimensional conformation and resume normal function. 6) Proteins that are damaged beyond repair are recognized by the UPS and ubiquitinated to target them for degradation by the 26S proteasome. 7) Failure of one or both of these cellular protein quality control mechanisms can lead to the accumulation of misfolded proteins leading to protein aggregation which can be toxic to the cell or even cause cell death.



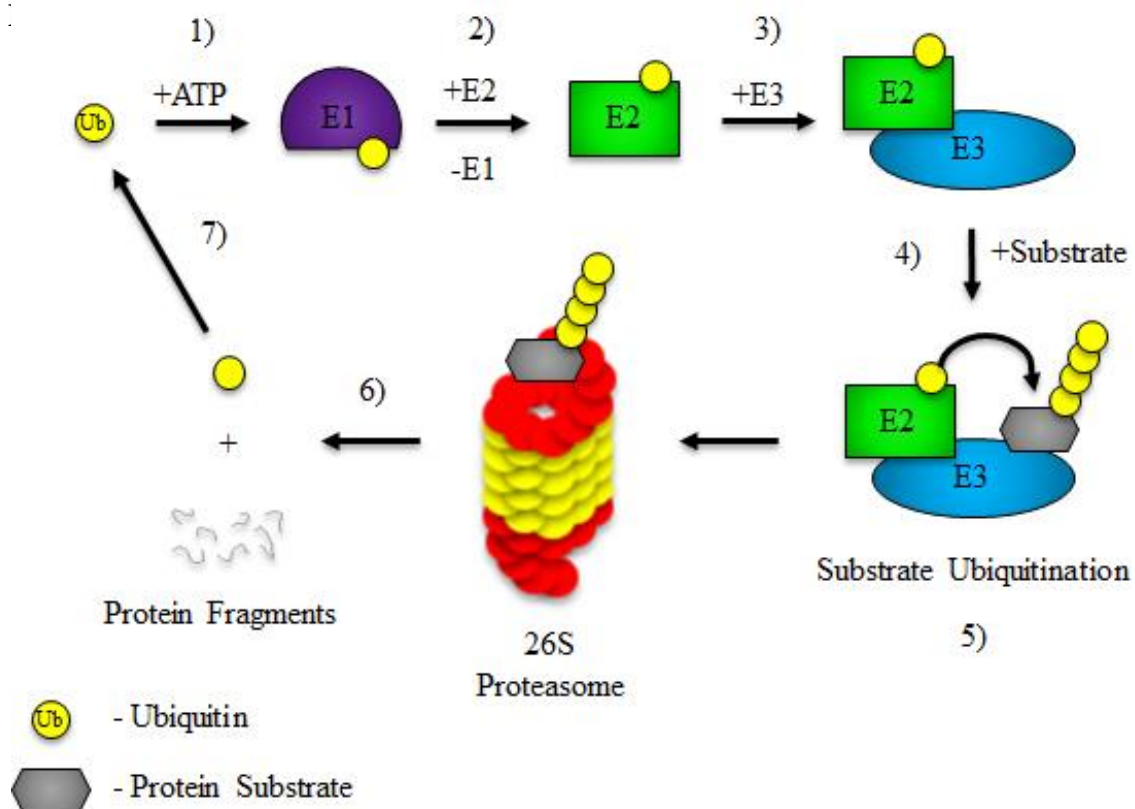


Figure 1-2. The ubiquitin proteasome system (UPS). 1) Unmodified ubiquitin is activated with the use of ATP and bonded to an E1, ubiquitin activating enzyme. 2) Activated ubiquitin is transferred from an E1 to an E2, ubiquitin conjugating enzyme. 3) An E2 ubiquitin conjugate interacts or docks with an E3, ubiquitin ligase. 4) The E2-E3-ubiquitin complex comes in contact with a protein substrate which is properly oriented by the E3. 5) A poly-ubiquitin chain is built on the substrate protein either by direct transfer of ubiquitin from the E2 enzyme, or through a sequential transfer of ubiquitin from E2 to E3 to substrate. 6) The ubiquitinated substrate is directed to the 26S proteasome where the substrate protein is degraded into proteolytic fragments. 7) Ubiquitin is recycled and is ready for use in the UPS or other cellular pathways.

1.2 Neurodegenerative Disease

Many neurodegenerative diseases are caused by genetic mutations. These genetic or familial forms often present a more severe phenotype and an earlier onset than sporadic cases. Notably, neurodegenerative-associated genes and proteins have distinct functions and structures, cause dysfunction and cell death in distinct sets of neurons, and cause distinct symptoms. That being said, there are several features that are common and central to many, if not all neurodegenerative diseases.

One common feature of neurodegenerative diseases, that can also cause other human diseases, is loss of function (LOF) mutations, whereby an inherited mutation in a specific gene causes a protein to lose its proper function, leading to cell death. Examples of neurodegenerative diseases caused by heritable loss of function mutations include non-sense mutations causing premature transcriptional termination of the glutamine superoxide dismutase (SOD1) protein causing ALS (28), and any of the several heritable mutations of in the *PARK* gene family causing PD (29).

The second common feature of neurodegenerative diseases is toxic gain of function (GOF) mutations. Similar to LOF mutations, GOF mutations can be genetically inherited or acquired over time. Instead of losing their proper function, GOF mutations often cause proteins to misfold and aggregate, dragging other essential proteins into large insoluble protein aggregates that can be cytotoxic (30). The accumulation of protein aggregates overloads the protein quality control machinery, causing further stress to the cell by disrupting normal cellular processes. An example of neurodegeneration caused by toxic

GOF mutations is α -synuclein mutations causing the formation of Lewy Bodies leading to PD (31, 32).

Another hallmark of neurodegenerative disorders is the accumulation of damaged or misfolded proteins into insoluble plaques or aggregates. The accumulation of aggregated or misfolded proteins has been proposed to be cytotoxic. Recent studies have suggested, however, that protein aggregation can indeed play a protective role in cells by sequestering potentially toxic protein species, thereby reducing their potential to damage the cell (33). Some well-established examples of disease-associated protein aggregates include neurofibrillary tangles made of the protein tau and plaques made of amyloid fibrils of the $A\beta$ peptide in AD (34), nuclear and cytosolic aggregates made of polyglutamine repeat proteins in HD and Spinocerebellar Ataxia Type 1 (36), and Lewy Bodies made primarily of α -synuclein in PD (37). As stated above, the major cellular systems that neutralize or eliminate misfolded proteins are 1) refolding via molecular chaperones and 2) degradation via the UPS or autophagy.

Although research over the past decades has discovered the genetic cause of many of these diseases, the underlying mechanisms of how they cause neuronal damage and cell death are still widely unknown. Furthermore, there is even less understanding of what causes the much more common sporadic cases of neurodegenerative diseases and their underlying mechanisms.

1.2.1 Alzheimer's Disease

AD is the most common neurodegenerative disorder and the most common cause of dementia, accounting for 60-70% of all cases of dementia (38). Like most

neurodegenerative disorders, this disease generally has a late age of onset, usually presenting after 65 years of age. Patients experience progressive neurological deterioration with the most common symptom being memory loss. There are cases of early onset AD which are more frequently seen in cases of familial inheritance. Pathology of Alzheimer's patients presents with the classical protein aggregates, referred to as plaques, which overload the protein quality control machinery. Alzheimer's plaques are predominantly made of A β , a short amino acid peptide made of fragments of the amyloid precursor protein (APP). The tau protein, whose normal function is to stabilize microtubules, can also be found in Alzheimer's protein aggregates, but this is likely due to mis-sorting of the protein caused by A β . Although environmental exposure and lifestyle choices, such as smoking, can increase the risk of developing Alzheimer's disease, there is no evidence that there is any way to prevent disease development (38,39). There is currently no cure for Alzheimer's disease and no available treatment to slow or prevent disease progression. Treatment options, which consist of five different compounds, are only intended to manage neurological symptoms (41).

1.2.2 Huntington's Disease

Unlike most other neurodegenerative diseases, HD is solely caused by one protein known as huntingtin (Htt). HD occurs as a result of the expansion of a polyglutamine (polyQ) region within Htt, which causes the protein to misfold and form aggregates, again stressing the protein quality control machinery. The regular function of the Htt protein is still unknown, but it is expressed at the highest levels in the brain and testes (42). HD generally presents between 35 and 45 years of age, but symptoms can begin during infancy

or late in life depending on the size of the polyQ expansion. The wild-type Htt protein contains less than 36 glutamine repeats and expansion of the polyQ track causes increased disease severity and leads to an earlier age of onset which is directly correlated to the length of the polyQ expansion. HD heritability is dominant, where one mutant copy of the gene can drag normal copies of the protein into Htt aggregates. There are currently no treatments available to prevent or eliminate Htt aggregates, but several treatments have been used to manage symptoms which include jerky, random, and uncontrollable movements known as chorea.

1.2.3 Amyotrophic Lateral Sclerosis

ALS, made famous by the baseball player Lou Gehrig, is different than most other neurodegenerative diseases as it affects motor neurons in the periphery rather than in the brain. ALS is progressive, with neurons in the extremities being affected first which leads to movement difficulties that gradually causes paralysis of the arms and legs. Patients generally do not experience any cognitive symptoms but they eventually lose the ability to speak, chew, or swallow, and typically succumb to respiratory failure after cell death occurs to motor neurons controlling the diaphragm. This condition is also different from most other neurodegenerative diseases because of its rapid progression. After onset, patients typically survive for only three to four years. ALS can be heritable, whereby mutations in the genes encoding SOD1 (43), FUS, TDP-43 (44), C9Orf72 (45), the recently discovered RGNEF (46, 47), and more can cause ALS, but these only account for a small proportion of all ALS cases. Pathology of ALS patients is a proteinopathy where proteins form potentially toxic aggregate as seen in other neurodegenerative diseases. There is

currently no cure for the disease and the only available treatment is a drug called riluzole, which only extends patients' lifespan by approximately three months.

1.3 Parkinson's Disease

PD is the second most common neurodegenerative disease affecting more than 100 000 Canadians and typically has a late age of onset, which occurs around 70 years of age (48). Patients experience progressive neurodegeneration that results in a variety of physical manifestations including resting tremors, rigidity, postural instabilities, and staggered gait. PD cases can be classified into two categories: familial and non-familial, also referred to as sporadic or idiopathic PD; in both cases, patients experience loss of dopaminergic neurons in the substantia nigra resulting in decreased dopamine uptake at neural synapses (49). Inherited forms of PD have been linked to seven genes with various functions (**Table 1-1**). One of the most common pathologies seen in PD patients is the formation of Lewy Bodies composed primarily of α -synuclein which can be inherited in an autosomal dominant manner (50). Although inherited PD is associated with one or more mutations in the *PARK* family of genes, these only account for approximately 10% of all cases of PD. In cases of idiopathic PD, which account for the remaining 90% of PD cases, the relationships between these proteins is extremely complex. Although pathogenic mutations in single genes have been identified in familial PD (51), it is plausible to speculate that there is an intricate interplay between these genes that cause cases of sporadic PD (52–54). This study focuses predominantly on the role of parkin (*PARK2*) in idiopathic PD and how dysregulation of the protein quality control machinery may also be involved.

Table 1-1. *PARK* family of genes involved in inherited Parkinson's disease.

Gene	Protein	Inheritance	Function
PARK1	α -synuclein	Dominant	Presynaptic protein
PARK2	parkin	Recessive	Ubiquitin E3 ligase
PARK5	UCH-L1	Dominant	Ubiquitin hydrolase
PARK6	PINK1	Recessive	Mitochondrial kinase
PARK7	DJ-1	Recessive	Chaperone
PARK8	LRRK2	Dominant	Kinase
PARK13	HTRA2	Unknown	Serine proteinase

1.3.1 *Parkin – An E3 Ubiquitin Ligase*

Research on parkin began in 1998 with the discovery of a mutation in the *PARK2* gene, which is located on the long arm of chromosome 6, by Tohru Kitada *et al.* in a Japanese family (55). This study showed that parkin contains amino acid similarity to ubiquitin from residues 1-76 and high cysteine content in the remainder of the protein. They also established, based on exon deletions found in five patients, that parkin is linked to Autosomal Recessive Juvenile Parkinsonism (AR-JP), an early onset form of PD that affects individuals less than 40 years of age. AR-JP is pathologically very similar to PD, as patients exhibit the same decreased sensitivity to dopamine in the substantia nigra and experience the same progressive neurodegeneration and loss of motor control at a much younger age. Also similar to PD, AR-JP mutations are often inherited in an autosomal recessive manner, many of which map to the *PARK2* gene encoding parkin (**Figure 1-3**).

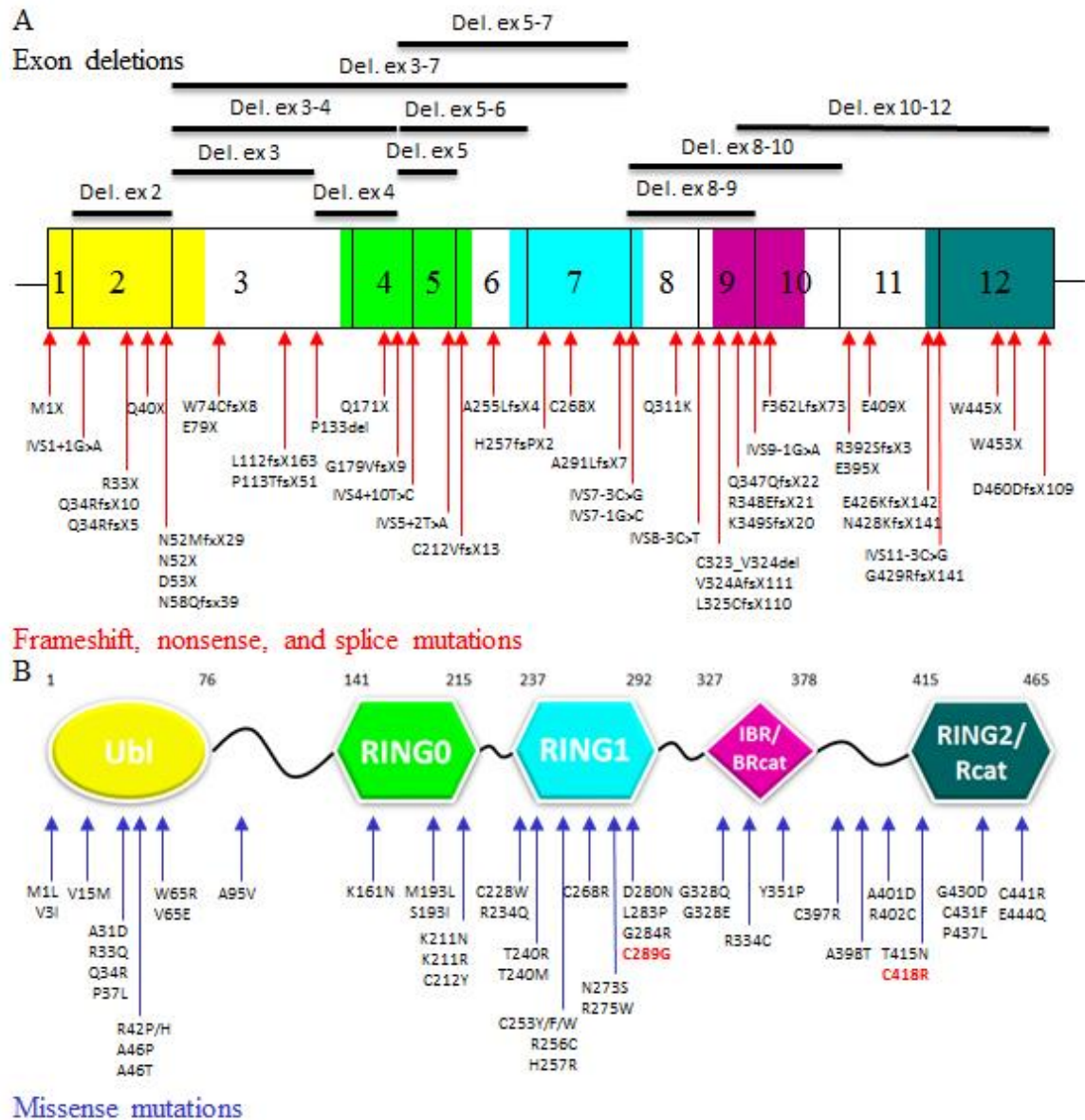


Figure 1-3. Mutations and deletions in the *PARK2* gene causing Parkinson's disease.

A) Schematic representation of the *PARK2* gene showing known exon deletions, frameshift mutations, non-sense mutations, and splicing mutations causing Parkinson's disease. B) Schematic representation of the parkin protein encoded by the *PARK2* gene and its functional domains showing known nonsense mutations causing Parkinson's disease. The highlighted red missense mutations in B) were used in this study to assess parkin misfolding. Modified from (55, 56).

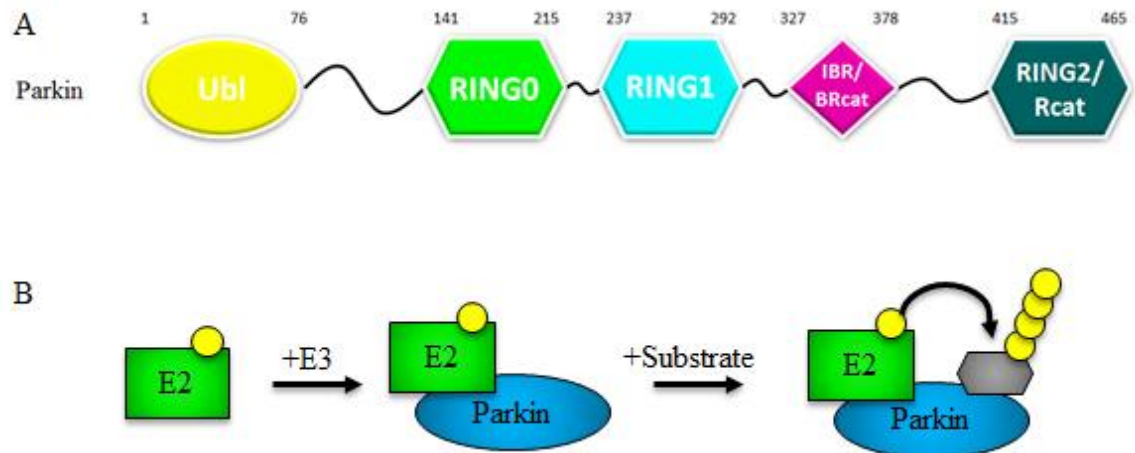


Figure 1-4. Parkin is an E3 ubiquitin ligase involved in the UPS. (A) Schematic representation of parkin domains based on structural determination by NMR containing an N-terminal Ubl domain, which acts to auto-inhibit parkin activity, and a C-terminal Rcat/RING2 domain required for catalytic transfer of ubiquitin. (B) The role of parkin as an E3 ligase in UPS which acts to transfer ubiquitin from E2 to target substrate.

Following its initial discovery in the context of AR-JP, work by several groups focused on deciphering parkin's regular function and its altered function that causes PD development. Initially, sequence homology was used to define the functional domains within parkin where, in addition to the N-terminal ubiquitin-like domain, three additional domains were proposed based on sequence homology, which included two Really Interesting New Gene (RING) domains (58). Since its discovery, a fifth domain (RING0) has also been described within parkin, and our understanding of its function has vastly increased (59).

We now know that human parkin is a 465 residue protein made up of five domains and functions as an E3 ubiquitin ligase in the UPS (**Figure 1-4**). Parkin is classified as an RBR (RING1-BRcat-Rcat, formerly known as RING1-inBetweenRING-RING2) E3 ligase (60). Its functions are twofold during the process of ubiquitin transfer: 1) it acts as a scaffold to orient the E2 enzyme for the transfer of ubiquitin to substrate proteins, and 2) parkin accepts ubiquitin onto a catalytic cysteine located in the Rcat/RING2 domain before transferring it to the substrate protein. This action differs from the RING class E3 enzymes that only act as a scaffold between the E2 and protein substrate (61) and from homologous to the E6-AP carboxyl terminus (HECT) E3 ligases that accept activated ubiquitin onto a catalytic site before interacting with and subsequently ubiquitinating substrate proteins (62). Parkin can therefore be classified as a RING/HECT hybrid. Previous work in our lab, in addition to work by several other groups, has studied parkin structure, exploring its regulation and the dynamics involved in ubiquitin transfer using nuclear magnetic resonance (NMR) spectroscopy and other methods (63–65). These studies have shown that the N-terminal Ubl domain of parkin acts to inhibit parkin ubiquitination by folding back

on itself, blocking surfaces of the protein required for ubiquitin transfer and E2 docking. They have also shown that this inhibition can be regulated through phosphorylation of the Ubl domain and ubiquitin, both at Serine 65 by PTEN-induced putative kinase 1 (PINK1), a PD-associated kinase. Structural studies have also established that the four C-terminal domains of parkin each coordinate two Zn^{2+} ions that are essential for structural stability of the protein (59).

In addition to the extensive research aimed at understanding parkin at a structural level, there have also been significant efforts made to understand parkin function at a cellular level. Prior to the recent discovery of the connection between parkin and PINK1, which will be discussed below, the majority of parkin related research was focused on its role as an E3 ligase. AR-JP causing loss-of-function mutations are found across the entire length of the *PARK2* gene. These mutations are comprised of point mutations (missense, nonsense or frame shift) and deletions across one or more exons, resulting in early termination or truncation (66, 67). Functional studies have implied the ubiquitination and subsequent degradation of many different proteins by parkin, including CDrel-1, a GTPase expressed in the nervous system, and Pael-R, a G-protein coupled transmembrane protein expressed in dopaminergic neurons. The literature also describes hundreds of potential parkin substrates that have been detected by high throughput screens (68) and *in vitro* testing (69). Most of these substrates have not been confirmed independently and it remains to be determined whether there are changes in the levels of these proteins upon dysregulation of parkin.

Although many studies associate parkin to PD through its inability to prevent the accumulation of damaged protein, work by several groups suggest that pathogenic parkin

mutants induce parkin misfolding and aggregation. Schlehe *et. al* have shown that the AR-JP causing R42P is actively degraded by the proteasome upon expression (70). Similar aggregation patterns have been shown by Wen-Jie *et. al* using mutations of two cysteine residues that normally co-ordinate binding of structural zinc ions. They show that these mutants not only form perinuclear aggregates, but also disrupt the co-localization of parkin with two different E2 enzymes, UbcH7 and UbcH8 (71). 1-methyl-4-phenylpyridinium (MPP+) is a positively charged molecule that induces ROS accumulation by inhibiting complex I, interfering with oxidative respiration. Parkin has been found in insoluble fractions of SH-SY5Y cells experiencing excess accumulation of MPP+ induced ROS and in non-familial PD patient brain samples (72). In addition to these results, the proposed association of parkin with alpha-synuclein within Lewy bodies (73, 74) gives additional support to the claim that aggregation of insoluble mutants or oxidatively damaged parkin plays an important role in the pathogenesis of idiopathic PD. Overall, it remains mostly unclear how parkin is oxidized under stress conditions and how missense mutations cause misfolding and subsequent PD.

1.3.2 *Parkin's Role in Mitophagy*

Parkin has been implicated in the degradation and turnover of damaged mitochondrial proteins and entire mitochondria (mitophagy, (75, 76)), and it is suggested that this activity is induced by PINK1 mediated phosphorylation (77, 78). PINK1 is a serine/threonine kinase that contains an N-terminal mitochondrial targeting sequence (MTS) that is used to direct and anchor PINK1 to the mitochondria and a C-terminal kinase domain (79). Currently there is not a clear consensus on where PINK1 is anchored to the

mitochondria as some studies suggest that it undergoes processing and cleavage at the inner mitochondrial membrane (80), while others propose that PINK1 is directed to and interacts with the outer membrane in response to loss of membrane potential, leaving the C-terminal kinase lobe facing the cytosol to interact with ubiquitin, parkin, or other proteins (77, 81). There are over 50 recessive mutations to PINK1 that can cause PD and studies suggest that these mutations inhibit parkin mediated protein degradation by inhibiting PINK1 phosphorylation and recruitment of parkin, or by preventing PINK1 translocation to the mitochondria, also preventing parkin activation (82).

Narendra *et. al* have shown that PINK1 is normally degraded in the cytosol in HeLa cells, but upon mitochondrial damage following carbonyl cyanide m-chlorophenyl hydrazone (CCCP) treatment, damaged mitochondria lose their membrane potential. CCCP damages mitochondria by uncoupling the proton gradient established by the electron transport chain during oxidative respiration (83). This study showed that the loss mitochondrial membrane potential causes PINK1 to be selectively recruited and anchored to the outer mitochondrial membrane. They further showed that parkin only localizes to mitochondria of CCCP treated cells when PINK1 is present (84). Although this study provides strong evidence that PINK1 is required for parkin recruitment, this does not explain the mechanism by which this recruitment of parkin to mitochondria and the ensuing mitophagy occurs. **Figure 1-5** shows one potential model of how PINK1 recruits and activates parkin. Previous studies suggest that parkin recruitment is activated by: 1) phosphorylation of free ubiquitin to activate parkin (85), 2) by phosphorylation of one of several mitochondrial proteins, such as TOM20 or mitofusin 2, to recruit parkin

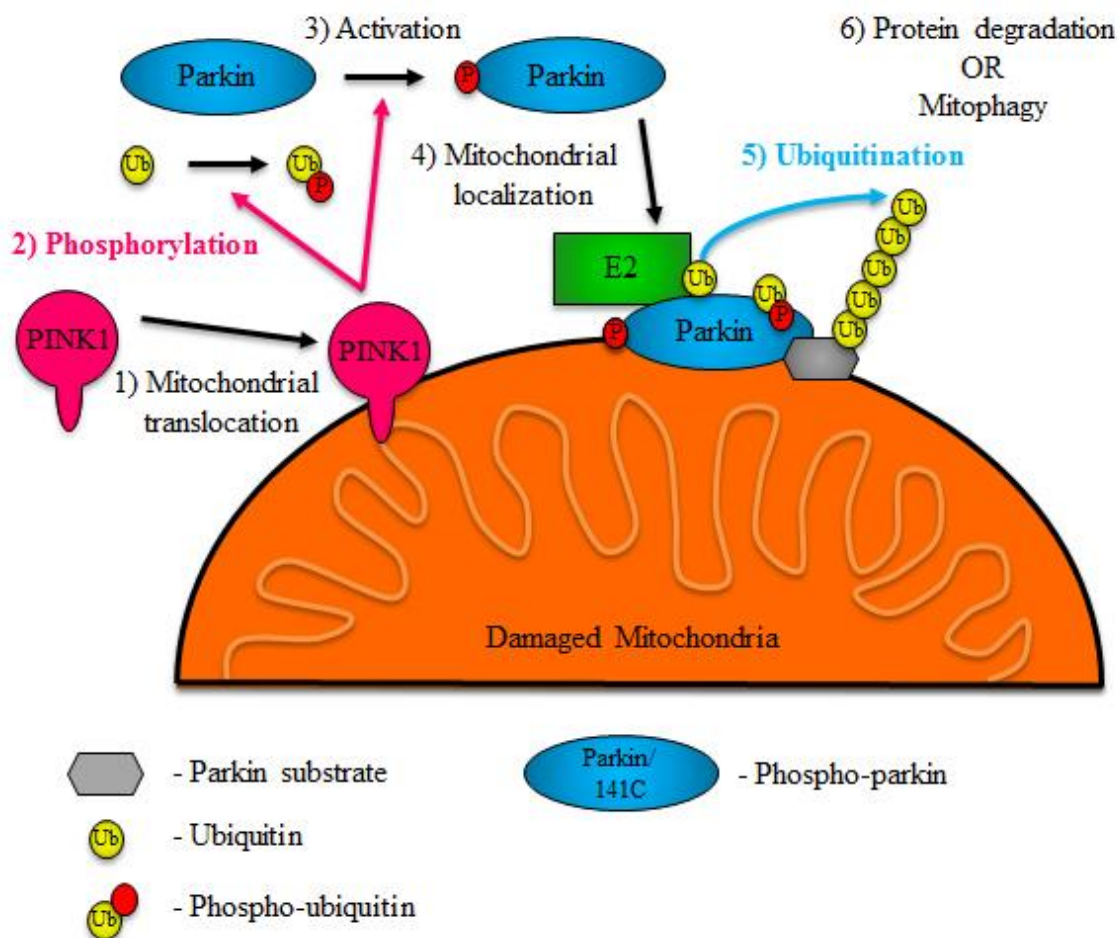


Figure 1-5. Activation of parkin mediated mitophagy of damaged mitochondria by PINK1. 1) Following its transport to damaged mitochondria, 2) PINK1 phosphorylates parkin and ubiquitin. 3) Phospho-parkin undergoes a closed-to-open conformational change and becomes more active, 4) directing it to damaged mitochondria, while PINK1 phosphorylation of ubiquitin is required to activate parkin. 5) While at the mitochondrial membrane, activated phospho-parkin ubiquitinates damaged mitochondrial proteins leading to 6) their degradation by the 26S proteasome or lysosomal degradation of damaged mitochondria (mitophagy).

for ubiquitination (86, 87), or 3) direct phosphorylation of S65 in the ubiquitin-like domain of parkin by PINK1, which converts parkin to an open or “active” conformation, priming it for ubiquitination (88). Ultimately, the recruitment of parkin to damaged mitochondria causes ubiquitination of damaged mitochondrial proteins, and subsequently, lysosomal degradation. Notably, these models are highly controversial because the published experimental data has not allowed researchers to draw a definite conclusion regarding the mechanism of parkin activation by PINK1. Additionally, a direct interaction between PINK1 and parkin has yet to be demonstrated.

1.4 Yeast Models

Saccharomyces cerevisiae, commonly known as baker’s or brewer’s yeast, is a model organism that has many advantages that make that it an excellent model system to study human diseases. Yeast is a single celled eukaryote that contains membrane bound organelles found in higher order eukaryotes and as a result, many key cellular pathways and processes relevant to human disease are conserved. As a unicellular organism, yeast can be grown in isolation as they do not require the release of growth factors from neighboring cells, which is often required for mammalian systems. In the laboratory, yeast is relatively easy to handle and has extremely short generation times, but the greatest power of the system comes from the ease of genetic manipulation. The yeast genome is considerably smaller than that of humans, with about 25% of the total number of genes found in humans (89). This smaller size has enabled the identification and characterization of each and every yeast gene to test whether they are essential and identify any phenotypes associated with deletion or over-expression. To this end, comprehensive deletion and over-

expression libraries have been generated that allow for high-throughput screening for genetic interactions, which is not possible in any model other organism. Furthermore, yeast can exist in both a diploid and haploid state, so it can be used to study the effects of heterozygous deletions or mutations.

1.4.1 Yeast Models of Neurodegeneration

Many established yeast models have been and are currently used to study human disease and one prominent class of human diseases studied in yeast are neurodegenerative disorders. One of the best-established yeast models of neurodegeneration is the polyglutamine expansion causing HD. Yeast HD models have established that polyQ expanded Htt exhibits tendencies to aggregate that are reminiscent of those found in human cells and have also shown the same toxicity associated with polyQ expansion (90, 91). Since its establishment, this model has been used to study how protein misfolding and aggregation can be modulated by molecular chaperones like heat shock protein (HSP) 70 and has identified this class of proteins as a potential for therapeutic intervention (92, 93). Other established yeast models for neurodegenerative diseases include A β models of Alzheimer's disease (94–96), and ALS models investigating SOD1, FUS, and TDP-43 aggregation and toxicity (97, 98).

1.4.1.1 Parkinson's Disease Yeast Models

There are also several established yeast models for PD associated genes and mutations. Of these genes, α -synuclein is the most well characterized model (99–101). Yeast models of α -synuclein, like yeast Htt models, closely mimic α -synuclein behavior in mammalian cells, showing transport of α -synuclein to the cell membrane under normal

levels of expression (102) and following accumulation (mimicked by overexpression), α -synuclein forms cytoplasmic inclusion that are similar to Lewy Bodies in human patients (103). With this established model, researchers have been able to further characterize the effects of specific point mutants (100), clearance of α -synuclein aggregates (104), and the effects of the ribosomal chaperone RPS3A (105). Yeast models have also been used to characterize the PD associated chaperone DJ-1. Under normal conditions in human cells, DJ-1 is a redox sensitive chaperone that acts to prevent α -synuclein aggregation (106, 107). Yeast models frequently use the *Saccharomyces cerevisiae* protein HSP31, which is a member of the DJ-1 superfamily of chaperones. Although HSP31 deletion strains do not exhibit a phenotype compared to wild-type yeast under normal conditions, they do have an increased sensitivity to oxidative stress (108). There has also been one recent parkin yeast model published in 2015 (109).

It must be noted that because yeast is a simple model system, results obtaining using this model may not always directly translate into human cells, therefore, they must be carefully interpreted and validated in other system. Nevertheless, yeast models can give new insight into protein function and potential therapeutics by focusing on conserved pathways including protein quality control, UPS, and protein misfolding, making it a highly versatile and capable model system.

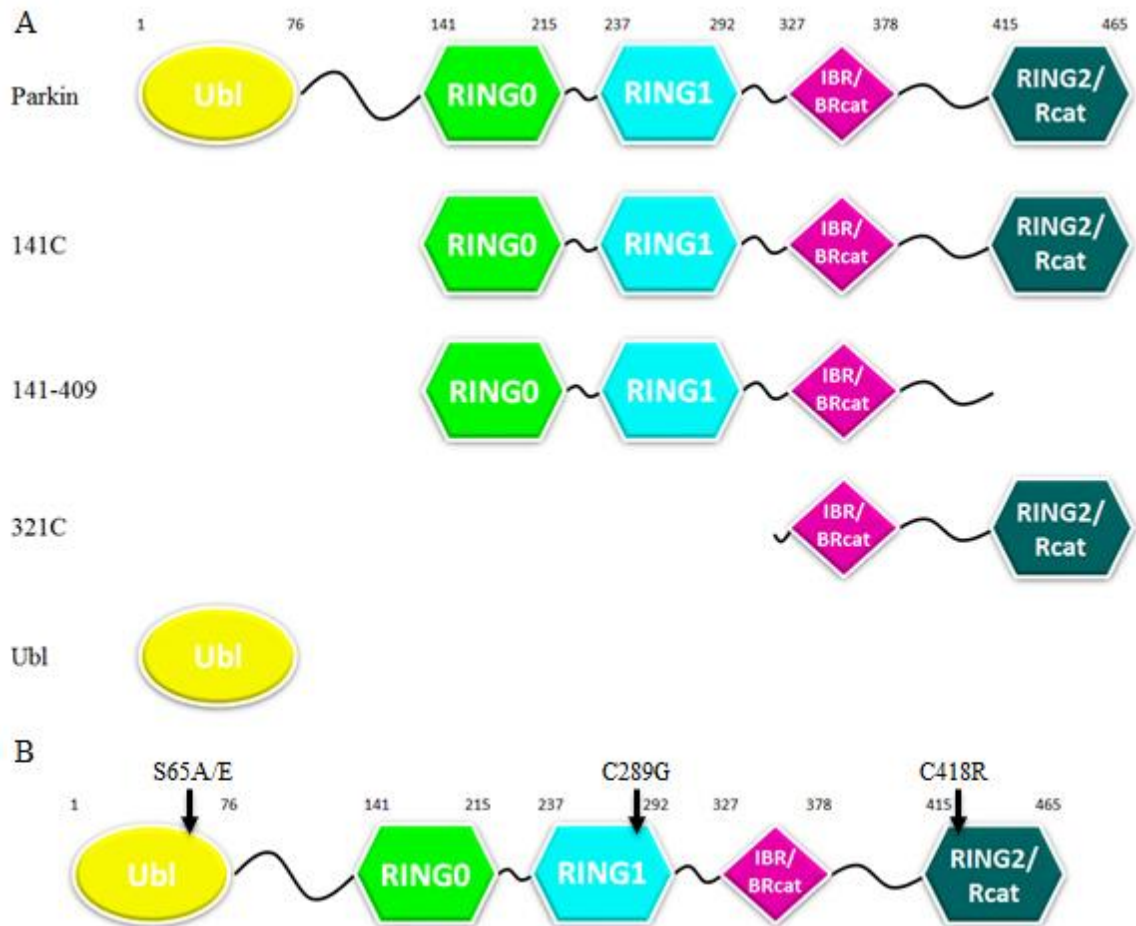


Figure 1-6. Parkin truncation variants and point mutants. Schematic representation of generated parkin (A) truncation variants and (B) point mutants used in this study.

1.5 Rationale, Hypothesis, Objectives, and Significance

1.5.1 Rationale

Parkin dysfunction can cause PD, but the underlying mechanisms causing disease development and progression remain unresolved. Independent evidence suggests that regulation by PINK1, loss of function caused by mutations, and misfolding can all contribute to PD development. Additionally, there currently is not an effective animal model that has clarified the role of parkin misfolding and ensuing cellular outcomes that lead to PD.

1.5.2 Hypotheses

- 1) Parkin truncations and point mutations alter cell growth and disrupt normal parkin localization.**
- 2) Parkin is involved in genetic interactions with genes required for oxidative stress management and preventing protein misfolding.**
- 3) Oxidative stress damages parkin resulting in misfolding and altered cellular localization.**
- 4) PINK1 interacts with parkin to disrupt parkin localization and stability**

1.5.3 Objectives

1) Establish a functional parkin yeast model

A yeast model expressing parkin and several parkin mutants (**Figure 1-6**) was established. The system was used to identify how dysregulation of parkin affected growth, and altered localization with the use of growth assays and fluorescence microscopy, respectively. Parkin variants bearing N- and C-terminal truncations allowed mapping and characterization of results based on functional knowledge of each domain. Additionally, two parkin point mutants were selected that have an increased propensity to misfold. These mutants were used to compare oxidative stress induced misfolding to aggregation caused by pathogenic AR-JP mutants. Two additional mutations to S65, the serine residue phosphorylated by PINK1 (88), were used to monitor how parkin aggregation and toxicity changed in the absence of PINK1-mediated phosphorylation.

2) Identify genetic interactions that alter parkin misfolding and toxicity

We tested how parkin localization is affected by the deletion of key genes involved in managing oxidative stress and protein misfolding by performing a pilot screen using yeast deletion libraries. Changes in growth and parkin localization were examined by spotting assays and fluorescence microscopy, respectively.

3) Assess how oxidative stress alters folding and localization of parkin

The effects of oxidative stress treatment towards parkin localization, toxicity and stability were examined in yeast by fluorescent microscopy, growth assays, and Western blot analysis following treatment with stress inducing chemicals.

4) Identify how PINK1 modifies parkin stability and cell toxicity

We tested how parkin toxicity, localization, and stability were altered by co-expression of PINK1 in yeast using growth assays, fluorescent microscopy, and Western blot analysis.

1.5.4 Significance

The use of genetic screens gave insight into alternate cellular pathways that parkin may be involved in that contribute to PD. This built a strong rationale to conduct a high throughput screen using the entire deletion and over-expression yeast libraries, which may uncover previously unidentified genetic interactions with parkin and elucidate previously undescribed pathways that may modulate parkin localization and function. By assessing how mutations, truncations, oxidative stress, and PINK1 co-expression, altered parkin localization, toxicity, and stability, we also established that parkin misfolding and regulation contribute to its dysfunction. Continuing research on these aspects of parkin dysregulation will certainly provide a better understanding of how parkin contributes to PD.

Chapter Two: Materials and Methods

2.1 Materials

2.1.1 *Escherichia coli* Strains - DH5 α Genotype $F-\Phi 80lacZ\Delta M15 \Delta(lacZYA-argF) 169$
recA1 endA1 hsdR17 (rK-, mK+) phoA supE44 λ - thi-1 gyrA96 relA1

2.1.2 Bacterial Media

2.1.2.1 *Luria-Bertani (LB)* - 10 g/L NaCl (Sigma Aldrich), 10 g/L tryptone (Sigma Aldrich) and 5 g/L yeast extract (Sigma Aldrich), supplemented with antibiotics: 100 μ g/mL ampicillin (Amresco) or 50 μ g/mL kanamycin (Amreseco).

2.1.2.2 *2xYT* - Full nutrient media for non-selective bacterial growth in liquid culture.

16 g/L tryptone, 10 g/L yeast extract (Sigma Aldrich) and 5 g/L NaCl.

2.1.3 *Saccharomyces cerevisiae* Strains - W303 MAT a (genotype: *leu2-3,112 trp1-1 can1-100 ura3-1 ade2-1 his3-11,15*) were used in all growth assays and protein work. BY4742 MAT a (Genotype *his3 Δ 1 leu2 Δ 0 lys2 Δ 0 ura3 Δ 0*) were used in all fluorescence microscopy experiments. BY4741 MAT α (Genotype *his3 Δ 1 leu2 Δ 0 lys2 Δ 0 ura3 Δ 0*) were used for screening genetic deletion strains.

2.1.4 *Yeast Media*

2.1.4.1 *Yeast Peptone Dextrose (YPD)* - Full nutrient media for non-selective yeast growth in either liquid or agar plates. 10 g/L yeast extract (Amresco), 20 g/L peptone (Sigma-Aldrich), and 20 g/L dextrose (Sigma-Aldrich).

2.1.4.2 *Selective Dextrose (SD)* - Media lacking essential amino acids required for growth of yeast deficient in amino acid biosynthesis in liquid media or on agar plates. 2% Glucose, YNB (Sigma-Aldrich) as nitrogen source, and amino acid powder as required for selection. 100X general amino acid solutions (6 g/L L-isoleucine, 2 g/L L-arginine, 4g/L L-lysine HCl, 6 g/L L phenylalanine, 1 g/L L-threonine, and 1g/L L-methionine); 100X selective amino acids (4g/L L-tryptophan, 6g/L L-leucine, 2 g/L L-histidine-monohydrate); 0.2% (w/v) adenine hemisulfate in 0.1 M NaOH; 0.4% (w/v) uracil in 0.1M NaOH.

2.1.4.3 *Selective Galactose/Raffinose (SGal/Raff)* - Media lacking essential amino acids required for growth of yeast deficient in amino acids biosynthesis; used to induce genes carried on vectors under control of Gal promoter. 2% Galactose (Sigma-Aldrich), 2% Raffinose (Sigma Aldrich), YNB as nitrogen source, and amino acid powder as required for selection.

2.1.5 *Mammalian Cell Lines* – Cervical cancer derived HeLa cells, human embryonic kidney (HEK) 293 cells stably expressing transfected FLAG-Parkin, and neuroblastoma derived SH-SY5Y cells were used in this study.

2.1.6 *Cell Culture Media* - Dulbecco's Modified Eagle Medium (DMEM, Corning) with 4.5 g/L or 1 g/L glucose was supplemented with 10% fetal bovine serum (FBS, Gibco),

100 I.U./mL penicillin (Corning Cellgro), 100 µg/mL streptomycin (Corning) and 1x glutamine (Sigma Aldrich).

2.1.7 Sources of DNA used for Cloning - Human parkin DNA used to clone parkin and parkin truncation variants was acquired from Dr. Shaw (Western). Yeast specific PINK1 DNA used in cloning and human PINK1 and kinase dead PINK1 DNA used for expression in mammalian was provided by was generously provided by Dr. Endo (Kyoto Sangyo University)

2.1.8 Chemicals

2.1.8.1 General Chemicals

All chemicals were purchased from Sigma Aldrich unless stated otherwise.

2.1.8.2 Protease Inhibitors

Protease and Phosphatase Inhibitor Cocktail (Thermo Scientific)

SIGMAFAST™ Protease Inhibitor Tablets (Sigma Aldrich)

N-Ethylmaleimide (NEM, Sigma Aldrich)

Phenylmethanesulfonyl fluoride (PMSF, Sigma Aldrich)

2.1.9 *Antibodies***Table 2-1. Antibodies used in this study.**

Antigen	Epitope	Supplier	Use	Concentration
Parkin	Ubl	Novus	WB	1-1000
			IF	1-200
Parkin	RING1	Abcam	WB	1-1000
			IF	1-500
Parkin	RING2	Cell Signaling	WB	1-10000 (Yeast)
			WB	1-2000 (Mam)
			IF	1-200
Parkin	Unknown	Santa Cruz	IF	1-200
PGK1	N/A	Antibodies-online	WB	1-10000 – 1-20000
Tubulin	N/A	Abcam	WB	1-5000
FLAG	N/A	Sigma Aldrich	WB	1-1000 – 1-2000
Polyubiquitin	N/A	Enzo	WB	1-2000
PS65-Ubiquitin	N/A	Boston Biochem	WB	1-500

2.2 Methods

2.2.1 Cloning

2.2.1.1 Polymerase Chain Reaction (PCR) – PCR is a technique used to create parkin variant templates to be used in Gateway® recombination cloning. Reaction mixtures included: 10 mM dNTPs (2 µL), variable concentration template (1 µL), 100 mM forward primer (2 µL), 100 mM reverse primer (2 µL), Q5 polymerase (1µL) (New England Biolabs), 5x buffer (20 µL) (New England Biolabs), and ddH₂O (72 µL). Samples were run for 25 cycles with denaturing, annealing, and extension temperatures of 95°C, 58°C, and 72°C respectively. DNA products were resolved by agarose gel electrophoresis (See **Table 2-2** for primer design).

2.2.1.2 Agarose Gel Electrophoresis - 1% agarose powder was dissolved in TAE (40 mM Tris, 20 mM acetic acid and 1 mM ethylenediaminetetraacetic acid (EDTA)) buffer with 1µg/mL ethidium bromide (Sigma Aldrich) and allowed to solidify at room temperature.

2.2.1.3 Gel Purification of DNA - AccuPrep® Gel Purification Kit (Bioneer) was used to purify DNA products from agarose gel. DNA bands were excised from the agarose gel and purified as described in the supplier instruction manual.

2.2.1.4 Mini Prep - High Speed Plasmid Mini Kit (Geneaid) uses standard alkaline lysis followed by neutralization and ethanol wash on DNA binding columns to extract dsDNA plasmids from E. coli. E. coli were grown in 3 mL cultures of LB supplemented with

ampicillin or kanamycin. Cells were lysed and DNA was extracted following the protocol described in the supplier instruction manual.

2.2.1.5 *Midi/Maxi Prep* - PureLink® HiPure Plasmid Midi/Maxiprep Kits provided by Invitrogen were used to prepare DNA for transfection of HeLa cells. 250-500 mL LB Amp cultures of *E. coli* were grown and isolated as per the instruction manual.

Table 2-2. Custom designed primers used to generate constructs for use in Gateway® cloning.

Clone and Orientation	Sequence (5' to 3')
Parkin/Ubl Fw	ggggacaagtttgtaaaaaagcaggctatgatagtgttgtcaggttcaact
141C/141-409 Fw	ggggacaagtttgtaaaaaagcaggctatgtcaatctacaacagctttatgtgt
321-465 Fw	ggggacaagtttgtaaaaaagcaggctatggaggagtgtgtcctgcagatggggg
Parkin/141C/321-465 Rv w/ Stop	ggggaccactttgtacaagaaagctgggtctacacgtcgaaccagtggcccc
Parkin/141C/321-465 Rv No Stop	ggggaccactttgtacaagaaagctgggtccacgtcgaaccagtggccccatg
141-409 Rv w/ Stop	ggggaccactttgtacaagaaagctgggtctaaaatacggcactgcactcccctca
141-409 RV No Stop	ggggaccactttgtacaagaaagctgggtcaaatacggcactgcactcccctca
Ubl Rv w/ Stop	ggggaccactttgtacaagaaagctgggtctaacctttctccacgggtctctgcaca
Ubl Rv No Stop	ggggaccactttgtacaagaaagctgggtcacctttctccacgggtctctgcaca
PINK1 Fw	ggggacaagtttgtaaaaaagcaggctatggtcagagaacagaaggccaag
PINK1 Rv w/ Stop	ggggaccactttgtacaagaaagctgggtcacttatcatcatcatcctata

2.2.1.6 Preparation of Competent DH5 α Cells – Two mL 2xYT culture of DH5 α were inoculated and incubated for six hours at 37°C during the day. Ten μ L of culture was transferred into 2 mL fresh 2xYT and incubated overnight at 37°C. The culture was diluted 1:100 in 1xYT media and incubated at 37°C. During this time, the culture OD₆₀₀ was checked 30 minutes after the first 2 hours and every 15 minutes after that. Cultures were grown to OD₆₀₀ 0.4-0.5. All the following steps occurred on ice. Cultures were chilled on ice 10 minutes by pouring equal volumes into two 50 mL conical PP centrifuge tubes. Samples were spun at 2,000xg for 15 minutes at 4°C in RT6000 Sorvall centrifuge with Swinging Bucket Rotor and resuspended with a 10mL pipet in 10 mL of CaCl₂ solution (60 mM CaCl₂.2H₂O, 10 mM PIPES pH 7.0 and 15% glycerol) per 50 mL tube with a 10 mL disposable pipet. Samples were spun again at 2,000xg for 10 minutes at 4°C in RT6000 Sorvall centrifuge with Swinging Bucket Rotor and resuspended with 10 mL pipet in 10 mL total volume of CaCl₂ solution before incubating on ice for 30 minutes. Following the incubation on ice, samples were spun at <2,000xg for 10 minutes at 4°C in RT6000 Sorvall centrifuge with Swinging Bucket Rotor and resuspended with 5 mL pipet into 1 mL volume of CaCl₂ Solution per 50 mL volume starting culture. Using P1000 pipet solutions were aliquoted in 100 μ L volumes into chilled tubes and quickly frozen to -80°C.

2.2.1.7 Gateway® Cloning – Gateway® Cloning is technique that utilizes homologous recombination to selectively insert the desired gene product into one of several destination vectors (110). After isolating PCR generated dsDNA constructs, the BP recombination reaction was first used transfer PCR template DNA into an intermediate cloning vector. Reaction mixtures included BP Clonase (1 μ L) (Invitrogen), pDONR vector (1 μ L) (Invitrogen), gel purified PCR DNA (3 μ L). The reaction was incubated at 37°C overnight.

Following the overnight incubation, the reaction was quenched with 1 μ L Proteinase K (Invitrogen) and incubated for 10 minutes at 37°C. Three μ L of reaction mixture was transformed into competent DH5 α cells via E. coli transformation protocol (see below) and plated on LB agar plates containing 50 μ g/ml Kan. Single colonies were isolated and grown in liquid LB Kan media overnight at 37°C. DNA was isolated from the E. coli using the High Speed Plasmid Mini Kit (Geneaid) and sequenced using the sequencing services provided by Robarts Research Institute at Western University to verify successful incorporation of the DNA into the pDONR201 vector.

After successfully isolating the desired construct in the pDONR backbone, the LR recombination reaction was used to transfer from the intermediate vector to one of several possible destination vectors. Reaction mixtures included: LR Clonase (4 μ L) (Invitrogen), destination vector (2 μ L), pDONR vector as source of recombinant DNA (2 μ L), and TE (10mM Tris pH 8.0, and 1 mM EDTA) buffer (12 μ L). The reaction was incubated at 37°C overnight followed by quenching with 2 μ L Proteinase K, which was incubated for 10 minutes at 37°C. Ten μ L of the reaction was transformed into competent DH5 α cells via E. coli transformation protocol and plated on LB agar plates containing 100 μ g/mL ampicillin (Amp). Again, single colonies were isolated, grown in LB AMP overnight at 37°C and the DNA was extracted and sequenced to verify successful recombination into the destination vector. A list of constructs and destination vectors used in this study can be found in **Table 2-3**.

2.2.1.8 Bacterial Transformation – Transformation is a protocol for introducing double stranded plasmid DNA into E. coli cells for replication/expression. One hundred μ L

aliquots of competent DH5 α cells were removed from -80°C and allowed to thaw on ice for five minutes. 1-5 μ L of plasmid DNA was added and samples were left to incubate on ice for 30 minutes. Samples were heat shocked at 42°C for 100 seconds followed by a two minutes incubation on ice. 900 μ L of 2xYT was added to each sample to make to total volume of 1mL. Samples were then incubated at 37°C shaking for at least one hour. After recover, cells were pelleted at 15 000xg for one minute and the supernatant was removed. The pellet was resuspended in 100 μ L LB or 2xYT and plated on LB agar plates with antibiotic.

Table 2-3. List of constructs and expression vectors used in this study.

Construct	Vector	Expression Control	Expression System
Parkin (WT)	pRS423	Galactose Induced	Yeast
Parkin (WT)	pRS423-YFP	Galactose Induced	Yeast
Parkin (WT)	pcDNA3.1	Constitutive	Mammalian
Parkin S65A	pRS423	Galactose Induced	Yeast
Parkin S65A	pRS423-YFP	Galactose Induced	Yeast
Parkin S65A	pcDNA3.1	Constitutive	Mammalian
Parkin S65E	pRS423	Galactose Induced	Yeast
Parkin S65E	pRS423-YFP	Galactose Induced	Yeast
Parkin S65E	pcDNA3.1	Constitutive	Mammalian
Parkin C289G	pRS423	Galactose Induced	Yeast
Parkin C289G	pRS423-YFP	Galactose Induced	Yeast
Parkin C289G	pcDNA3.1	Constitutive	Mammalian
Parkin C418R	pRS423	Galactose Induced	Yeast

Parkin C418R	pRS423-YFP	Galactose Induced	Yeast
Parkin C418R	pcDNA3.1	Constitutive	Mammalian
141C	pRS423	Galactose Induced	Yeast
141C	pRS423-YFP	Galactose Induced	Yeast
141C	pcDNA3.1	Constitutive	Mammalian
141-409	pRS423	Galactose Induced	Yeast
141-409	pRS423-YFP	Galactose Induced	Yeast
141-409	pcDNA3.1	Constitutive	Mammalian
321C	pRS423	Galactose Induced	Yeast
321C	pRS423-YFP	Galactose Induced	Yeast
321C	pcDNA3.1	Constitutive	Mammalian
Ubl	pRS423	Galactose Induced	Yeast
Ubl	pRS423-YFP	Galactose Induced	Yeast
Ubl	pcDNA3.1	Constitutive	Mammalian
PINK1 (WT)	pRS416	Galactose Induced	Yeast
PINK1 (WT)	pDENTIG	Constitutive	Mammalian
Kinase Dead PINK1	pRS416	Galactose Induced	Yeast
Kinase Dead PINK1	pDENTIG	Constitutive	Mammalian

2.2.2 *Yeast Culturing Techniques*

2.2.2.1 *Yeast Transformation* - Yeast cells were inoculated in 3 mL YPD or SD media and grown overnight at 30°C. Starter cultures were used to inoculate a 30ml culture in YPD or SD to an OD₆₀₀ = 0.200. Cells were grown for 4-5 hours at 30°C to OD₆₀₀ = 0.500. Equal volumes of the culture were poured into two 50mL sterile centrifuge tubes and centrifuge

for 5 minutes at 2000xg at 4°C. Supernatant was discarded and cell pellets were resuspended in 5 mL sterile H₂O per 50 mL tube. Samples were centrifuged again for 5 minutes at 2000xg at 4°C after which the supernatant was aspirated and cell pellets were resuspended in 2 mL of 100 mM Li-Acetate/TE and incubate for 10 minutes at 30°C. Samples were once again centrifuged for 5 minutes at 2000xg at 4°C and the supernatant was removed. One hundred mM Li-Acetate/TE was used to resuspend cells in the necessary volume for the number of transformations + 1 (100 µl/transformation). One hundred µl of yeast cell suspension was aliquoted into labeled tubes and to each tube add in order: 250 µl transformation buffer (1 X TE, 40% polyethylene glycol and 100 mM Li-Acetate), 12 µl salmon sperm DNA, 1 µl mini-prep cDNA and 25 µl DMSO (Sigma-Aldrich). After resuspension, samples were heat shocked for 20 minutes at 42°C shaking. Samples were chilled on ice for 5 minutes before centrifuging for 1 minute at 1000xg, after which the supernatant was aspirated. Cells were then resuspended in 50 µl TE. The entire suspension was plated onto selective agar plates.

2.2.2.2 Protein Induction – Yeast cells maintained on selective agar plates were used to inoculate liquid cultures in SD media. Cultures were incubated overnight at 30°C with constant shaking. After approximately 16 hours of growth, cultures were spun at 3000xg to pellet cells. The supernatant was aspirated and the cells were resuspended in sterile ddH₂O. This process was repeated and cells were washed a second time with ddH₂O before spinning one more time at 3000xg and aspirating the supernatant. The cells were then resuspended in SGal/Raff media to induce expression of constructs under control of the

Gal promoter. Cells were allowed to incubate in inducing media for 8-10 hours at 30°C before analysis or preparation for protein extraction.

2.2.3 *Growth Assays*

2.2.3.1 *Spotting Assays* - Yeast cells were inoculated into 3 mL liquid cultures of SD media and incubated with constant shaking overnight at 30°C. These cultures were diluted 1:10 in water and the OD₆₀₀ was measured as a proxy for cell density. In 96 well plates, yeast cultures were diluted in sterile ddH₂O to 200 µl with an OD₆₀₀ = 1.0. The subsequent five wells were filled with 120 µl of ddH₂O. Serial dilution of 1:4 volume from top well into subsequent 5 wells were prepared by transferring 30 µl from well to well. Equal volumes of each well were transferred onto agar plates using a 48 prong spotting tool (“frogger”). Samples were plated on YPD media to ensure equal cell concentrations as well as SGal/Raff plates to detect affects caused by protein induction. Plates were dried for 10-15 minutes prior to spotting to prevent samples from running. After spotting the plates were incubated at 30°C for 2-5 days. Pictures were taken to document growth differences between samples at the indicated incubation times.

2.2.3.2 *Growth Curves* – Yeast cultures were inoculated in SD media and grown overnight at 30° C with constant shaking. After approximately 12-16 hours, cultures were spun at 3000xg for 5 minutes and washed twice with sterile ddH₂O after removing the supernatant. Following the wash step, protein expression was induced by resuspending the cells in SGal/Raff media. Culture density was measured at a 600nm wavelength using a spectrophotometer. After measuring the OD₆₀₀, cultures were diluted to an OD₆₀₀ = 0.2 in SGal/Raff media and 300 µL of the culture was added to each well of a honeycomb plate.

Plates were incubated for 2-3 days in a Bioscreen C instrument (Oy Growth Curves Ab Ltd) at 30°C. OD₆₀₀ measurements were taken every 15 minutes after the plates were agitated for 15 seconds prior to reading.

2.2.3.2.1 Quantification of Growth Curves – Means of OD₆₀₀ measurements at mid-log growth were compared using GraphPad Prism 6 software to calculate statistical significances. Means and standard deviations were compared using either an unpaired T-test for experiments with two samples or a One-way ANOVA for experiments containing three or more samples. All sample means were compared to a vector control at an equivalent time point to assess growth inhibition.

2.2.4 Fluorescent Microscopy - Imaging of YFP (yellow fluorescent protein) tagged parkin variants expressed in BY 4742 MAT a following 10 hours of galactose induction were performed on a Leica TCS SP5 II Confocal microscope using a HCX PL APO 63x oil objective. Images were captured using an equipped CCD camera using Leica Application Suite Advance Fluorescence Life V2.6.0 software.

2.2.5 Cell Lysis

2.2.5.1 Yeast - Following 10 hours of induction in SGal/Raff media at 30°C, yeast cultures were spun at 3000xg for 5 minutes to pellet cells. After aspirating the supernatant, the pellets were washed with sterile ddH₂O. These steps were repeated to wash the cells a second time, after which, the cells were spun one more time. Again the supernatant was aspirated and cell pellets were put through one freeze thaw cycle at -20°C to assist with lysis. Cells were resuspended in equal volumes cold lysis buffer (50 mM Hepes pH 7.5, 150 mM NaCl, 5 mM EDTA, 1% Triton X-100, SIGMAFAST™ Protease Inhibitor

(Sigma), and 50 mM NEM or 2 mM PMSF) and glass beads. Yeast cells were lysed by vortexing in a Disruptor Genie (Scientific Industries) 6 times for 30 seconds with 1 minute incubations on ice between vortexes. After lysis, samples were spun at 20000xg for 10 minutes at 4°C. The supernatant was collected and the protein concentration of each sample was determined and normalized using the bicinchoninic acid (BCA) kit (Promega) using bovine serum albumin (BSA) as a standard.

2.2.5.2 Mammalian - Cells were washed with cold PBS which was then aspirated off. A cell scraper was used to detach cells into cold lysis buffer (50 mM Hepes pH 7.5, 150 mM NaCl, 5 mM EDTA, 1% (v/v) Triton X-100, and SIGMAFAST™ Protease Inhibitor) after which, extracts were frozen at -20°C. After thawing on ice, extracted were lysed using a Branson Sonifier® ultrasonic cell disruptor for two 3-5 second pluses. Lysed samples were centrifuged at 20000xg for 10 minutes at 4°C. The supernatant was collected and protein concentrations were determined using the BCA kit (Promega) using BSA as a standard.

2.2.5.3 NaOH Based Yeast Lysis – NaOH based lysis is an alternative method of yeast lysis used to address post lysis protease dependent protein degradation. The protocol was followed as described by Von der Haar T. (111) with adaptations made using 5ml cultures and adapting total volumes accordingly.

2.2.6 Western Blotting – Thirty µg of normalized protein samples in 1x sample buffer (2% sodium dodecyl sulphate (SDS), 5% glycerol, 50 mM EDTA, 200mM Tris-HCl pH 6.8) with or without reducing agents (1% β-mercaptoethanol (BME) and 100 mM dithiothreitol (DTT)) were loaded onto 12% or 15% acrylamide gels. Once resolved, the protein samples were transferred to nitrocellulose membranes (Bio Rad) using the Trans

Blot Turbo Transfer System (Bio Rad) following the manufacturer's instructions. Membranes were blocked with blocking buffer (PBST 0.01% Tween-20, 2% BSA (Sigma Aldrich), and 2% goat serum) for 1 hour at room temperature and then incubated with primary antibodies (concentrations can be found in **Table 2-1**) in PBST with 2% BSA overnight at 4°C. Primary antibodies solutions were removed and membranes were washed with PSBT for 10 minutes 6 times before adding secondary antibody solutions and incubating at room temperature for 1 hour. After removing secondary antibody solutions, the membranes were again washed 6 times with PBST. Samples were imaged at infrared wavelengths using the LiCor system (Odyssey) using Odyssey V3.0 software.

2.2.7 SYTOX® Green Cell Death Assay - Yeast cells maintained on selective agar plates were used to inoculate liquid cultures in SD media. Cultures were incubated overnight at 30°C with constant shaking. After approximately 16 hours of growth, cultures were spun at 3000xg to pellet cells. The supernatant was aspirated and the cells were resuspended in ddH₂O. This process was repeated and cells were washed a second time with ddH₂O before spinning one more time at 3000xg and aspirating the supernatant. The cells were then resuspended in SGal/Raff media to induce expression of constructs under control of the Gal promoter. Cells were allowed to incubate in inducing media for 8-10 hours at 30°C before adding 5 µL of SYTOX® Green Nucleic Acid Stain (Thermo-Fisher) to 1 mL of culture to a final concentration of 25 µM. The cultures were vortexed and allowed to incubate at room temperature for ten minutes. Three 200 µL aliquots of the SYTOX® treated culture were added to 96 well plates followed by analysis using the Victor3V Plate Reader using the Perkin Elmer 2030 Manager Software. SYTOX® emission were read at

535nm and culture density was measured at 595nm. STYOX® measurements were corrected to culture density and values used for analysis.

2.2.8 Semi Denaturing Detergent Agarose Gel Electrophoresis (SDD AGE) – SDD AGE is a technique used to resolve amyloid-like protein aggregates using mild detergents. Protein expression in yeast was performed, as described above. After 10 hours of protein induction, cells were washed twice in ddH₂O before resuspending in equal volumes of cold SDD PAGE lysis buffer (100 mM Tris pH 7.5, 200 mM NaCl, 1mM EDTA, 5% glycerol, 1 mM PMSF, 50mM NEM, Phosphatase and Protease Inhibitor Cocktail (Sigma Aldrich), and SIGMAFAST™ Protease Inhibitor) and glass beads. Yeast cells were lysed by vortexing in a Disruptor Genie (Scientific Industries) 6 times for 30 seconds with 30 second incubations on ice between vortexes. After lysis, samples were spun at 1000xG for 10 minutes to pellet insoluble debris. The supernatant was collected and protein extracts were normalized by BCA assay (Pierce) using BSA as a standard. Sample buffer (1x TAE, 5% glycerol, and 0.2% SDS) was added to protein extracts and 30 µg total protein was loaded into each lane. Samples were resolved by electrophoresis through a 1.8% agarose gel containing 0.1% SDS. After rinsing the gel in TBS (10 mM Tris pH 7.5, and 150 mM NaCl) samples were transferred to a nitrocellulose membrane (Bio Rad) through capillary force using pre-assembled TurboBlotter™ Rapid Downward Transfer System packs (GE

Healthcare). Once samples were transferred to the nitrocellulose membrane, samples were treated and imaged in the same way as standard Western blots (described above).

2.2.9 Cell Culture

2.2.9.1 *Cell Maintenance and Passaging* - Cervical cancer derived HeLa, human embryonic kidney (HEK 293) stably expressing FLAG-Parkin, and neuroblastoma derived SH-SY5Y cell lines were used in this study. Cells were continually passaged on culturing plastics (Starsted) in Dulbecco's Modified Eagle Medium (DMEM) containing 4.5g/L glucose supplemented with 10% fetal bovine serum (FBS), 100 I.U./mL penicillin (Corning Cellgro), 100 µg/mL streptomycin (Corning Cellgro), and 1x glutamine (Sigma Aldrich) at 37°C with ~5% CO₂. Cell lines were passaged using standard 0.25% trypsin with 2.21 mM EDTA incubation followed by washing with fresh DMEM and re-seeding to new sterile culture plastics.

2.2.9.2 *Transfection* - Cells were grown to approximately 90% confluency in DMEM before transfecting cells using Lipofectamine® 2000 (Thermo Fisher) following the supplier recommended concentrations in Opti-MEM® low serum media. Transfections were incubated for 16-20 hours at 37°C before washing with PBS. Cells were returned to DMEM media to recover for 24 hours before passaging into 6 well plates or 8 chamber

microscopy slides. Cells were allowed to recover for 24 hours after passaging before further treatment or analysis.

2.2.10 Chemical Stress Treatment

2.2.10.1.1 Yeast - Spotting assays and Bioscreen growth curve experiments were performed with selective agar or liquid media, respectively, containing 50 μM H_2O_2 , 100 μM H_2O_2 , 1 mM H_2O_2 , 500 μM azetidine-2-carboxylic acid (AZC, Sigma-Aldrich), 10 μM peroxyntirite (Enzo), 2 mM DTT, 25 μM radicicol (Sigma-Aldrich), or 50 μM antimycin A (Sigma Aldrich). Spotting assays were grown for 3-5 days at 30°C under stress conditions where as Bioscreen growth experiments were incubated for 2-3 days at 30°C with agitation every 15 minutes

2.2.10.1.2 Mammalian - Mammalian cells were treated with either 75 μM H_2O_2 , 10 μM MG132, 1 mM LAZC, 50 μM antimycin-A, or 10 μM peroxyntirite for either 8 hours or 16 hours in DMEM at 37°C with 5% CO_2 . Following treatment, cells were washed with PBS and used for Western Blotting or Immunofluorescence microscopy (IF).

2.2.11 Viability Assay – SH-SY5Y cells expressing endogenous parkin and PINK1, HEK 293 cells stably expressing FLAG-parkin but no PINK1, or HeLa cells transiently transfected with parkin, various parkin mutants, wild-type (WT) PINK1, and/or a kinase dead (KD) mutant PINK1 were used to perform viability assays. Following transfection or standard passaging, cells were given either 1 or 4 days to recover in rich media (DMEM with 10% FBS and 4.5 g/L glucose) or minimal media (DMEM with 1% FBS and 1 g/L glucose) before performing the luminescence based Cell Titer-Glo® Luminescent Cell Viability Assay (Promega). Samples were prepared as recommended by the supplier and

loaded into 96 well plates. Plates were then measured using the Victor3V Plate Reader (Perkin Elmer) using the Perkin Elmer 2030 Manager Software.

2.2.12 Immunofluorescence Microscopy - 8 well chamber slides (Lab-Tex) were coated with Poly-L-Lysine (Sigma Aldrich) before passaging cells into wells. Culturing media was removed after a 24 hour recovery period and cells were fixed with 4% paraformaldehyde in PBS pH 7.4 for 20 minutes at room temperature. Cells were rinsed with PBS every 5 minutes for 30 minutes followed by permeabilization with 0.1% Triton X-100 (Sigma Aldrich) in PBS for 10 minutes. The Triton X-100 solution was removed and cells were washed 6 times with PBS before blocking in PBST (PBS + 0.01% Tween 20) with 6% BSA and 2% goat serum for 1.5 hours at room temperature. Following blocking, cells were incubated in primary antibody solution for 1 hour at room temperature with antibody titers corresponding to **Table 2-1** in section 2.1.9. Cells were then washed with PSBT every 5 minutes for 30 minutes. This was followed by incubation with secondary antibody solution for 1 hour at room temperature. Cells were washed again for 30 minutes at 5 minutes intervals with PBST before mounting with SlowFade® Gold anti-fade reagent with DAPI (Life Technologies) mounting media. Samples were then visualized using a Zeiss Axio Vert A1 Inverted fluorescent microscope using a 40x objective. Images were captured using an AxioCam Icc5 camera operating on the Zen 2 Lite software.

2.2.13 Shutoff

2.2.13.1 Yeast – After ten hours of protein induction, glucose was added to the cultures to a final concentration of 2% to quench expression under control of the gal promoter. At the point of glucose addition, 50µM MG132 or an equivalent volume of DMSO were added to

cultures. Δ erg1, Δ erg3 W303 MAT yeast strains were used in these experiments to inhibit export of MG132 from the cells. Aliquots of the culture were taken at various time points following expression inhibition, and frozen at -80°C until all time points were collected. All time points were then lysed as described above, used to perform western blots, and band intensities were quantified using Odyssey V3.0 software.

2.2.13.2 Mammalian – Following transfection or normal passaging, mammalian cells were treated with $200\ \mu\text{g}/\text{mL}$ cycloheximide (Sigma Aldrich) and $10\ \mu\text{M}$ MG132 or an equivalent volume of DMSO in fresh culturing media (DMEM with 10% FBS and 4.5 g/L glucose). Cells were harvested as described above at various time points and kept at -20°C until all time points were collected. Samples were then lysed as previously described, used for western blotting, and band intensities were quantified using Odyssey V3.0 software.

Chapter Three: Results

3.1 Parkin Sequence Analysis

To gain a better understanding how the amino acid composition of parkin affects its sensitivity to damage by oxidation, which can lead to altered parkin function, we performed an amino acid sequence analysis. Using sequence files obtained from Uniprot.org, we conducted a comprehensive analysis, aligning the parkin sequences of 38 difference species (Appendix 2). For clarity, a representative alignment of four species (Homo sapiens, Mus musculus, Drosophila melanogaster, and Caenorhabditis elegans) is shown in **Figure 3-1**. These four species cover a wide spectrum of species divergence from roundworm to insects and mammals. Amino acids C431, H433, and E444, which make up the catalytic triad involved in human parkin's E3 ubiquitin conjugation activity (112), are highly conserved in these species. C431 and H433 are completely conserved across all four species, and E444 is substituted for an acidic aspartate residue in *C. elegans*.

Analysis of the human parkin amino acid sequence revealed that 35 of the 465 residues are cysteines, equating to 7.52% of the total protein. This proportion of cysteines is approximately two times higher than the calculated random incorporation of 3.28% based on the two of 61 possible sense codons encoding cysteine residues and, more importantly, nearly three times higher than the average for all analyzed human proteins, which is 2.26% (8). Twenty-nine of parkin's 35 cysteines (82.8%) are conserved between all four species and all of these residues are located within the boundaries of structurally determined functional domains. When *C. elegans* is excluded from this analysis, this number increases to 32 of the possible 35 cysteines (91.4%).

Figure 3-1. Parkin sequence alignment. (A) Schematic representation of parkin domains based on structural determination by NMR. (B) Amino acid sequences acquired from UniProt were aligned using Clustal Omega software. Cysteine residues are in red and amino acid residues of the functional domains in the human sequence are highlighted in the corresponding colour as shown in panel A. Asterisks (*) indicate positions with fully-conserved residues; colons (:) indicate conservation between groups of strongly similar properties, and periods (.) indicate conservation between groups of weakly similar properties.

Many of these cysteines are known to be involved in coordinating Zn^{2+} ions, which is required for proper folding and stability of parkin (59). However, this unusually high cysteine content also suggests a high susceptibility to oxidative damage and disulfide formation caused by exposure to reactive oxygen species (ROS) *in vivo*.

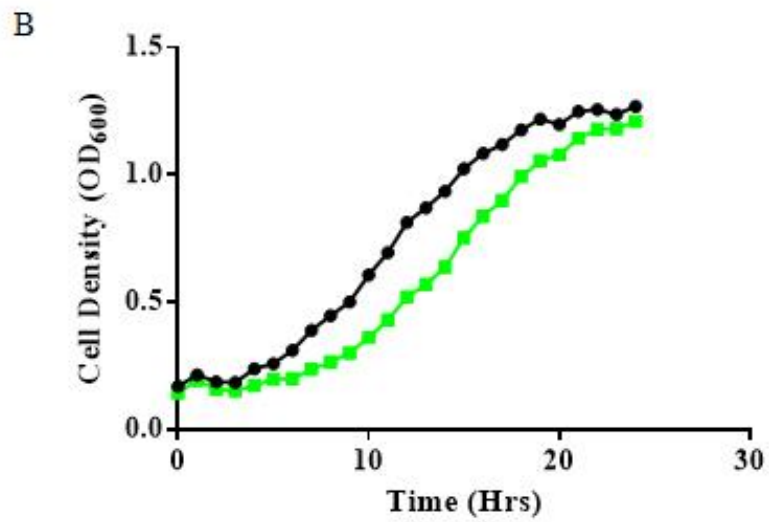
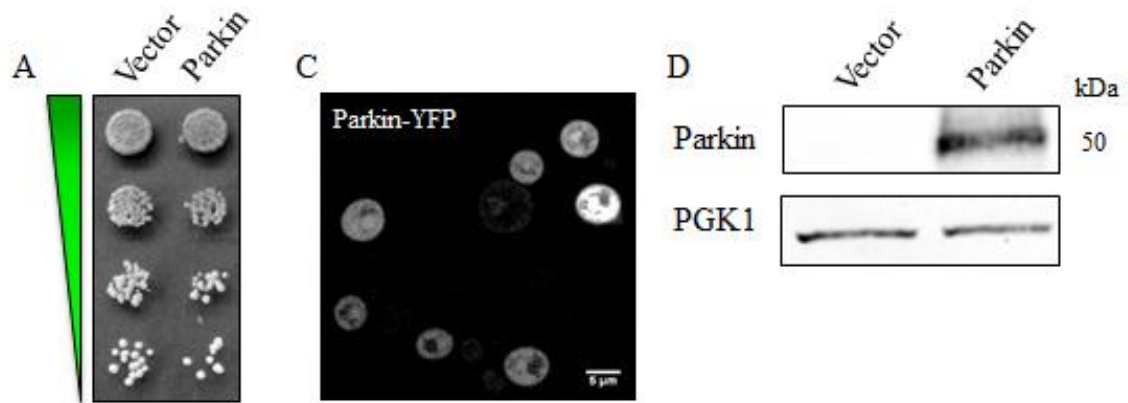
3.2 The Parkin Yeast Model

The yeast genome does not contain a *PARK2* orthologue. We therefore used human parkin to establish a yeast model to study how parkin is affected by truncations, point mutations, PINK1 mediated phosphorylation, or various types of chemical stress including oxidative, nitrogenous, or membrane stress. Recombination-based cloning (Gateway) was used to generate yeast expression vectors for human parkin: one expressing the unmodified wild-type protein, and one containing a carboxy-terminal (C-terminal) yellow fluorescent protein (YFP) fusion protein (parkin-YFP) to visualize cellular localization by fluorescence microscopy. These parkin expression vectors contain a galactose inducible promoter (GAL1) to allow controlled expression of parkin. Unlike many constitutive promoters used in many mammalian systems, yeast enables the use of various promoters that can be selectively induced. This allows yeast to be grown on media containing glucose as a primary carbon source which causes them to grow and divide like wild-type yeast, but switching to a galactose based media induces parkin translation, allowing for controlled expression. Additionally, yeast expressing parkin can be switched back to glucose based media to selectively inhibit parkin expression without altering transcription of all other cellular proteins. Both the YFP-tagged and untagged parkin expression vectors were transformed into yeast. We first assessed whether the expression of human parkin has an

effect on the growth of yeast cultures under normal conditions. Spotting assays on agar plates and growth curves in liquid media showed an extremely mild growth defect associated with the over expression of untagged human parkin (**Figure 3-2 A and B**). Notably, control yeast (transformed with empty vector) and those over-expressing parkin had a similar growth rate during exponential growth phase as documented by a similar maximum slope of the curve during the first 12-18 hours of growth (**Figure 3-2 B**). Cells expressing parkin took two to three hours longer to enter logarithmic growth, indicating a prolonged lag phase.

We next assessed parkin localization of parkin-YFP by fluorescent microscopy. After ten hours of inducing parkin-YFP expression, parkin-YFP was diffusely localized throughout the yeast cytosol (**Figure 3-2 C**) as previously reported in mammalian systems (113, 114). A minor proportion of yeast cells showed small cytosolic foci of increased signal intensity which could indicate subcellular accumulation of parkin (data not shown). Western blots showed that after ten hours of galactose induction, parkin was stably expressed in the transformed yeast (**Figure 3-2 D**). These data established our yeast parkin model and set the baseline to determine how cellular stress conditions and genetic modifications alter parkin toxicity, localization, stability, and degradation.

Figure 3-2. Establishing a parkin yeast model. (A) Liquid cultures of W303 were grown to stationary phase in non-inducing selective media and diluted to $OD_{600} = 1.0$ and serially diluted 1:5 before spotting on selective inducing agar media and incubated at 30°C for 2-4 days before imaging to assess the effects of parkin expression on wild type W303. (B) Liquid cultures grown to stationary phase in non-inducing selective media were washed twice with sterile H_2O and resuspended in inducing selective media before diluting to $OD_{600} = 0.2$ and incubating at 30°C . OD_{600} measurements were taken every 15 minutes and plotted to generate a growth curve. Standard deviations did not exceed a maximum $OD_{600} = 0.02$. At mid-log growth parkin growth was statistically different from the control with a P value ≤ 0.001 as determined from an unpaired T-test. ● (Black) - Vector; ● (Green) - parkin (C) BY cells expressing parkin-YFP were grown in inducing liquid media for 8 hours and fluorescent images were captured using a Leica TCS SP5 II confocal microscope at 63x magnification. The scale bar represents $5\mu\text{m}$. (D) Thirty μg total protein of cell extracts from wild type W303 and W303 expressing parkin were resolved by SDS-PAGE, transferred to nitrocellulose membranes and expression of parkin was detected using immunodetection and imaged using infrared conjugated secondary antibodies. PGK1 was used to assess equal loading.



3.3 Genetic Modulators of Parkin Toxicity and Localization

Yeast can be used to perform extremely powerful genetic screens that cannot be carried out in any other model systems. These screens make use of the exhaustive over-expression and deletion libraries that have been generated in yeast. Based on previous descriptions of parkin's involvement in degradation of damaged proteins and turnover of damaged mitochondria (mitophagy), we decided to perform a genetic screen with parkin in a select library of 17 yeast deletions strains of genes involved in managing oxidative stress and protein misfolding which are described in **Table 3-1**.

Parkin and parkin-YFP expressing yeast plasmids were transformed into the selected yeast strains. Deletion strains expressing untagged parkin were spotted onto inducing media and growth was assessed against a wild-type control strain expressing parkin (**Figure 3-3 A**). This screen revealed three deletion strains that show reduced growth due to the over-expression of human parkin: 1) deletion of SOD2, encoding a mitochondrial superoxide dismutase that protects against toxicity caused by superoxide radicals (115, 116); 2) deletion of YAP1, encoding a transcription factor required for oxidative stress tolerance that is activated by H₂O₂ (117); and 3) deletion of BTN2, encoding a v-SNARE binding protein that facilitates protein retrieval from a late endosome to the Golgi and contributes to prion curling (118). Deletion strains expressing parkin-YFP were used for fluorescent microscopy to assess changes in parkin localization. Only two strains, deletion of SOD2 and SGT2, showed changes in parkin localization, showing subcellular accumulation of parkin into bright puncta; all other strains showed diffuse parkin localization as seen in wild-type yeast cells. SGT2 is a cytoplasmic co-chaperone

that is part of a protein complex required to mediate post-translational insertion of tail-anchored proteins into the endoplasmic reticulum (ER) membrane (119), suggesting that altered capability of cells to undergo proper protein trafficking and folding affects parkin localization. These results indicate that genetic interactions can cause growth retardation and parkin accumulation, but these phenotypes are not necessarily dependent on one another. The results from this limited pilot screen built a strong rationale to conduct a high-throughput screen using the entire deletion and over-expression yeast libraries. A high-throughput screen may uncover novel genetic interactions with parkin and elucidate pathways that modulate parkin localization and parkin function that have not been described previously.

Figure 3-3. Pilot screen for genetic modulators of parkin toxicity and localization.

Parkin or parkin-YFP was transformed into a selected set of BY deletion strains of genes involved in managing oxidative stress and protein misfolding. (A) BY deletion strains expressing parkin were spotted to assess the effects of parkin expression on BY deletion strains. (B) BY deletion strains expressing parkin-YFP were grown in inducing liquid media for 8 hours and fluorescent images were captured using a Leica TCS SP5 II confocal microscope at 63x magnification to detect changes in parkin localization. The scale bar represents 5 μm .

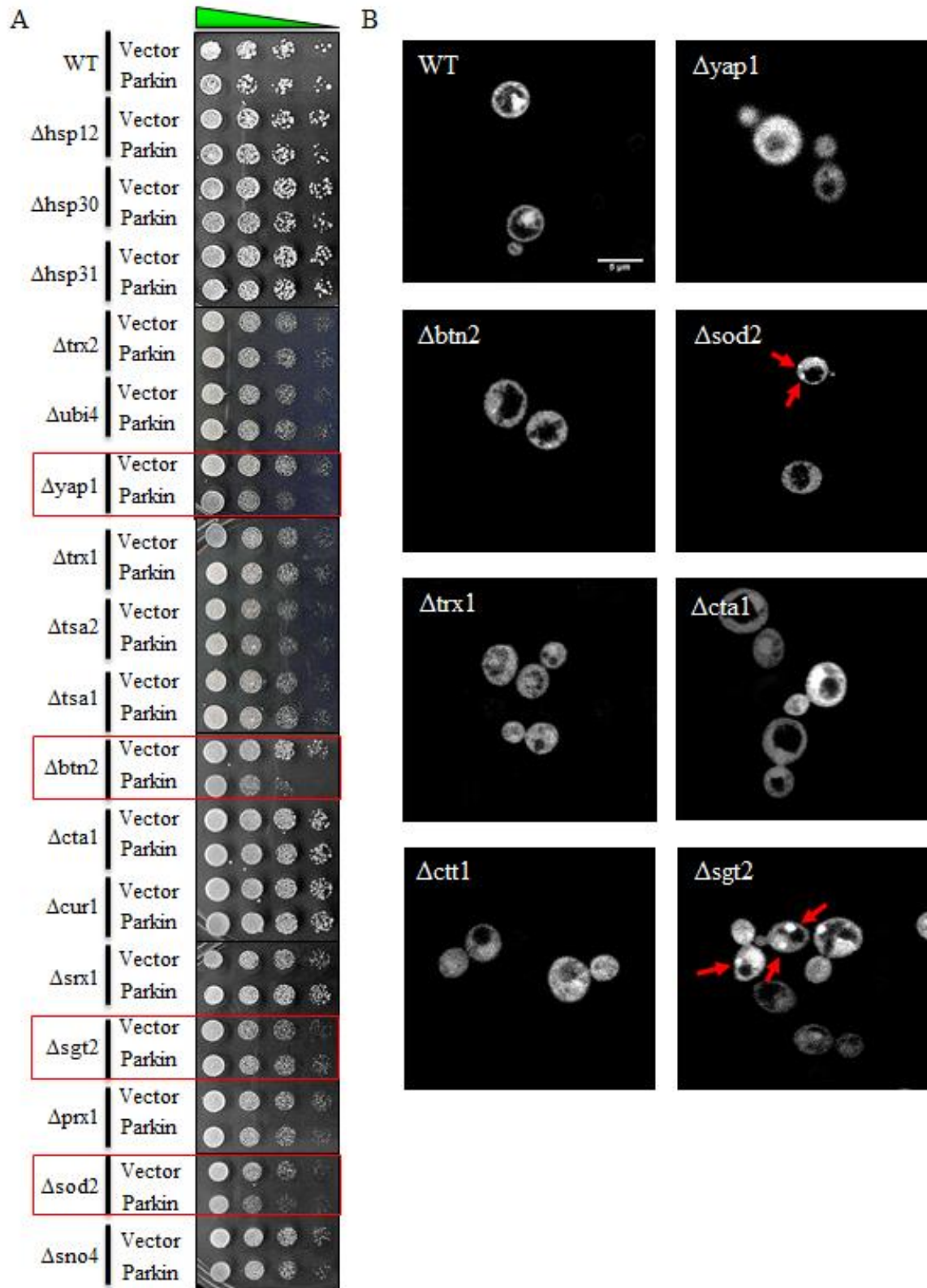


Table 3-1. List of yeast deletions and corresponding gene function used to screen for parkin genetic interactions. Cellular functions and phenotypes associated with gene deletions. Modified from the Saccharomyces Genome Database.

Gene	Function	Null Phenotype	Reference(s)
HSP12	Plasma membrane protein involved in maintaining membrane organization; involved in maintaining organization during stress conditions; induced by heat shock, oxidative stress, osmotic stress, stationary phase, glucose depletion, oleate and alcohol.	Slow growth phenotype, increased sensitivity to cell-wall affecting drugs, and increased flocculation.	(120, 121)
HSP30	Negative regulator of the H(+)-ATPase Pma1p; stress-responsive protein.	No growth phenotype.	(122)
HSP31	Methylglyoxalase that converts methylglyoxal to D-lactate; involved in oxidative stress resistance.	No growth phenotype; increased sensitivity to oxidative stress and accumulation of ROS.	(121)
TRX2	Cytoplasmic thioredoxin isoenzyme; part of thioredoxin system which protects cells against oxidative and reductive stress.	Increased heat sensitivity and decreased resistance to hydrogen peroxide.	(123, 124)
UBI4	Ubiquitin; becomes conjugated to proteins, marking them for selective degradation via the ubiquitin-26S proteasome system; essential for the cellular stress response.	Increased sensitivity to elevated temperature, zinc deficiency, nitrogen starvation, and oxidative stress.	(125, 126)
YAP1	Basic leucine zipper (bZIP) transcription factor; required for oxidative stress tolerance; activated by H ₂ O ₂ through the multistep formation of disulfide bonds.	Increased mutation frequency, decreased resistance to oxidizing and reducing agents.	(117)
TRX1	Cytoplasmic thioredoxin isoenzyme; part of thioredoxin system which protects cells against oxidative and reductive stress.	Decreased chromosome and plasmid maintenance.	(123, 124)
TSA1	Thioredoxin peroxidase; acts as both ribosome-associated and free cytoplasmic antioxidant; self-associates to form high-molecular weight chaperone complex under oxidative stress.	Hypersensitive to oxidative stress and shows decreased anaerobic growth rate.	(127, 128)
TSA2	Stress inducible cytoplasmic thioredoxin peroxidase; cooperates with Tsa1p in the removal of reactive oxygen, nitrogen and sulfur species using thioredoxin as hydrogen donor.	Decreased growth rate in exponential phase.	(129, 130)

BTN2	v-SNARE binding protein; facilitates specific protein retrieval from a late endosome to the Golgi; modulates arginine uptake, possible role in mediating pH homeostasis between the vacuole and plasma membrane H(+)-ATPase.	Decreased resistance to acidic pH.	(118, 131)
CTA1	Catalase A; breaks down hydrogen peroxide in the peroxisomal matrix formed by acyl-CoA oxidase (Pox1p) during fatty acid beta-oxidation.	Decreased resistance to oxidative stress and decreased superoxide accumulation.	(132, 133)
CUR1	Sorting factor, central regulator of spatial protein quality control; physically and functionally interacts with chaperones to promote sorting and deposition of misfolded proteins into cytosolic compartments.	Increased prion formation and abnormal protein distribution.	(11, 131)
SRX1	Sulfiredoxin; contributes to oxidative stress resistance by reducing cysteine-sulfinic acid groups in the peroxiredoxin Tsa1p, which is formed upon exposure to oxidants.	Decreased oxidative stress resistance and increased sensitivity to hydrogen peroxide.	(134)
SGT2	Glutamine-rich cytoplasmic co-chaperone; serves as a scaffold bringing together TRC complex members required to mediate posttranslational insertion of tail-anchored proteins into the ER membrane; plays a role in targeting chaperones to prion aggregates.	Increased heat sensitivity and decreased resistance to hygromycin B.	(119)
PRX1	Mitochondrial peroxiredoxin with thioredoxin peroxidase activity; has a role in reduction of hydroperoxides.	Decreased resistance to oxidative stress.	(135)
SOD2	Mitochondrial manganese superoxide dismutase; protects cells against oxygen toxicity.	Increased apoptosis, and decreased chronological and replicative lifespan. Increased sensitivity to oxidative stress, heat, and ionic stress	(115, 116)
SNO4	Possible chaperone and cysteine protease; required for transcriptional reprogramming during the diauxic shift and for survival in stationary phase	Decreased oxidative stress resistance and increased accumulation of ROS.	(136)

3.4 Oxidative Stress and Parkin Accumulation

Before testing the effects of stress inducing treatments on parkin expressing cells, we tested to see if parkin is modified from naturally occurring stress inducing chemicals, such as reactive oxygen or nitrogen species that can be by-products of normal cellular processes (137, 138). Based on the high cysteine content of parkin, we hypothesized that parkin would be highly susceptible to oxidative modification *in vivo*. Western blots were performed with protein lysates from yeast cells expressing parkin (**Figure 3-4 A**). Before resolving by SDS-PAGE, samples were prepared in loading buffer either with or without reducing agents (β ME/DTT). In the absence of reducing agents, parkin migrated through the gel at a faster pace than parkin treated with reducing agents. N-Ethylmaleimide (NEM) irreversibly modifies cysteine residues by adding an alkyl group to the sulphur atom on their side chains. When protein lysates from yeast cells expressing parkin were treated with 50 mM NEM, the molecular weight shift of parkin observed by Western blot with non-reducing buffer was eliminated (data not shown). A closer analysis of the parkin signal of under non-reducing conditions (**Figure 3-4 A lane 2**) revealed a predominant species around 50kDa with a smeared signal above and below the predominant band. These results suggest that parkin is modified by oxidative damage under normal growth conditions in yeast.

To test if this result was an artefact caused by the non-native environment of a yeast cell, similar experiments were performed with three human cell lines expressing different forms of parkin. HeLa and HEK 293 cells were chosen as simple model mammalian

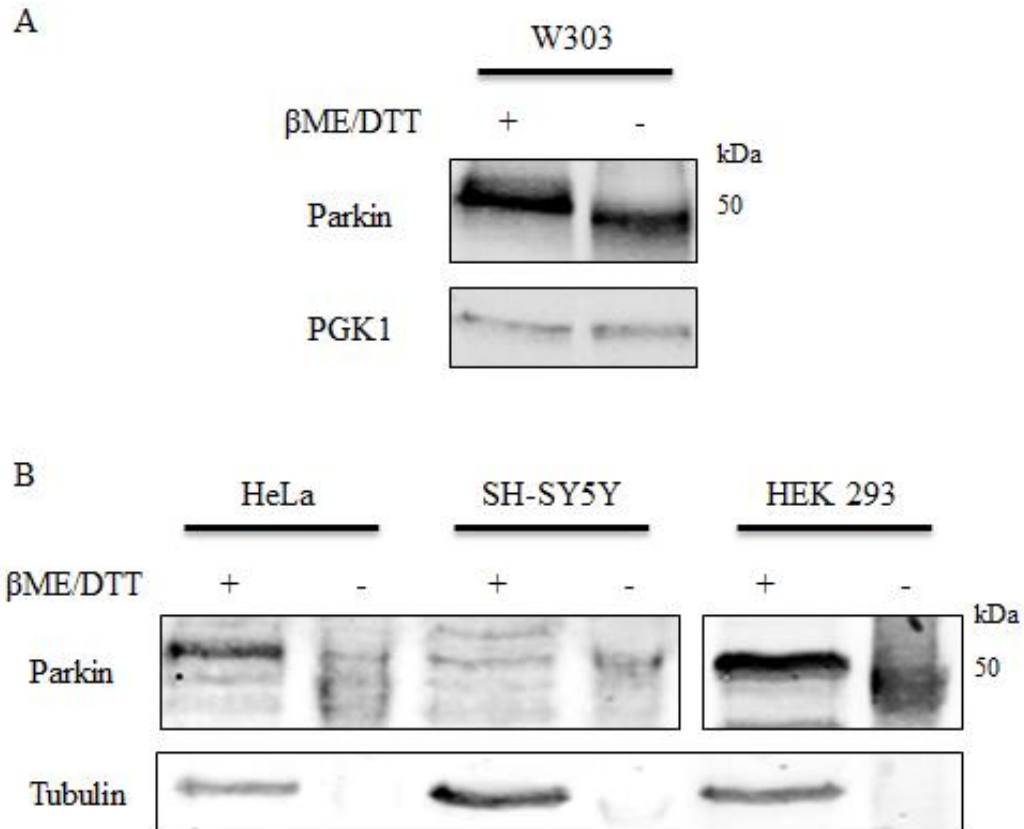
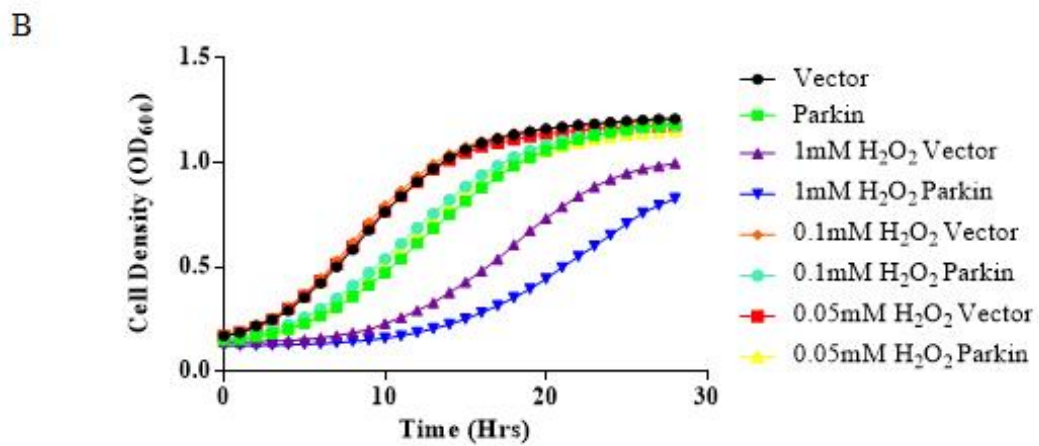
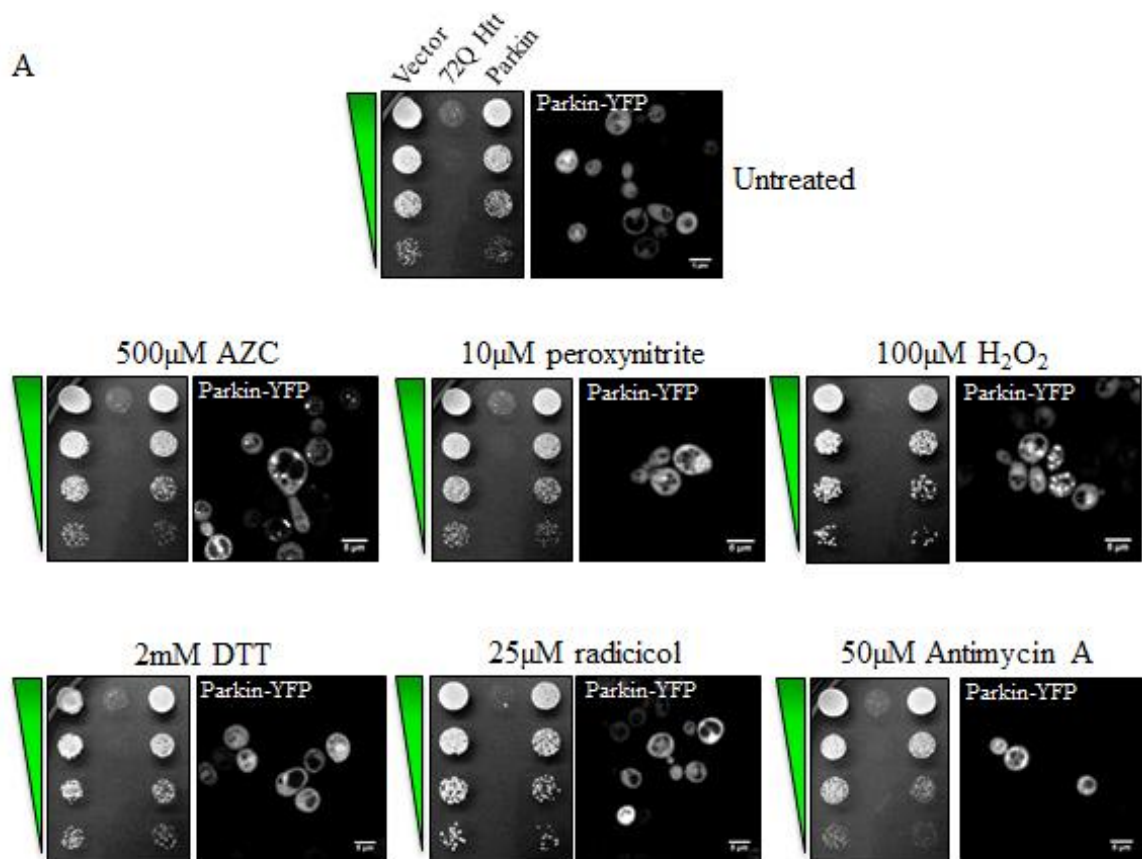


Figure 3-4. Parkin is oxidatively modified in vivo. Cell lysate from W303 (A) or various mammalian cells (B) expressing parkin (W303), transiently transfected parkin (HeLa), endogenous parkin (SH-SY5Y), or stably transfected FLAG-parkin (HEK 293) were used to perform western blots and probe for parkin. 30 μ g (A) or 80 μ g (B) of total protein from cell extracts were prepared in loading buffer with or without reducing agents (1% BME and 100mM DTT). Samples were resolved by SDS-PAGE, transferred to nitrocellulose membranes and expression of parkin was detected using immunodetection and imaged using infrared conjugated secondary antibodies. PGK1 and tubulin were used to assess equal loading for yeast or mammalian extracts respectively.

systems, and SH-SY5Y cells were selected based on their neuron-like characteristics. HeLa cells used were transiently transfected with human parkin. HEK 293 cells stably expressing parkin tagged amino (N)-terminally with the FLAG epitope (FLAG-parkin) were provided by Dr. Rylett (Robarts, Western University) and SH-SY5Y cells used express endogenous parkin. Western blots were performed with protein lysates from these three cell lines (**Figure 3-4 B**) which showed that there is a similar molecular weight shift for parkin in mammalian cells in the absence of reducing agents. This trend occurred with varying degrees of intensity, which is likely due to the various levels of parkin expression in the different cell lines and different levels of ROS. The HeLa and HEK 293 cell lines, which constitutively express parkin, showed the most significant shift in molecular weight, whereas SH-SY5Y lysates expressing endogenous parkin at lower levels showed a less significant shift.

We next sought to test the effects of adding additional stress inducing chemicals on parkin. Spotting assays and fluorescent microscopy were performed with yeast cells expressing parkin in the presence of various stress inducing chemicals (**Figure 3-5 A**). At the concentrations used in these experiments, no significant changes were seen in the growth rate of parkin expressing yeast cells, but treatment with H₂O₂ and L-Azetidine-2-carboxylic acid (AZC) caused parkin-YFP to accumulate into subcellular puncta. Western blot analysis of lysates of cells expressing parkin grown in the presence of stress inducing chemicals (**Figure 3-6**) showed no noticeable difference in parkin's migration patterns, as parkin extracted from stress-treated cells showed the same shift in molecular weight in the absence of reducing agents as seen in untreated yeast and mammalian cells (**Figure 3-4**). Treatment with two oxidative stress inducing reagents, Antimycin A and peroxynitrite,

Figure 3-5. Stress treatment alters parkin localization in yeast. (A) W303 cells used for spotting growth assays and BY cells used for fluorescent microscopy were transformed with parkin and parkin-YFP, respectively. W303 expressing parkin were spotted onto inducing media containing 500 μ M AZC, 10 μ M peroxyntirite, 100 μ M H₂O₂, 2 mM DTT, 25 μ M radicicol, or 50 μ M antimycin A. BY cells expressing parkin-YFP were grown in inducing liquid media for 8 hours containing the above drug concentrations and fluorescent images were captured using a Leica TCS SP5 II confocal microscope at 63x magnification. The scale bars represents 5 μ m. (B) W303 expressing parkin were grown in media containing 1 mM, 0.1 mM, or 0.05 mM H₂O₂ and incubating at 30°C. OD₆₀₀ measurements were taken every 15 minutes and plotted to generate a growth curve. Standard deviations did not exceed a maximum OD₆₀₀ = 0.05. At mid-log growth all samples were statistically different from the control with a P value \leq 0.0001 as determined from a One-way ANOVA.



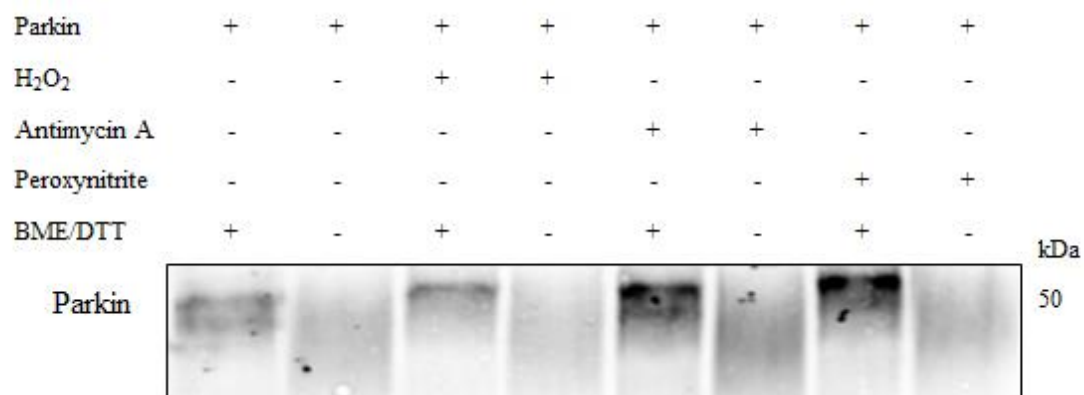


Figure 3-6. Stress treatment does not change oxidative modification of parkin in yeast.

Cell extracts from W303 expressing parkin grown in the presence of 100 μ M H₂O₂, 10 μ M peroxynitrite, or 50 μ M antimycin A were prepared in loading buffer with or without reducing agents (1% BME and 100mM DTT). Samples were resolved by SDS-PAGE, transferred to nitrocellulose membranes and expression of parkin was detected using immunodetection and imaged using infrared conjugated secondary antibodies.

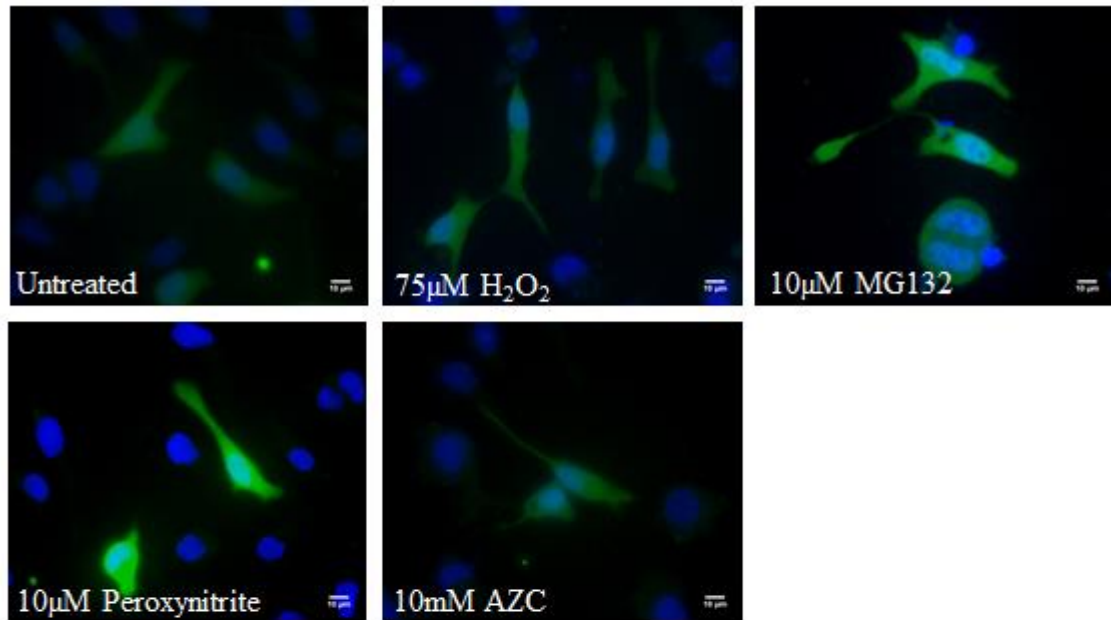
appear to cause and increase in overall parkin levels, but the experiment would need to be repeated in order to determine if this trend is statistically significant.

H₂O₂ was chosen for subsequent experiments based on its relevance to disease associated cell damage. Growth curves with increasing concentrations of H₂O₂ showed that up to a concentration of 100 μM, H₂O₂ had no effect on cell growth in the presence or absence of parkin (**Figure 3-5 B**). Increasing the concentration of H₂O₂ to 1 mM caused a slowed entry in logarithmic growth phase as well as a slower growth rate during exponential growth as indicated by the maximum slope of the curve for both control cells and cells expressing parkin. Although cell growth is affected by the increased H₂O₂ concentration, the difference between wild-type cells and cells expressing parkin did not seem to change when compared to untreated cells.

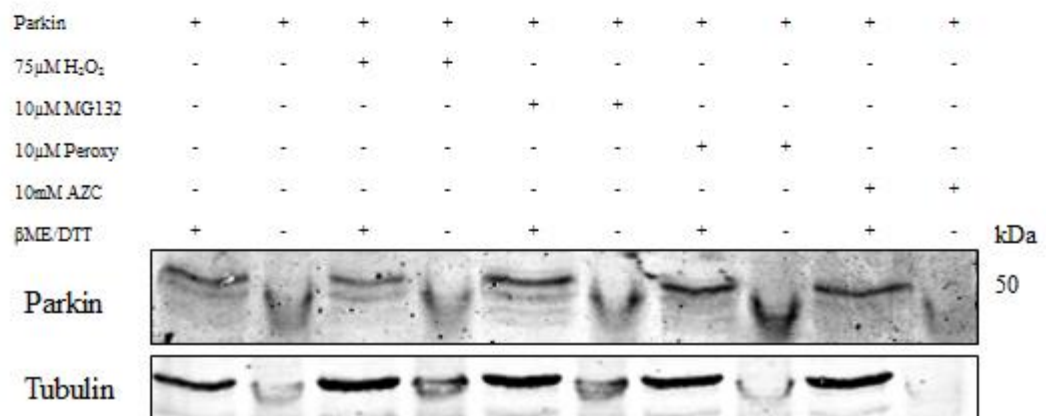
Next we tested if stress treatment would cause similar changes to parkin localization in mammalian cells. HeLa cells transiently transfected with parkin were treated with stress inducing chemicals and parkin localization was assessed using immunofluorescence microscopy (**Figure 3-7 A**). In contrast to the results found in yeast, HeLa cells treated with stress chemicals showed no change in parkin localization as we observed the same diffuse parkin localization seen in untreated cells. Western blots (**Figure 3-7 B**) showed that parkin also undergoes a molecular weight shift in the absence of reducing agents and this effect seems unchanged by the presence of stress inducing chemicals. Overall, there were only minor effects caused by stress treatment that seemed mostly exclusive to yeast. The lack of observed effects in HeLa cells could be a result of the increased capability of mammalian cells to cope with various types of cellular stress.

Figure 3-7. Parkin is unaffected by stress treatment in HeLa cells. HeLa cells transiently transfected with parkin were used to assess the effects of stress treatment on parkin in mammalian cells. After transfection, cells were given 24 hours to recover in full media before treating for 8 hours with 75 μ M H₂O₂, 10 μ M MG132, 10 μ M peroxynitrite, or 10 mM AZC. Following treatment (A) cells were passaged to 8 chamber microscopy slides and prepared for immunofluorescence imaging. Parkin was visualized using an AlexaFluor-488 conjugated secondary antibody and nuclei were stained with DAPI. Images were captured a Zeiss Axio Vert A1 Inverted fluorescent microscope using a 40x objective. Scale bars represent 10 μ m. Parkin is stained green and nuclei are stained blue. (B) Cells lysates (30 μ g total protein) were analyzed by Western blotting detecting parkin in the presence or absence of reducing agent in the loading buffer.

A



B



3.5 Subcellular Localization of Parkin Truncations and Point Mutations

Extensive experimentation has been performed to structurally characterize each of the functional domains of parkin and to determine how different domains interact and move within the entire parkin protein while executing its enzymatic activity (63, 65). Based on this knowledge, we generated functional truncation variants of parkin that we used to characterize and map changes to specific domains of the protein. Four truncation variants were generated and transformed into yeast. These variants include: 1. 141C, which has a N-terminal truncation of the first 140 residues that include the autoinhibitory Ubl domain and an unstructured linker region of approximately 70 amino acids; this parkin variant has increased activity compared to the wild-type protein and can be used to monitor how dysregulation of parkin affects misfolding and toxicity; 2. 141-409, which is similar to 141C with an additional 56 residue C-terminal truncation of the catalytic C-terminal Rcat/RING2 domain. This variant is unable to perform the catalytic transfer of ubiquitin from E2 to substrate proteins; 3. 321C, which has a 320 residue N-terminal truncation leaving only the two most C-terminal domains (Brcat/IRB and Rcat/RING2) intact. This variant is capable of ubiquitination activity, albeit with reduced efficiency; and 4. Ubl, which only has the most N-terminal 76 residues that make up the ubiquitin-like (Ubl) domain; this domain performs an autoinhibitory function within the parkin protein.

Furthermore, we employed a set of four point mutants selected based on structural and functional features of parkin. Two of these point mutants were used previously by Wen-Jie *et. al* (71). C289G and C418R, and have been identified as AR-JP causing

mutations. These parkin variants contain amino acid changes of cysteine residues that coordinate Zn^{2+} ions required for proper parkin folding (60). By altering these residues, parkin is unable to properly bind Zn^{2+} ions and loses its structural integrity, and thus has an increased propensity to misfold. These mutants were used to compare oxidative stress induced misfolding to aggregation caused by pathogenic AR-JP mutants. The other two mutations were to S65, the serine residue in parkin's Ubl domain, which is phosphorylated by PINK1 (88). The S65A mutant was used to monitor how parkin aggregation and toxicity changes in the absence of PINK1-mediated phosphorylation. The S65E mutant was used as a phospho-mimic to determine whether aggregation and toxicity was caused by S65 phosphorylation.

We first developed yeast models of all the truncation variants, testing toxicity, localization and expression. Spotting assays and growth curves revealed that all of the truncation variants caused a mild growth retardation that was identical to that caused by wild-type full-length parkin (**Figure 3-8 A and B**). Localization studies were performed with C-terminally YFP-tagged parkin truncation variants (**Figure 3-8 C and D**). Fluorescent microscopy showed that like parkin, Ubl and 321C were diffusely spread throughout the cytosol, but 141C and 141-409 had altered subcellular localization (**Figure 3-8 E**). 141C formed small subcellular puncta, similar in size and distribution to those caused by AZC or H_2O_2 treatment on parkin-YFP expressing cells (**Figure 3-5 A**) with some diffuse staining. 141-409 caused more severe changes, forming either several large or many small puncta with no diffuse staining occurring in any cells. These findings

Figure 3-8. Truncations cause subcellular accumulation of parkin without altering growth in yeast. W303 transformed with parkin truncation variants (A/B) or C-terminally YFP tagged parkin truncation variants (C/D) were used to perform growth assays. Spotting assays (A/C) were performed by growing liquid cultures of W303 to stationary phase in non-inducing selective media. Cultures were diluted to $OD_{600} = 1.0$ and serially diluted 1:5 before spotting on selective inducing agar media and incubated at 30°C for 2-4 days before imaging to assess the effects of parkin truncations with and without C-terminal YFP tags compared to wild type parkin. Growth curves (B/D) were performed by growing liquid cultures to stationary phase in non-inducing selective media. Cultures were washed twice with sterile H₂O and resuspended in inducing selective media before diluting to $OD_{600} = 0.2$ and incubating at 30°C. OD_{600} measurements were taken every 15 minutes and plotted to generate a growth curve. Standard deviations did not exceed a maximum $OD_{600} = 0.02$. At mid-log growth all samples were statistically different from the control with a P value ≤ 0.001 as determined from a One-way ANOVA • (Black) – Vector; ■ (Green) – Parkin or Parkin-YFP; ▲ (Purple) – 141C or 141C-YFP; ▼ (Blue) – 141-409 or 141-409-YFP; ◆ (Orange) – 321C or 321C-YFP; ● (Teal) – Ubl or Ubl-YFP. (E) BY transformed with N-terminally YFP tagged parkin truncation variants were grown in inducing liquid media for 8 hours and fluorescent images were captured using a Leica TCS SP5 II confocal microscope at 63x magnification. The scale bars represent 5 μ m.

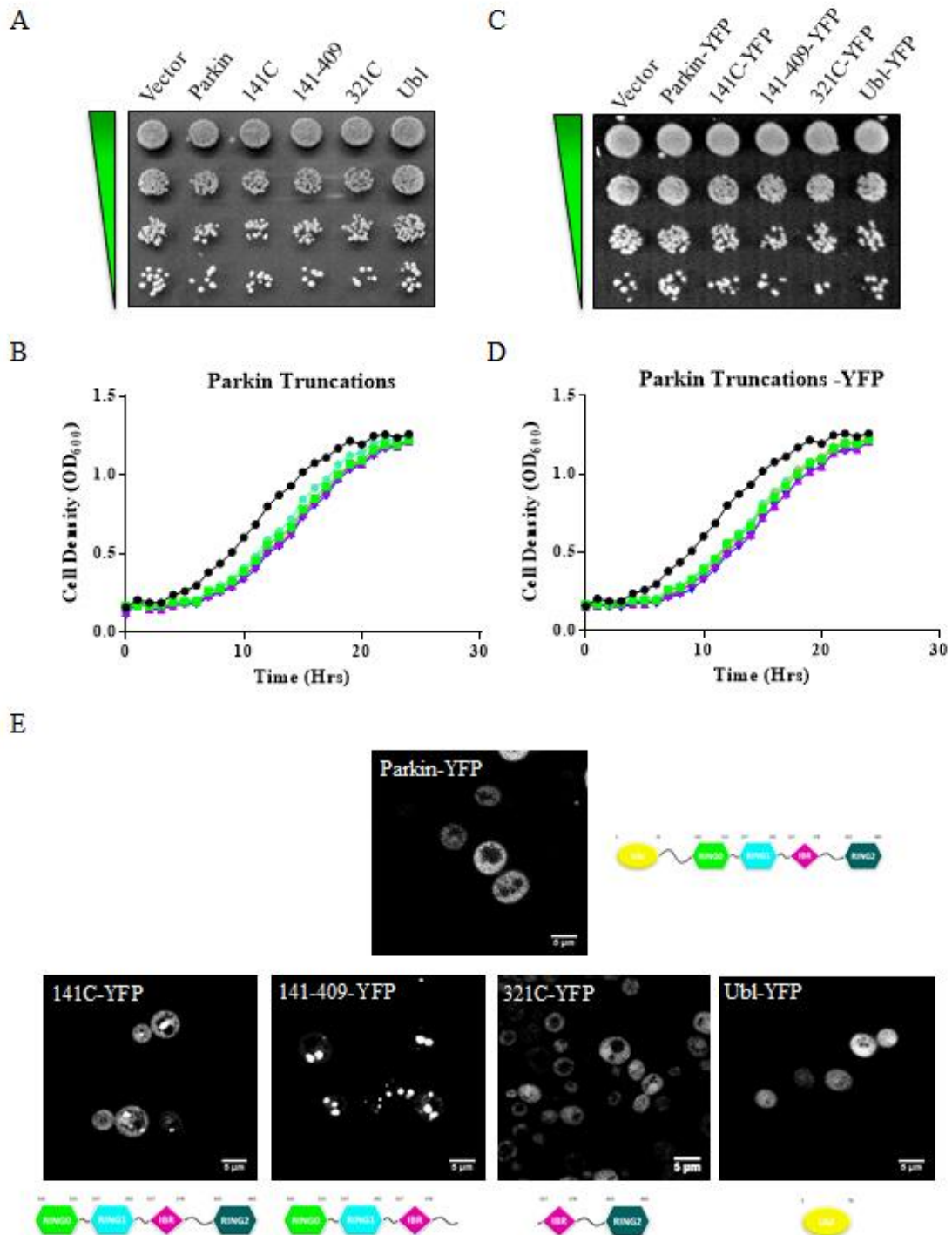
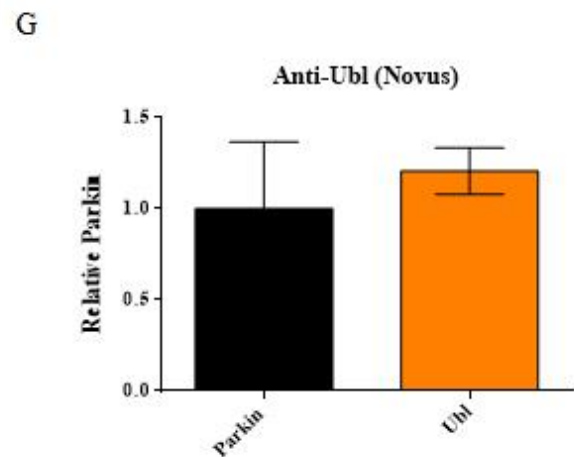
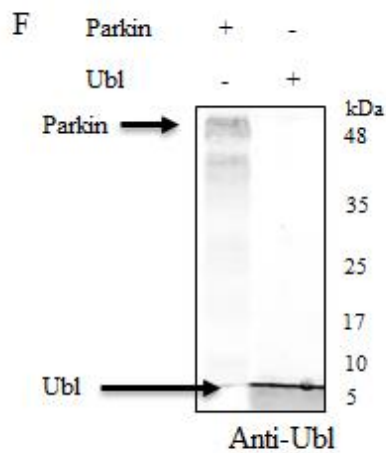
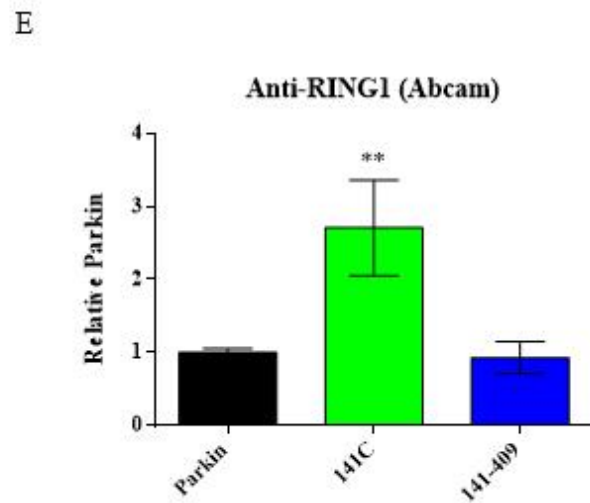
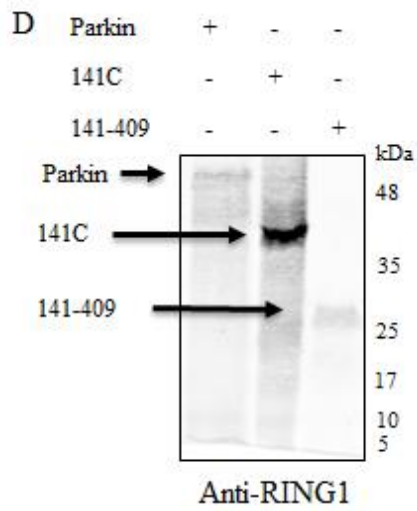
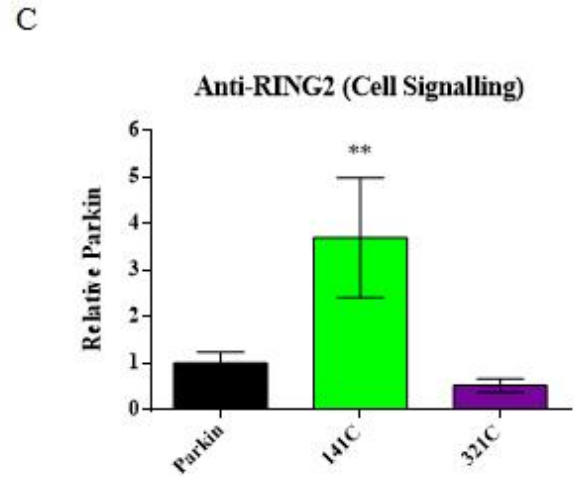
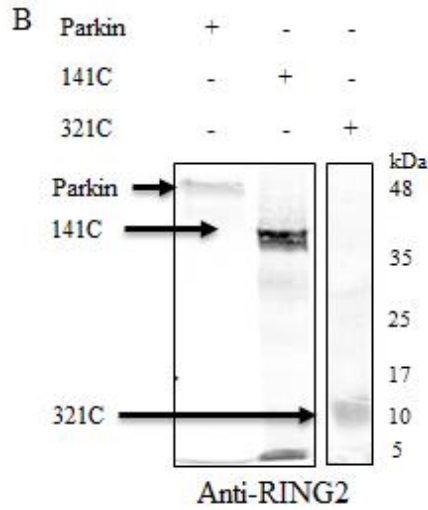
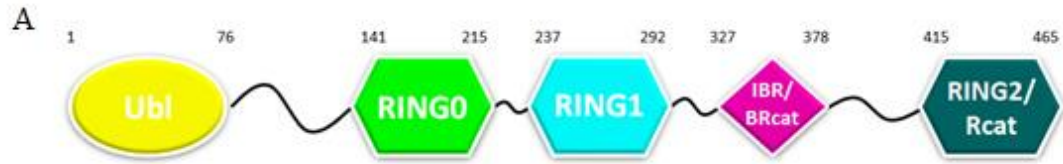


Figure 3-9. Parkin 141C truncation is expressed at higher levels than wild type parkin in yeast. (A) Schematic representation of parkin and its domains. Thirty μg total protein were used for Western blots detecting parkin. Primary antibodies with epitopes specifically recognizing various domains were used to detect parkin and the various truncation variants and compare relative expression. A RING2 specific antibody was used to detect parkin, 141C, and 321C (B), a RING 1 specific antibody was used to detect parkin, 141C, and 141-409 (D), and a Ubl specific antibody was used to detect parkin and Ubl (F). Signal intensities were measured and quantified, setting the value of wild-type parkin expression to 1. Means were compared using a one-way ANOVA (C and E) or an unpaired T-test (G). Two asterisks (**) indicates a statistical difference with a p value ≤ 0.01 . . Black – Parkin; Green – 141C; Purple – 321C; Blue – 141-409; Orange – Ubl.

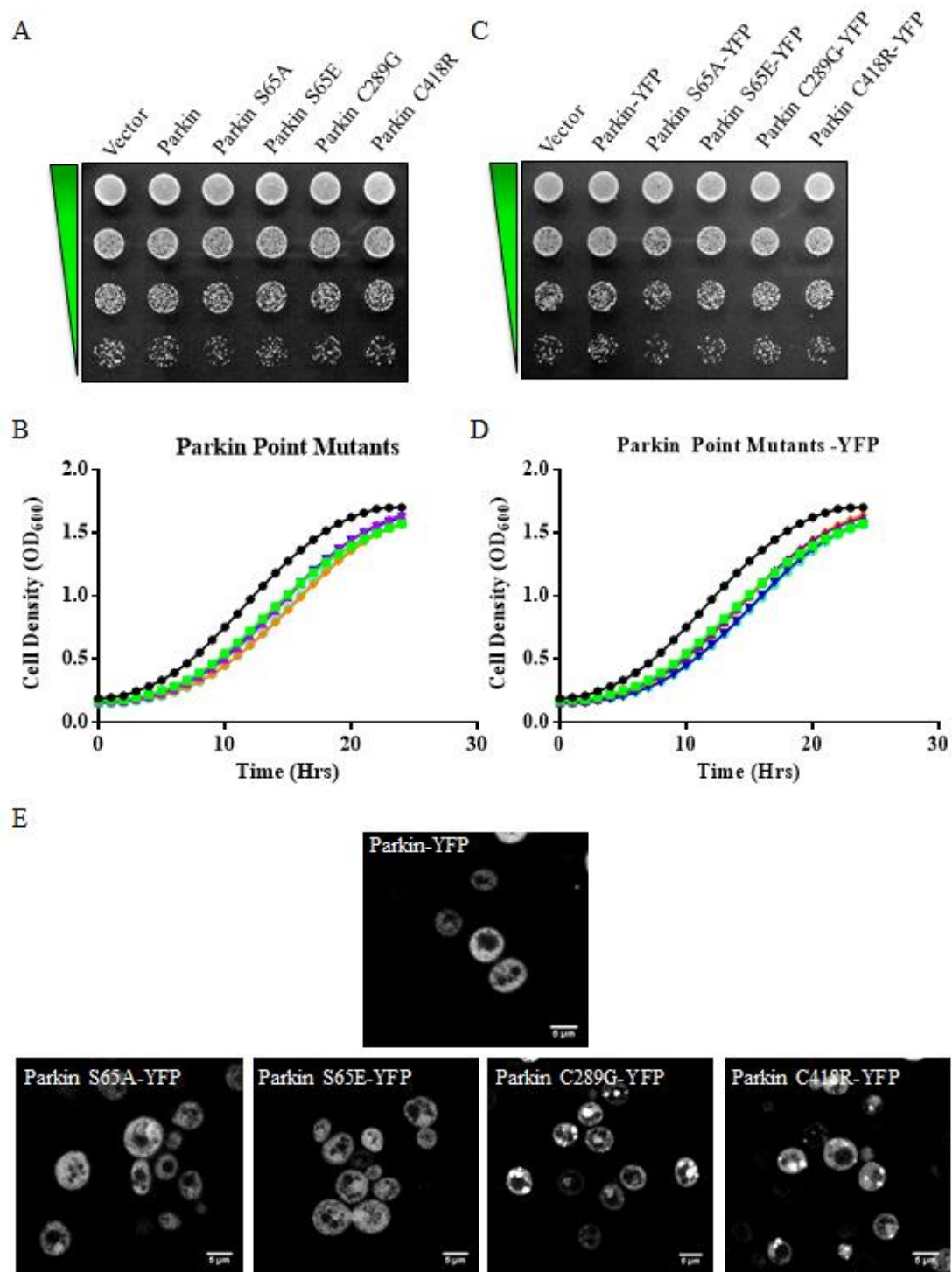


suggest that the Rcat/RING2 domain removed in the 141-409 variant plays a role in maintaining proper parkin folding and localization.

We next tested expression levels of the parkin truncation variants in yeast. Because it was not possible to compare all variants using the same antibody, three different primary anti-parkin antibodies were used to quantify the expression of the different truncation variants. In each case, the level of wild-type full length parkin expression was arbitrarily set to one, and the relative intensity of the truncation variants was compared to wild-type parkin (**Figure 3-9**). Although the α -Rcat/RING2 1° antibody (Cell Signalling) yielded approximately a three-fold stronger signal than the α -RING1 1° antibody (Abcam) for wild-type parkin using the same lysates (data not shown), in both cases, nearly three times more 141C was expressed than wild-type parkin (**Figure 3-9 C and E**). The three remaining truncation variants were expressed at relatively similar levels to wild-type full-length parkin (**Figure 3-9 C, E, and G**).

We then performed the same set of experiments to test the four parkin point mutants. All four point mutants had the same growth phenotypes as wild-type parkin in the presence or absence of C-terminal YFP tags, showing only mild growth restriction (**Figure 3-10 A, B, C, and D**). Fluorescent microscopy revealed that the C289G and C418R mutants formed subcellular aggregates (previously shown in mammalian cells (71)), but both S65 mutants showed diffuse cytosolic localization (**Figure 3-10 E**). The aggregates formed by the C289G and C418R mutants resemble those formed by the 141C variant (**Figure 3-8 E**), forming one or more small puncta per cell with some diffuse staining still occurring. Analysis of expression levels showed that all four point mutants had similar expression levels compared to wild type parkin (**Figure 3-11 A and B**). Only

Figure 3-10. Parkin point mutants are non-toxic but alter parkin localization and expression levels in yeast. W303 cells expressing parkin point mutants (A and B) or C-terminally YFP tagged parkin point mutants (C and D) were used for growth assays. Spotting assays (A and C) were performed to assess the effects of parkin truncations with and without C-terminal YFP tags compared to wild type parkin. Growth curves (B and D) were performed by growing in inducing selective at 30°C. OD₆₀₀ measurements were taken every 15 minutes and plotted to generate a growth curve. Standard deviations did not exceed a maximum OD₆₀₀ = 0.05. At mid-log growth all samples were statistically different from the control with a P value ≤ 0.01 as determined from a One-way ANOVA. Samples tested were; ● (Black) Vector, ■ (Green) Parkin/Parkin-YFP, ▲ (Purple) Parkin S65A/Parkin S65A-YFP, ▼ (Blue) Parkin S65E/Parkin S65E-YFP, ◆ (Orange) Parkin C289G/Parkin C289G-YFP; and ● (Teal) Parkin C418R/Parkin C418R-YFP. (E) BY cells expressing C-terminally YFP tagged parkin point mutants were grown in inducing liquid media for 8 hours and fluorescent images were captured using a Leica TCS SP5 II confocal microscope at 63x magnification. The scale bars represents 5µm.



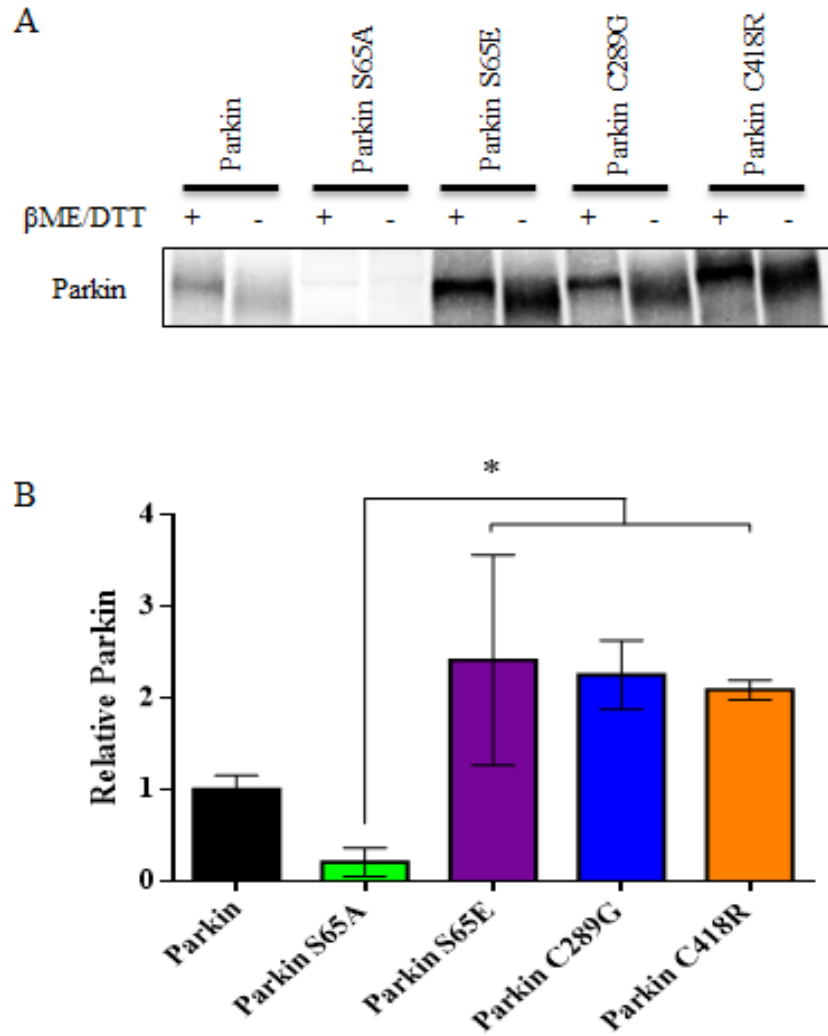


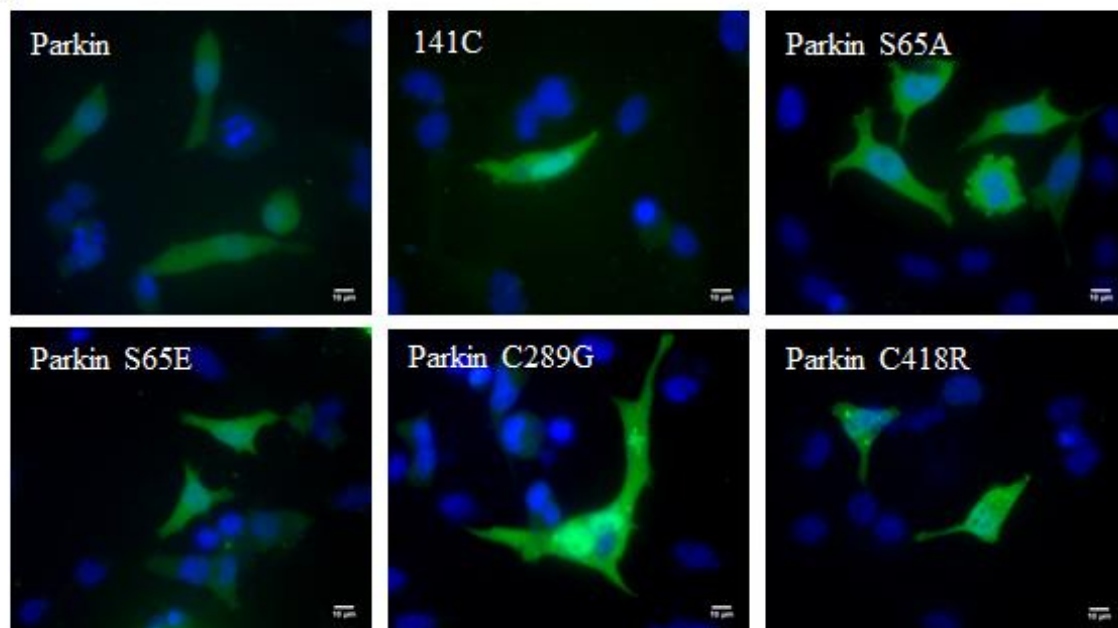
Figure 3-11. Point mutations change parkin levels in yeast. (A) 30 μ g total protein of cell extracts from W303 transformed with parkin or parkin point mutants were resolved by SDS-PAGE, transferred to a nitrocellulose membrane and expression was detected using immunodetection and imaged using infrared conjugated secondary antibodies. Samples were run in triplicate, quantified, and graphed (B) setting the value of wild type parkin expression to 1. Means were compared using a one-way ANOVA. An asterisk (*) indicates statistical difference with a p value ≤ 0.05 . Black – Parkin; Green – Parkin S65A; Purple – Parkin S65E; Blue – Parkin C289G; Orange – Parkin C418R.

the decreased level of the S65A mutant and the increased amount of the S65E, C289G and C418R mutants were statistically significant.

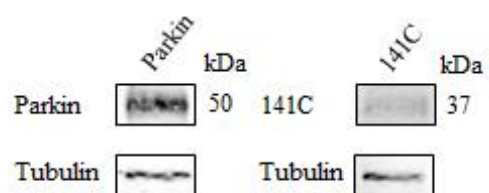
We next tested the expression of the parkin truncation variants and point mutants in mammalian cells to test if any of these results were artefacts caused by parkin expression in yeast, as shown for chemical stress treatment of parkin (**Figure 3-7**). Due to technical issues with strong background signals, the 141-409, 321C, and Ubl truncation variants could not be detected though immunofluorescence microscopy in transfected HeLa cells. Despite extensive testing and protocol adjustments, all four different parkin antibodies tested here showed significant background staining in untransfected HeLa cell that express no endogenous parkin (Appendix 3). Additionally, only the Rcat/RING2 primary antibody was able to detect parkin in Western blots, so the following experiments were performed with only the parkin point mutants and the 141C variant. Immunofluorescence microscopy staining revealed that 141C, S65A and S65E, like wild type parkin, were cellular diffuse, and the C289G and C418R mutants formed subcellular aggregates as previously shown (71) (**Figure 3-12 A**). Western blots of transfected cell lysates showed that, in contrast to results in yeast, 141C is expressed at significantly lower levels than parkin (**Figure 3-12 B and C**). Similarly, the S65A point mutant, that had lower expression in yeast, was expressed at nearly four-fold higher levels than wild-type parkin in transfected HeLa cells (**Figure 3-12 D and E**). Similarly, the S65E point mutant was expressed at even higher levels than S65A, suggesting that modification of the Ubl domain plays a significant role in parkin expression and stability in mammalian cells. In contrast, the expression levels of the two parkin cysteine mutants were similar to wild-type parkin (**Figure 3-12 D and E**).

Figure 3-12. Parkin point mutants and truncations have altered expression and cellular localization in HeLa cells. HeLa cells transiently transfected with parkin, parkin truncation variants, or parkin point mutants were used to assess the effects of parkin alterations in mammalian cells. After transfection, cells were given 24 hours to recover in full media before further treatment. (A) Transfected HeLa cells were passaged to 8 chamber microscopy slides and prepared for immunofluorescence imaging. Parkin, 141C, and four parkin point mutants were immunodetected with a RING2 specific primary antibody and subsequently visualized using an AlexaFluor-488 conjugated secondary antibody. Cell nuclei were stained with DAPI. Images were captured a Zeiss Axio Vert A1 Inverted fluorescent microscope using a 40x objective. Scale bars represent 10 μ m. Parkin, 141C, and parkin point mutants are stained **green**, nuclei are stained **blue**. (B and D) Cells used for Western blotting were washed and lysed before resolving 30 μ g total protein by SDS-PAGE. Samples were run in triplicate and signal intensities were quantified relative to the tubulin loading control and graphed (C and E), setting wild-type parkin levels to 1. Means were compared using an unpaired T-test (C) or a one-way ANOVA (E). Two, three, or four asterisks (**/***/****) indicates a statistical difference with a p value ≤ 0.01 , ≤ 0.001 , or ≤ 0.0001 , respectively. Tubulin was used to assess equal loading. . Black – Parkin; **Green** – 141C; **Purple** – Parkin S65A; **Blue** – Parkin S65E; **Orange** – Parkin C289G; **Teal** – Parkin C418R.

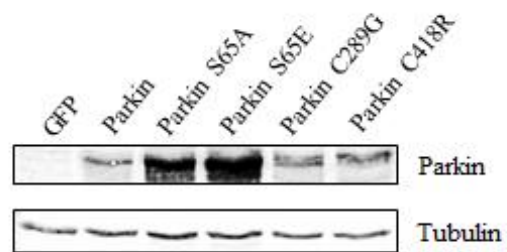
A



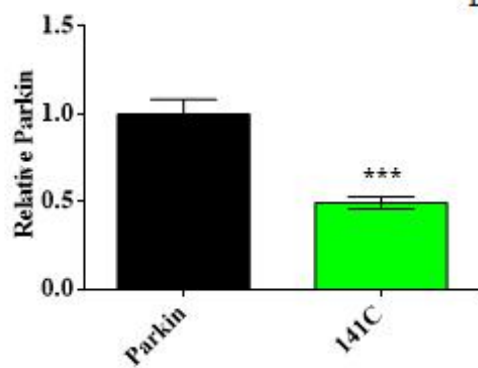
B



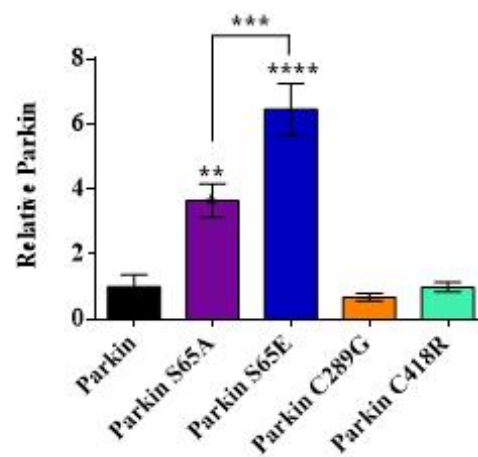
D



C



E



In summary, modification of key cysteine residues involved in zinc ion coordination (C289G and C418) significantly affected parkin solubility in both yeast and mammalian cells. Modification of S65 did not seem to affect parkin localization but had variable effects on expression in yeast and mammalian cells. 141C caused parkin aggregation and increased expression in yeast but had no effect on localization and showed reduced expression in HeLa cells.

3.6 PINK1 Modulates Parkin Localization, Toxicity, and Stability

With the recent explosion of literature focused on the relationship between parkin and PTEN-induced putative kinase 1 (PINK1), we next decided to study the effects of co-expressing these two proteins in yeast. Most of the parkin/PINK1 related literature focuses on how PINK1 activates parkin and the ensuing ubiquitination and turnover of damaged mitochondria (mitophagy). In contrast, our study aimed to explore PINK1 as a modifier of parkin folding and stability, and thereby determine how the addition of PINK1 affects parkin localization, expression, degradation, and toxicity.

Unlike most proteins, expression of the human form of PINK1 in yeast would not allow for proper function of the protein because human PINK1 appears to be degraded rapidly in yeast. Many studies suggest that PINK1 is anchored to the mitochondria via an N-terminal leader sequence that directs the protein to the mitochondrial membrane after translation (77). Unfortunately, this leader sequence is human-specific, and would not properly transport PINK1 to the mitochondria in yeast. A modified PINK1 clone containing a yeast specific N-terminal outer mitochondrial protein (OMP) leader sequence and a C-terminal FLAG tag was generously provided to us by our collaborator Dr. Endo (Kyoto

Sangyo University). This template was used to clone PINK1 into yeast vectors for expression in our model system. Also, the kinase activity of PINK1 was eliminated by mutating two key aspartic acid residues to alanine (D3682A and D384A). We used these mutations to create a kinase dead (KD) PINK1 mutant by mutagenic PCR and subsequently cloned into yeast expression vectors as a control.

3.6.1 *Co-expression of PINK1 and Parkin in Yeast*

These yeast specific PINK1 and KD PINK1 clones were co-expressed with parkin and the parkin truncation variants to test for toxicity (**Figure 3-13**). Interestingly, in yeast, PINK1 expression caused a mildly toxic phenotype on its own (**Figure 3-13 A lane 2**) which does not occur with the KD PINK1 mutant (**Figure 3-13 E lane 2**). When co-expressed with PINK1, wild-type parkin caused a severe toxic phenotype, almost completely inhibiting growth (**Figure 3-13 A lane 3**). Although parkin and PINK1 on their own caused only mild or slightly more severe growth inhibition, respectively, the co-expression of both had drastically increased (i.e. synergistic) growth inhibition. Interestingly, co-expression of PINK1 with the parkin truncation variants still exhibit artificial toxicity, even when expressed with variants lacking S65, including 141C, which is the site of PINK1 mediated phosphorylation of parkin (**Figure 3-13 A and B**).

PINK1 was then co-expressed with parkin-YFP and C-terminally YFP-tagged truncation variants (**Figure 3-13 C and D**) which showed a similar growth phenotype as their untagged counterparts with PINK1 and parkin-YFP causing the most significant toxicity, and reduced toxicity when PINK1 is co-expressed with 141C-YFP. In all cases, the addition of a C-terminal YFP tag slightly reduced the growth defect compared to their

Figure 3-13. Co-expression of parkin and PINK1 causes toxicity in yeast. W303 expressing PINK1-FLAG (A, B, C, and D) or kinase dead (KD) PINK1-FLAG (E and F) and parkin truncation variants (A, B, E, and F) or C-terminally YFP tagged parkin truncations (C and D) were used to perform growth assays. Spotting assays (A/C/E) were performed to assess the effects of parkin truncations with and without C-terminal YFP tags compared to wild type parkin in the presence of PINK1 or KD PINK1. Growth curves (B, D, and F) were performed by growing in inducing selective media at 30°C. OD₆₀₀ measurements were taken every 15 minutes and plotted to generate a growth curve. Standard deviations did not exceed a maximum OD₆₀₀ = 0.02. At mid-log growth all samples were statistically different from the control with a P value ≤ 0.01 as determined from a One-way ANOVA. The constructs tested were; ● (Black) Vector, ■ (Green) PINK1/KD PINK1, PINK1/KD PINK1 with ▲ (Purple) Parkin/Parkin-YFP, ▼ (Blue) 141C/141C-YFP, ◆ (Orange) 141-409/141-409-YFP, ● (Teal) 321C/321C-YFP, and ■ (Red) Ubl/Ubl-YFP.

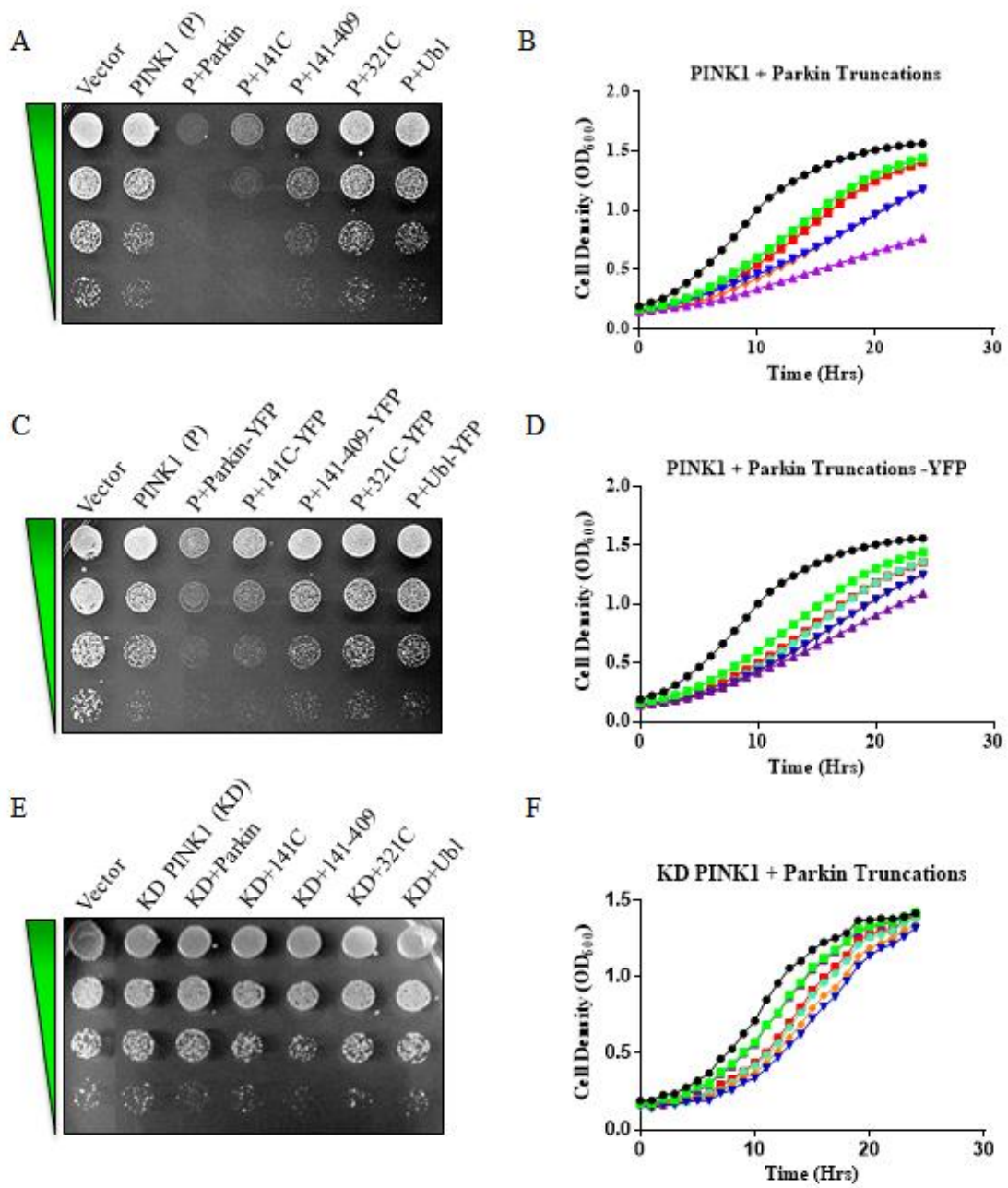
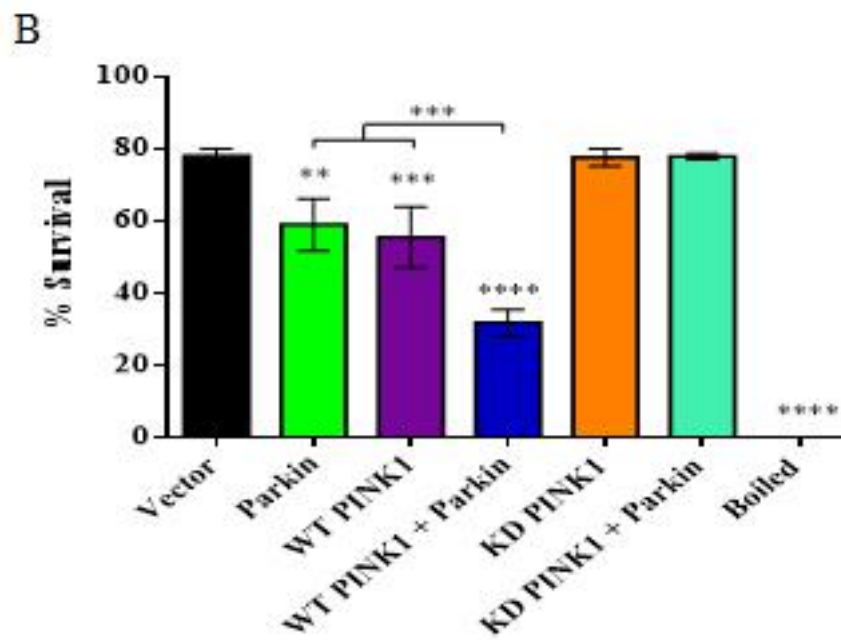
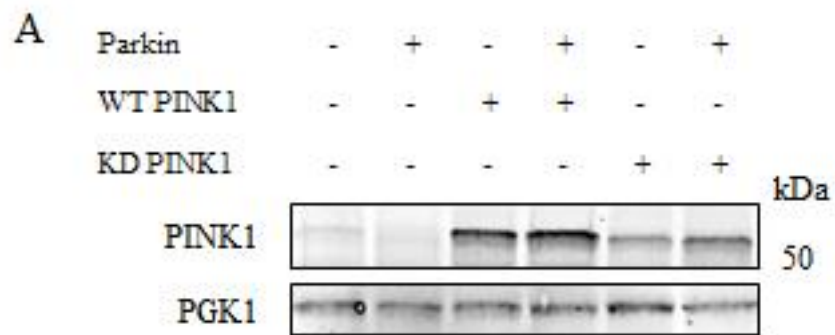


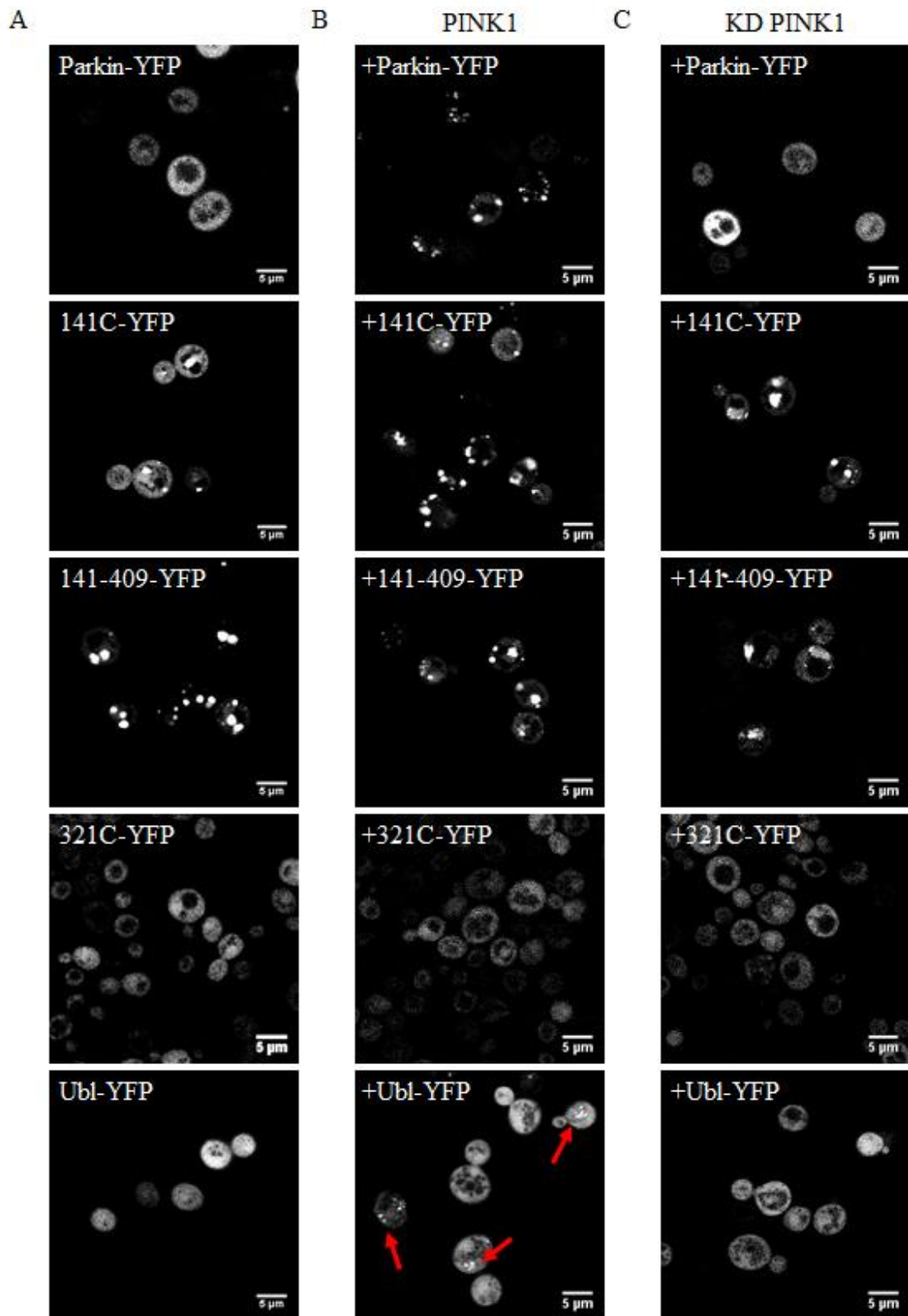
Figure 3-14. Co-expression of parkin and PINK1 causes yeast cell death. (A) Western blot using 30µg total protein of cell extracts from W303 expressing parkin, parkin and PINK1-FLAG, or parkin and KD PINK1-FLAG were probed with an anti-parkin antibody. PGK1 was used to assess equal loading. (B) SYTOX Green cell death assay was used to assess cell death from the co-expression of parkin with wild-type or KD PINK1 based on the dye's inability to enter live cells. After 8 hour of induction, cultures were incubated with SYTOX Green dye and emission was measured that was correlate to cell death. Values were corrected to culture density. Samples were run in triplicate, quantified, and graphed setting a boiled control to 100% cell death. Two, three, or four asterisks (**/***/****) indicate a statistical difference with a p value ≤ 0.05 , ≤ 0.001 , or ≤ 0.0001 respectively. Black – Vector; Green – Parkin; Purple – PINK1; Blue – PINK1 + Parkin; Orange – KD PINK1; Teal – KD PINK1 + Parkin; ■ Red – Boiled.



untagged counterparts. Co-expression of parkin and the parkin truncation variants with KD PINK1 were all non-toxic (**Figure 3-13 E and F**), suggesting that this toxic effect is dependent on the kinase activity of PINK1. We then ensured that wild-type (WT) and KD PINK1 were expressed properly in yeast. Western blots of yeast cell expressing WT or KD PINK1 in the absence and presence of parkin showed that PINK1 was stably expressed in yeast, but the KD mutant seemed to be expressed at lower levels than WT PINK1 (**Figure 3-14 A**).

To test whether the toxic effects caused by PINK1/parkin co-expression were based on growth inhibition or cell death, a SYTOX® Green based assay was used (**Figure 3-14 B**). SYTOX® Green is a nuclear stain that is membrane impermeable and can only enter dead cells. As shown above (**Figure 3-2 A and B and Figure 3-13 A and B**), parkin and PINK1 independently cause mild growth defects. The SYTOX® assay revealed that this defect is actually cell death, each resulting in approximately 75% viability compared to the control. The co-expression of the two proteins caused even more cell death showing approximately 45% viability compared to the control. Given that parkin and PINK1 independently cause about 25% cell death each, these results suggest that the amount of cell death caused by their co-expression is proportional to the combinatorial effects of the two. This contrasts our result seen in **Figure 3-13 A and B** in which PINK1/parkin toxicity appears to be synergistic, almost completely inhibiting growth. These findings would suggest that PINK1/parkin co-expression causes cell death while simultaneously inhibiting growth of viable yeast cells. As expected, expression of KD PINK1 causes no additional cell death compared to the control, but its co-expression with

Figure 3-15. PINK1 causes parkin accumulation in yeast. BY cells expressing parkin-YFP or C-terminally YFP tagged parkin truncations in the absence (As shown above in Figure 3-8) and presence of (B) PINK1 or (C) KD PINK1. Cells were grown in inducing liquid inducing media for 8 hours and fluorescent images were captured using a Leica TCS SP5 II confocal microscope at 63x magnification. The scales bar represent 5 μ m.



parkin eliminated the cell death caused by parkin alone, suggesting that KD PINK1 protects yeast from parkin toxicity.

We next performed fluorescent microscopy to test if PINK1 co-expression caused changes to parkin localization (**Figure 3-15**). The addition of PINK1 caused parkin-YFP to form subcellular aggregates and almost completely eliminated any diffuse parkin staining from the cytosol. Since 141C-YFP and 141-409-YFP already formed subcellular aggregates on their own, co-expression with PINK1 did not have an effect on their localization. 321C-YFP localization was also unaffected from the co-expression with PINK1 which is not surprising because PINK1 does not interact with or phosphorylate any residues within this parkin truncation. However, the co-expression of PINK1 did cause a subtle change to Ubl-YFP localization, causing the formation of extremely small fluorescent foci in a small number of cells.

Since PINK1 caused such a significant change in parkin localization, we next tested if parkin aggregates caused by the introduction of PINK1 had amyloid-like biophysical properties, such as robust insolubility in the presence of potent detergents. To test this, semi-denaturing detergent agarose gel electrophoresis (SDD AGE) was used (**Figure 3-16**). This technique utilizes mild lysis conditions in attempts to preserve subcellular aggregates. Protein samples are run through agarose with low sodium dodecyl sulfate (SDS) content, instead of polyacrylamide gel, where large amyloid-like complexes remain intact and run through the gel very slowly. This results in a high molecular weight species for insoluble, amyloid-like protein aggregates, as seen with the polyQ-expanded huntingtin protein (72Q) which was used as a positive control.

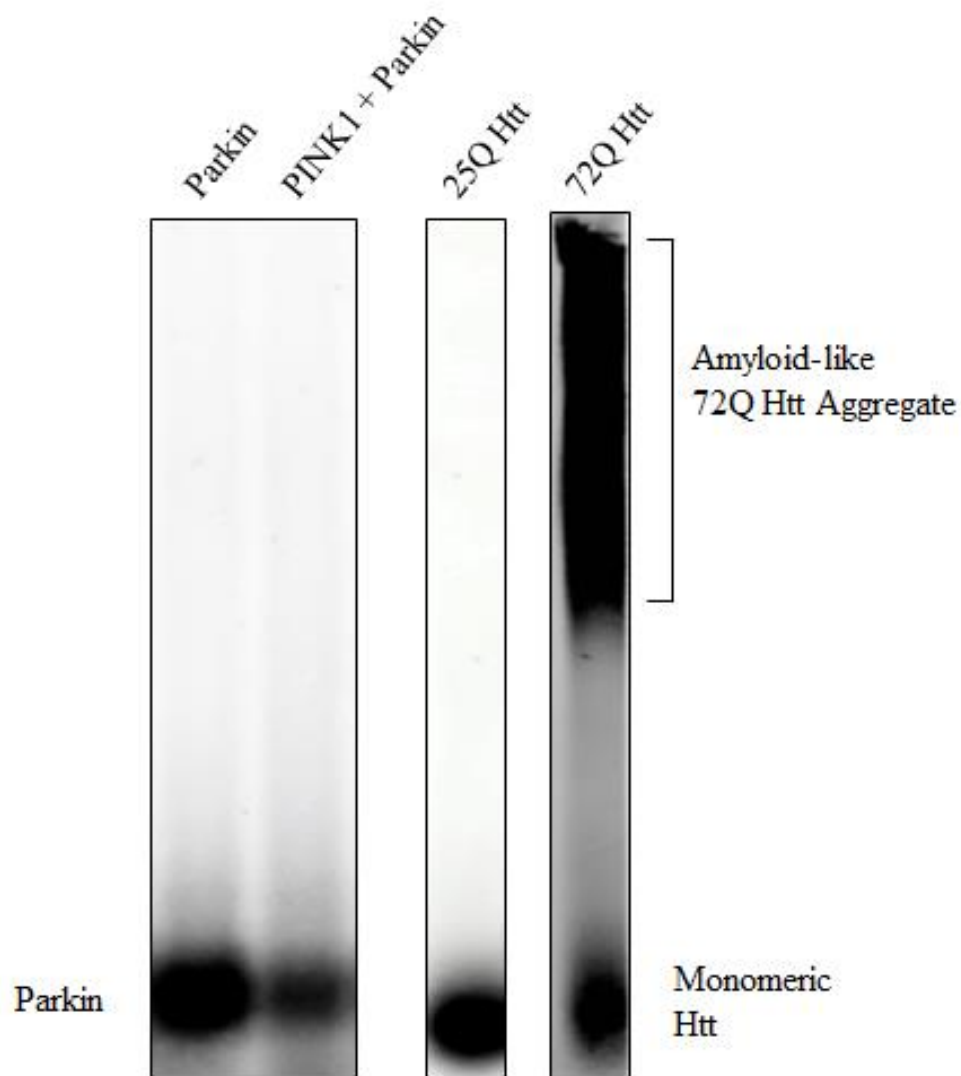


Figure 3-16. PINK1 induced parkin aggregates are not amyloid-like. 30 μ g total protein of cell extracts from W303 expressing parkin, or parkin and PINK1 were resolved by semi-denaturing detergent agarose gel electrophoresis (SDD AGE), transferred to nitrocellulose membranes via capillary force and expression of parkin was detected using immunodetection and imaged using infrared conjugated secondary antibodies. 25Q and 72Q huntingtin lysates were used as controls to show non amyloid-like and amyloid-like aggregation respectively.

In contrast, soluble, non-amyloid-like proteins run migrate through the gel as a monomer and show a single band at the expected molecular weight, as seen with the non-expanded huntingtin protein (25Q) which was used as a negative control. Despite testing several lysis and running conditions, as well as H₂O₂ treated parkin samples (data not shown), we did not detect amyloid-like protein aggregates composed of parkin in cells co-expressing parkin and PINK1.

We next tested how point mutations within parkin would affect PINK1 induced growth phenotypes in yeast. Growth assays were performed using WT and KD PINK1 co-expressed with the four parkin point mutants. All four of the point mutants showed significantly reduced toxicity compared to wild-type parkin (**Figure 3-17 A and B**). The results from spotting assays and growth curve assays were somewhat contradictory, as spotting assays performed on solid agar media showed strong reduction of toxicity (**Figure 3-17 A**), whereas growth curves performed in liquid media showed that the point mutants, when co-expressed with PINK1, are still more toxic than PINK1 alone (**Figure 3-17 B**). This discrepancy might be caused by the different growth patterns of yeast in liquid and on solid media. Results from spotting assays typically represent a later time point in the yeast growth cycle where the point mutants co-expressed with PINK could have caught up to cells expressing PINK1 alone. In both cases, wild-type parkin was significantly more toxic than all of the point mutants when expressed with PINK1, implying that the interaction of PINK1 and parkin is altered by parkin point mutations. Again, co-expression of the point mutants with the KD PINK1 abolished all toxicity (**Figure 3-17 C and D**).

Figure 3-17. PINK1/parkin toxicity is rescued by parkin point mutations. W303 cells expressing PINK1-FLAG (A and B) or kinase dead (KD) PINK1-FLAG (C and D) and parkin point mutants (A, B, C, and D) were used to perform growth assays. Spotting assays (A/C) were performed by growing on selective inducing agar media to assess the effects of parkin truncations with and without C-terminal YFP tags compared to wild type parkin in the presence of PINK1 or KD PINK1. Growth curves (B and D) were performed by growing liquid cultures in inducing selective media at 30°C. OD₆₀₀ measurements were taken every 15 minutes and plotted to generate a growth curve. Standard deviations did not exceed a maximum OD₆₀₀ = 0.02. At mid-log growth all samples were statistically different from the control with a P value ≤ 0.05 as determined from a One-way ANOVA. Samples tested were; ● (Black) Vector, ■ (Green) PINK1/KD PINK1, PINK1/KD PINK1 with ▲ (Purple) Parkin, ▼ (Blue) Parkin S65A, ◆ (Orange) Parkin S65E, ● (Teal) Parkin C289G, and ■ (Red) Parkin C418R.

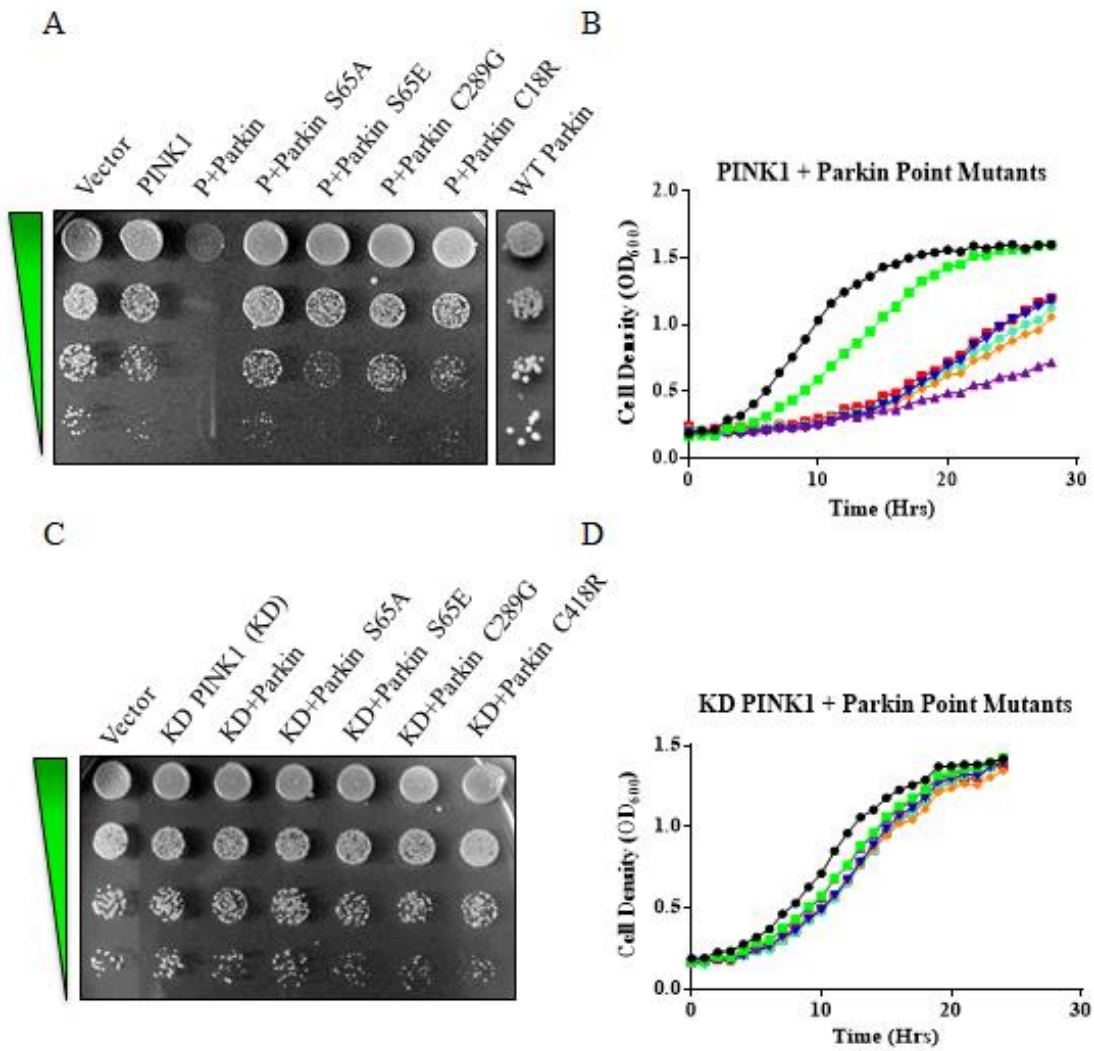


Figure 3-18. PINK1 mildly affects localization of mutant forms of parkin in yeast. BY cells expressing parkin-YFP or C-terminally YFP tagged parkin point mutants in the absence (As shown above in Figure 3-10) and presence of (B) PINK1 or (C) KD PINK1 were grown in inducing liquid media for 8 hours and fluorescent images were captured using a Leica TCS SP5 II confocal microscope at 63x magnification. The scales bar represent 5 μ m.

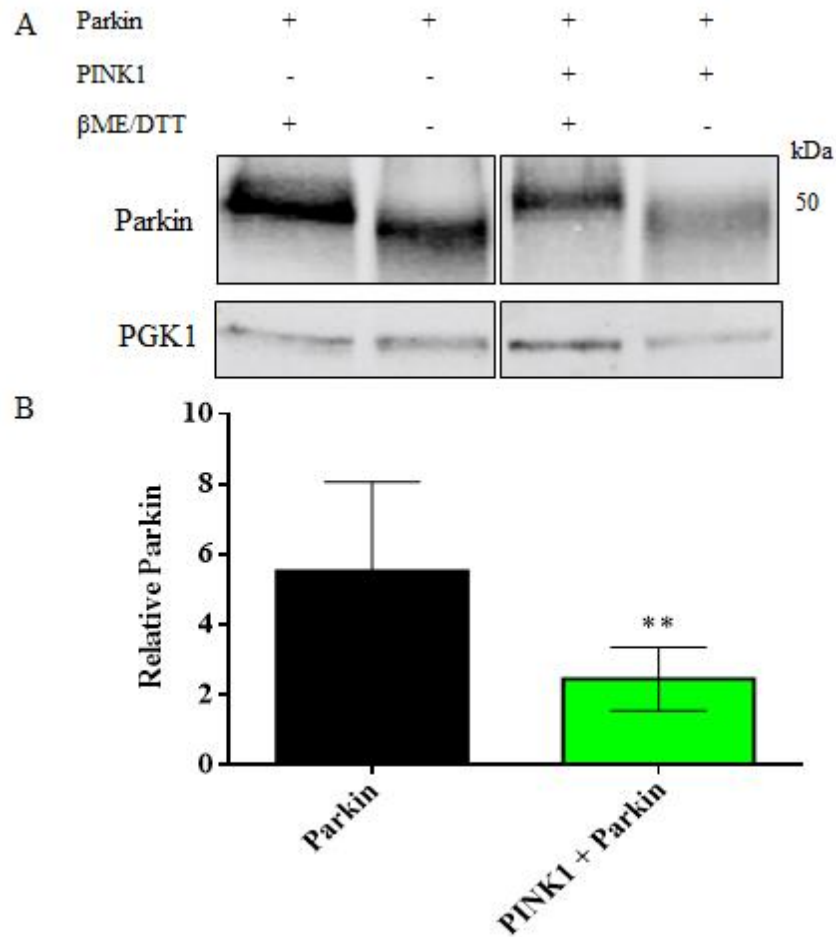


Figure 3-19. Parkin levels are decreased upon co-expression with PINK1 in yeast. (A) 30 μ g total protein of cell extracts from W303 expressing parkin or parkin and PINK1 were resolved by SDS-PAGE, transferred to nitrocellulose membranes and expression of parkin was detected using immunodetection and imaged using infrared conjugated secondary antibodies. (B) Parkin signal intensities from n=11 samples were measured and quantified relative to the PGK1 loading control and parkin levels in cells not co-expressing PINK1 was set to 1. Means were compared using an unpaired T-test and two asterisks (**) indicates a statistical difference with a p value ≤ 0.001 . PGK1 was used to assess equal loading. Black – Parkin; Green – PINK1 + Parkin.

Florescent microscopy was also performed with cells co-expressing the parkin point mutants and WT or KD PINK1 (**Figure 3-18**). We observed mild changes in the localization of parkin S65A and S65E mutants, which formed one to two puncta in a small proportion of cells. The drastically reduced effects on parkin localization caused by point mutations also suggest the PINK1/parkin interaction is modified by parkin point mutations.

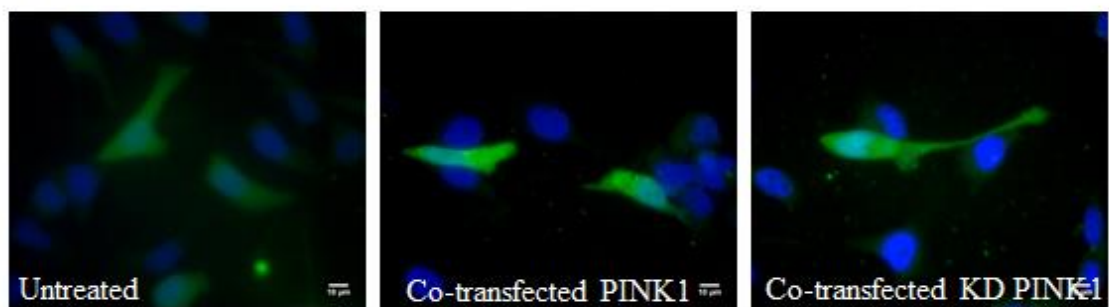
While testing the effects of co-expressing parkin and PINK1, we noticed that the levels of parkin being expressed in the presence of PINK1 seemed to be reduced compared to cells expressing parkin alone. Western blots were performed with protein lysates from yeast cells expressing parkin and co-expressing parkin and PINK1 using different combinations of protease inhibitors, and run in the presence and absence of reducing agents (**Figure 3-19 A**). The levels of parkin in cells co-expressing parkin and PINK1 were reduced by almost two and a half fold compared to cells expressing parkin alone (**Figure 3-19 B**).

3.6.2 Co-expression of PINK1 and Parkin in Mammalian Cells

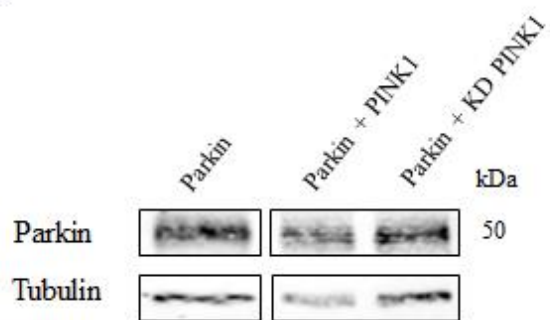
Since the expression of wild type parkin with PINK1 had the most drastic effects in yeast, we decided to focus on this interaction in mammalian cells. HeLa cells transfected with parkin, co-transfected with parkin and PINK1, or co-transfected parkin and KD PINK1 were analyzed for parkin localization and stability (**Figure 3-20**). Immunofluorescence microscopy revealed that the co-expression of parkin with WT PINK1 caused no changes in parkin localization, as parkin staining remained diffuse (**Figure 3-20 A**). This result is consistent with the literature which shows that cells endogenously expressing parkin and PINK1 do not show altered parkin localization

Figure 3-20. Co-expression of PINK1/parkin in HeLa cells. HeLa cells transiently transfected with parkin, parkin and PINK1, or parkin and kinase-dead (KD) PINK1 were used to assess the effects PINK1 on parkin localization and stability in mammalian cells. After transfection, cells were given 24 hours to recover in full media before further treatment. (A) Transfected HeLa cells were passaged to 8 chamber microscopy slides and prepared for immunofluorescence imaging. Parkin was visualized using an AlexaFluor-488 conjugated secondary antibody and nuclei were stained with DAPI. Images were captured on a Zeiss Axio Vert A1 Inverted fluorescent microscope using a 40x objective. Scale bars represent 10µm. Parkin is shown in **green** and nuclei are shown in **blue**. (B) Cell lysates of HeLa transfected with the indicated constructs were used for Western blotting detecting parkin and tubulin as a loading control (C) Parkin signal intensities were measured and quantified relative to the tubulin loading control and graphed. Parkin levels in non-co-transfected cells was set to 1. Means were compared using a one-way ANOVA. Black – Parkin; **Green** – PINK1 + Parkin; **Purple** – KD PINK1 + Parkin.

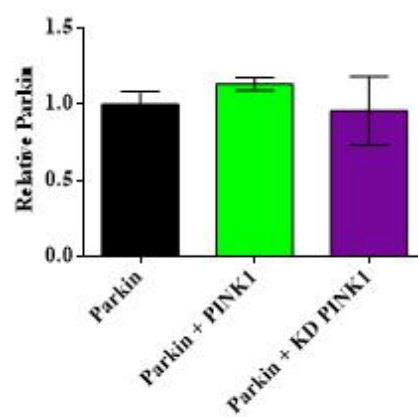
A



B



C

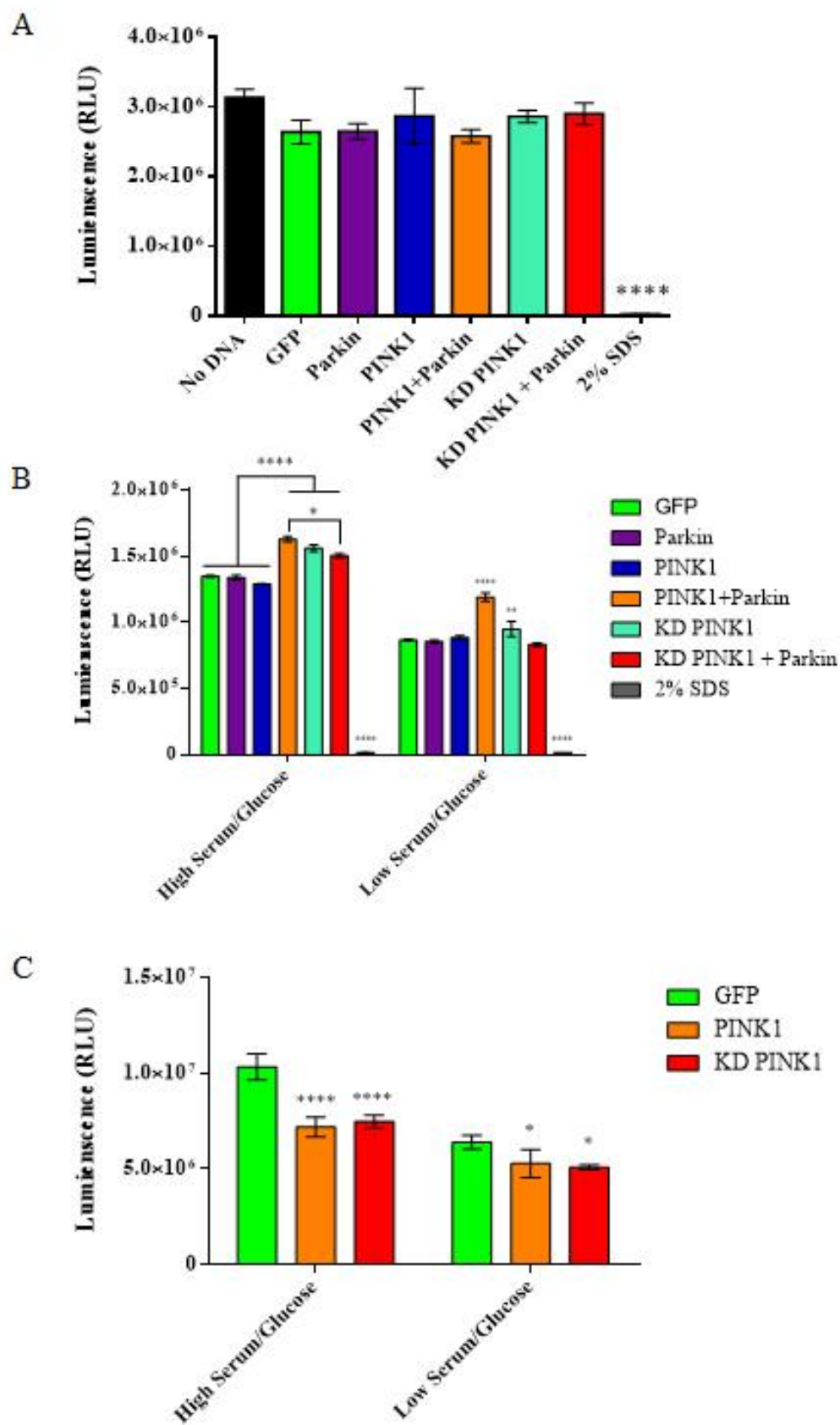


unless they are treated with the mitochondrial uncoupling agent CCCP (83) which causes the production of excessive amounts of ROS. Western blots were performed with lysates from these cells and quantification yet again revealed no changes in response to co-expression of parkin and PINK1 (**Figure 3-20 B and C**).

Our next goal was to test whether PINK1/parkin co-expression caused toxicity in mammalian cells. For these experiments, both HeLa and HEK 293 cell lines were used. Initially, HeLa cells were transfected with all possible combinations of parkin, wild-type PINK1 and KD PINK1. Following the transfection period, cells were given 24 hours to recover in full media (10% FBS and 4.5 g/L glucose) before testing cell viability (**Figure 3-21 A**). We observed no significant difference in cell viability for any combination of proteins. We speculated that the 24 hour recovery period was not long enough for the cells to accumulate sufficient amounts of the toxic species potentially caused by co-expressing PINK1 and parkin. To test this, HeLa cells were transfected with the same combination of proteins, but following the transfection period, cells were given four days to recover in either full media or minimal media (1% FBS and 1 g/L glucose) (**Figure 3-21 B**). Incubating cells in minimal media reduces their division rate and could allow for more accumulation of a toxic species.

Yet again, the co-expression of PINK1 and parkin was not detrimental to cell viability, but in fact, had the highest cell viability in both the full and minimal media recovery conditions. This would suggest that the co-expression of PINK1 and parkin actually plays a protective role in mammalian cells. Lastly, HEK 293 cells stably

Figure 3-21. PINK1 and parkin co-expression in mammalian cells is non-toxic. (A) HeLa cells transiently transfected with all permutations of parkin, PINK1, kinase dead (KD) PINK1, and GFP as a control were given 24 hours to recover in full media (4.5 g/L glucose and 10% FBS) before analyzing cell viability using an ATP based luminescence assay. (B) HeLa cells transfected in an identical manner as in A were given four days to recover in either full media or minimal media (1 g/L glucose and 1% FBS) before analyzing cell viability using an ATP based luminescence assay. (C) HEK 293 cells stably expressing FLAG-parkin were transfected with vectors for PINK1 or KD PINK1 expression and given four days to recover in either full media or minimal media before analyzing cell viability using an ATP based luminescence assay. For all data sets samples were run in triplicate, quantified and graphed. Means were compared using a one-way ANOVA. One, two, three, or four asterisks (*/**/****/*****) indicates a statistical difference with a p value ≤ 0.05 , ≤ 0.01 , ≤ 0.001 , or ≤ 0.0001 respectively. Black – No DNA; **Green** – GFP; **Purple** – Parkin; **Blue** – PINK1; **Orange** – PINK1 + Parkin; **Teal** – KD PINK1; **Red** – KD PINK1 + Parkin.



expressing FLAG-parkin were used to test how cells that are constantly expressing parkin are affected by the introduction of PINK1. Again cells were transfected to combine parkin expression with wild-type or KD PINK1 and allowed to recover for four days in full or minimal media (**Figure 3-21 C**). Again, cells expressing parkin and PINK1 were equally as viable as cells co-expressing parkin and KD PINK1, suggesting that the co-expression of parkin and PINK1 does not exhibit the same toxicity in mammalian cells as it does in yeast. These results suggest that the changes in parkin localization and stability caused by PINK1 are yeast-specific and could be due to their inability to cope with phospho-parkin as they do not inherently express orthologues of either of these two proteins.

3.7 Parkin Proteolysis and Degradation in Yeast

Throughout our investigations, we noticed that Western blots of parkin expressing yeast lysates showed multiple highly reproducible bands of a lower molecular weight than the expected 52 kDa size of the full-length protein. These additional banding patterns also seemed to be specific depending on the epitope of the 1^o antibody used (**Figure 3-22 B**). When using the α -Ubl antibody (**Figure 3-22 B panel 3**) or the α -Rcat/RING2 antibody (**Figure 3-22 B panel 1**), which correspond to the most N and C-terminal domains of parkin, respectively, multiple bands were visualized between the range of 50 and 10 kDa with an additional band of high intensity running close to the dye front at around 5-10 kDa. Alternatively, using an α -RING1 antibody (**Figure 3-22 B panel 2**), which is specific to a domain near the middle of parkin, showed fewer low molecular weight bands, and instead, showed two to three bands greater than 25 kDa. Given that these bands were clearly

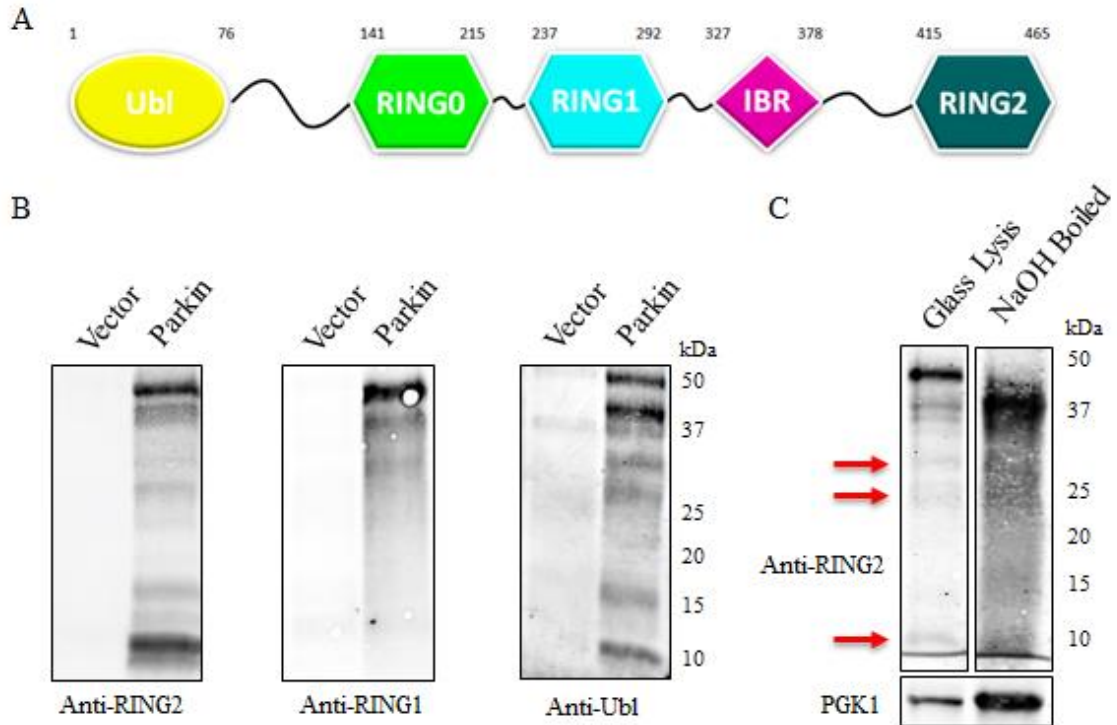


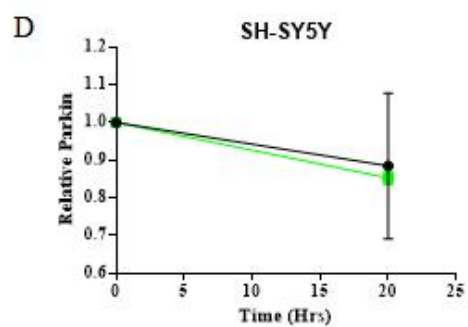
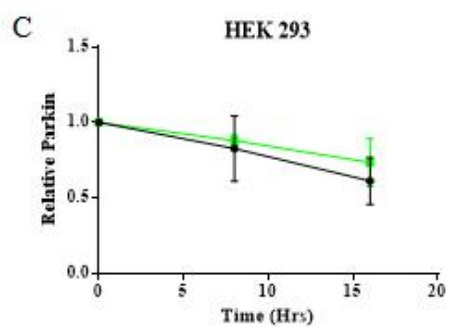
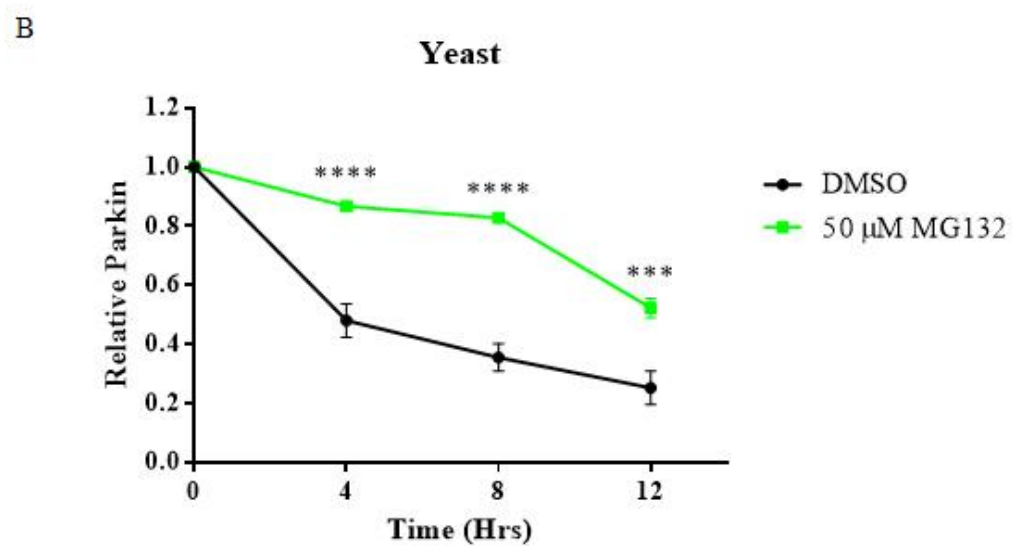
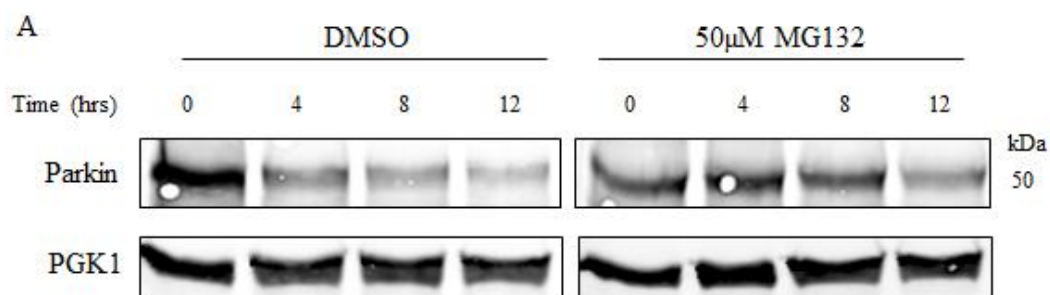
Figure 3-22. Parkin is degraded into distinct proteolytic fragments *in vivo*. (A) Schematic representation of parkin and its domains. (B) Thirty μg total protein of cell extracts from wild type W303 and W303 expressing parkin were analyzed by Western-blotting using three different primary antibodies with epitopes specific for distinct regions of parkin. (C) To assess if proteolytic cleavage products were being produced during or after cell lysis an alternate technique was used to prepare cell lysates. One W303 culture expressing parkin was equally split and lysed using two different techniques. The left lane used the standard glass bead lysis technique where cell are lysed in the presence of multiple different protease inhibitor. The right panel was lysed by boiling in a NaOH based lysis buffer and loading directly to the gel following neutralization, which does not allow post-lysis proteolysis. After lysis samples were resolved by SDS-PAGE and imaged in an identical manner as described in B.

parkin specific as they did not appear in wild type yeast cells, we believe that parkin is naturally undergoing proteolytic cleavage *in vivo*. To eliminate the possibility that this cleavage was occurring after lysis of the yeast cells, a NaOH based lysis technique was used, where cells were boiled in a NaOH based buffer, which would immediately denature all proteins and deactivate all proteases. After boiling, the samples were pH-neutralized and loaded directly into acrylamide gels, where they were resolved by SDS-PAGE next to a lysate that was prepared by glass bead lysis with protease inhibitors in the buffer (**Figure 3-22 C**). Western blots of these samples showed nearly identical size bands at approximately 30, 25 and 10 kDa in both lysates, suggesting that this proteolytic cleavage is occurring pre-lysis.

Next we tested if parkin was degraded in yeast cells by the 26S proteasome. Because yeast efficiently export many small molecules, including the proteasome inhibitor MG132, a yeast strain with deletions of the genes encoding PDR1 and PDR3, cell membrane transport proteins, were used to allow effective proteasome inhibition by MG132. *Δpdr1,3* yeast cells transformed with parkin were grown in inducing liquid media for ten hours to allow for parkin accumulation. Then expression of the galactose inducible GAL1 parkin promoter was quenched with the addition of glucose to a final concentration of 2%. Simultaneously, samples were treated with either 50 μ M MG132 to inhibit 26S proteasome dependent degradation or an equivalent volume of dimethyl sulfoxide (DMSO) as a control. Aliquots of the cultures were taken every four hours for twelve hours. Western blots were performed with these lysates and parkin levels were quantified relative to PGK1, which is a highly abundant stable protein in yeast. After setting the values of parkin at time

Figure 3-23. Inhibiting the 26S proteasome increases parkin stability in yeast. (A)

After 8 hours of induction in selective media W303 $\Delta pdr1,3$ cells expressing parkin were washed twice in sterile water and resuspended in non-inducing selective media (to prevent further parkin expression) with either 50 μ M MG132 or an equivalent volume of DMSO added. Aliquots of the cultures were taken every four hours for twelve hours. (C) Cultured HEK 293 cells stably expressing FLAG-parkin and (D) SH-SY5Y cells expressing endogenous parkin were treated with cycloheximide (Cx) and DMSO or 10 μ M MG132. Similar to the technique described in panel A, samples were harvested at various time points and frozen until all time points had been collected. (B/C/D) samples were lysed and 30 μ g of total protein was resolved by Western blotting for parkin (B) Samples were run in triplicate and parkin levels were quantified and normalized relative to the PGK1 loading control. (C and D) Sample were run in triplicate and parkin levels were quantified without normalization to a loading control. (B, C, and D) Parkin levels were independently set to 1 at time zero for the DMSO and MG132 treated samples. Means of the same time points were compared using a two-way ANOVA. Three or four asterisks (***/****) represent statistically significant differences with a p value ≤ 0.001 or ≤ 0.0001 respectively. Black – DMSO treated; Green – MG132 treated.



0 to 100%, the relative parkin intensities showed a decrease in overall parkin over the course of 12 hour for both the MG132 and DMSO treated controls, with significantly less degradation in the MG132 treated samples (**Figure 3-23 A and B**). After twelve hours about 30% of the original parkin remained in control cells whereas MG132 treated cells retained nearly double the amount of parkin. In these experiments only the predominant band representing the full length protein was quantified, although samples did exhibit lower molecular weight bands as described in **Figure 3-22** as well as high molecular weight smears that could represent poly-ubiquitinated parkin (data not shown). These data suggest that in yeast grown under normal conditions, parkin undergoes significant proteasome-dependent degradation.

Similar experiments were performed with HEK 293 cells stably expressing FLAG-parkin and SH-SY5Y cells expressing endogenous parkin. In these systems expression of all proteins was quenched using cycloheximide and samples were again treated with either MG132 or DMSO as a control (**Figure 3-23 C and D**). Cells were followed for either 16 or 20 hours before lysis and Western blotting. The results showed no statistical difference between MG132-treated or untreated samples in either cell line.

We next tested the effect on proteasome inhibition on parkin degradation without inhibiting protein expression. HeLa cells transfected with parkin-expressing vectors were treated to test the effects of decreased protein degradation. Following treatment with 10 μ M MG132 for 8 hours, proteins were extracted, and parkin stability was analyzed by Western blotting. We noticed an increase in parkin levels in MG132 treated cells compared

to untreated controls (**Figure 3-24 A and B**). This result indicates that transfected parkin is degraded by the 26S proteasome in HeLa cells.

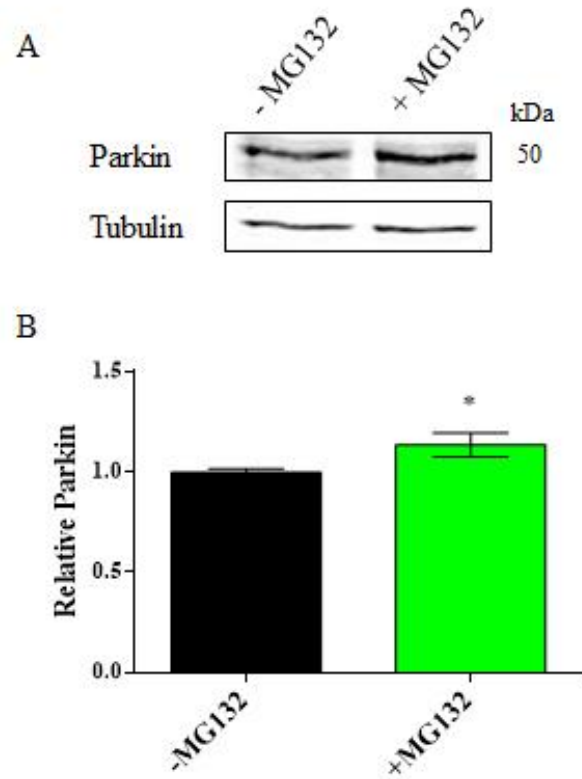


Figure 3-24. Parkin stability is mildly increased by MG132 in HeLa cells. Cell lysates of HeLa cells transfected with parkin were analyzed by Western blotting (A) to detect parkin. (B) Steady state levels of parkin were compared to cells treated with MG132 and parkin levels were quantified relative to the tubulin loading control. Parkin levels in untreated cells was set to 1. Means were compared using an unpaired T-test and an asterisk (*) indicates a statistical difference with a p value ≤ 0.05 . Tubulin was used to assess equal loading. Black – untreated; Green – MG132 treated.

Chapter Four: Discussion

4.1 Introduction – Parkin in PD

The E3 ubiquitin ligase parkin is essential for maintaining neuronal health in the substantia nigra and the dysfunction of parkin has been associated with familial and sporadic forms of PD (139). Parkin prevents the accumulation of damaged cellular proteins, particularly mitochondrial proteins, thus regulating the homeostasis of mitochondria, and consequently diminishing oxidative stress caused by ROS (140). PINK1, a serine/threonine kinase, has been implicated as a key regulator of parkin through two interrelated mechanisms: PINK1-mediated phosphorylation of parkin and PINK1-mediated phosphorylation of ubiquitin, which activates parkin (77, 78). In addition to insufficient phosphorylation of parkin by PINK1, damage to parkin by oxidative stress, loss of function mutations, and gain of function mutations resulting in parkin misfolding have also been associated with parkin dysfunction in PD (114, 139, 141, 142). Yet the cellular and molecular mechanisms by which parkin damage and misfolding contribute to PD remain poorly understood.

The overall goal of this thesis was to decipher how parkin regulation by PINK1, parkin misfolding and subsequent stress on the cellular protein quality control machinery, and oxidative damage to parkin contribute to parkin dysregulation and dysfunction in PD.

4.2 Summary of Findings and Significance

4.2.1 Sequence Analysis

Analysis of parkin's amino acid sequence demonstrated that the structurally and functionally determined catalytic triad consisting of C431, H433, and E444 located in parkin's Rcat/RING2 domain (112) is highly conserved across multiple different evolutionary distant species (**Figure 3-1**). Importantly, this analysis also revealed an unusually high level of conserved cysteine residues throughout the entire parkin protein with the exception of the N-terminal Ubl domain that contains only one cysteine. Thirty five of human parkin's 465 total amino acid residues are cysteines, giving it an overall cysteine content of 7.52%, which is nearly three times higher than the average for other human proteins (2.26% according to (7)). Structural studies have determined that 28 of these cysteine residues are required for coordination of eight Zn^{2+} ions in four distinct parkin domains (59). Accordingly, Zn^{2+} coordination does not account for all 31 of the conserved cysteines within parkin.

Cysteine residues are inherently sensitive to oxidative and nitrogenous modifications, and they can be essential for sensing and regulating levels of stress-inducing chemicals in the cell. For example, the Kelch-like ECH-associated protein 1 (Keap1) is an oxidative stress sensing protein that regulates the transcription factor Nuclear factor (erythroid-derived 2)-like 2 (Nrf2, (143)). Under normal cellular conditions Keap1 facilitates ubiquitination of Nrf2 in the cytosol, thus inducing rapid degradation of Nrf2. This prevents Nrf2 from entering the nucleus where it is transcriptionally active (143). Under condition of oxidative stress, C151 of Keap1 is oxidatively modified, causing a

conformational shift that releases Nrf2 and allows it to enter the nucleus and promote transcription of antioxidant genes.

Increased oxidative stress is a hallmark of PD (144, 145) and is closely associated with cellular damage. Additionally, oxidative stress induced by CCCP-mediated uncoupling of the electron transport chain causes a change in parkin localization, recruiting it to the mitochondria to activate its role in mitophagy (76, 78, 81). Also, Chung *et al.* have shown that parkin can be S-nitrosylated by nitric oxide (NO) and that this modification reduces its activity (146). In a similar manner, parkin could be modified in response to increased levels of oxidative stress, diminishing its E3 activity. A decrease in parkin activity could result in an increased load on the protein quality control machinery and activate one of many protective cellular stress responses programs.

In essence, parkin could act as a cellular sensor to detect and preemptively respond to oxidative stress and activate an anti-oxidant response. However, no previous studies have directly addressed oxidative damage to parkin and its ensuing misfolding. This would present a previously unknown function of parkin in stress homeostasis and in PD.

4.2.2 *Parkin Yeast Model*

Following successful examples of PD yeast models in the literature (99–109), we established a parkin yeast model, which we used as an experimental platform for further experimentation (**Figure 3-2**). In our model, parkin was diffusely localized throughout the yeast cytosol as previously observed in mammalian cells, including human neurons (113, 114, 147). We also showed that parkin is stably expressed and that it only slightly decreased

the growth rate of yeast. This effect can be attributed specifically to expression of parkin since expression of a similar sized protein in yeast does not inhibit growth (Appendix 5).

4.2.3 *Genetic Interactions of Parkin*

Using our parkin yeast model, we performed a small scale genetic screen with 17 yeast deletion strains deficient in genes required for oxidative stress management and protein quality control to unravel genetic interactions with parkin (**Figure 3-3**). In this screen one gene deletion (SGT2) was identified that significantly altered parkin localization and two gene deletions (YAP1 and BTN2) were identified that significantly reduced growth of yeast cells expressing parkin. Notably, only one gene deletion (SOD2) altered both parkin localization and reduced the growth of cells expressing parkin simultaneously.

Deletion of SOD2, encoding the mitochondrial superoxide dismutase, which prevents the accumulation of superoxide radicals, does not have a growth phenotype under regular conditions. Yet the expression of parkin caused a significant reduction in the growth rate of SOD2 deleted yeast. SOD2 deletion also altered parkin localization, causing small subcellular inclusions of parkin in addition to the diffuse localization pattern observed in wild-type cells. This result supports our idea that parkin acts as an oxidative stress sensor. The yeast SOD2 deletion strain accumulates excessive amounts of ROS (148), which may oxidatively damage parkin, result in parkin misfolding, and alter parkin's subcellular localization, thus inhibiting growth.

In order to confirm that these changes are indeed a result of increased levels of ROS, future experiments would need to test for increased levels of ROS and compare these

results to wild-type cells and cells exposed to chemically-induced oxidative stress. If parkin were properly functioning in wild-type yeast cells to degrade damaged proteins, the increase in ROS may modify parkin causing its aggregation, thereby inhibiting its protective function. This decrease in protective parkin activity could cause an increased burden on the protein quality control machinery, leading to growth inhibition.

Alternatively, the rise in ROS levels may not damage parkin itself. Instead, ROS may modify and damage other cellular proteins, increasing the number of proteins that require processing and degradation. The juxtaneuclear quality-control compartment (JUNQ) and perivacuolar insoluble protein deposit (IPOD) were first described by Kaganovich *et. al* in yeast as intracellular compartments that sequester misfolded cytosolic proteins (33). This research showed that when ubiquitinated, soluble misfolded proteins are directed to JUNQ, which contains a high concentration of proteasomes. JUNQ has been described as a site where misfolded proteins are sequestered when proteasome activity is impaired, often in response to cellular stress including heat shock. Following recovery from stress conditions, proteins sequestered to JUNQ can either be refolded via molecular chaperones or degraded by the proteasome. In contrast, proteins that were not ubiquitinated were directed to IPOD which is speculated to permanently sequester toxic amyloid-like proteins, thus preventing their toxic interaction with cytosolic proteins.

In the SOD2 deletion strain, parkin may be recruited to areas with increased need for UPS activity, like JUNQ, which would account for our observation of subcellular puncta with some remaining diffuse signal. In this scenario, an increased burden on the protein quality control machinery could also prevent normal growth by directing more

resources towards eliminating damaged proteins. Whether parkin or other cellular proteins are damaged by ROS in the SOD2 deletion strain, our data suggest that parkin responds to increased ROS in the cell. The relationship between SOD2 and parkin has not been thoroughly characterized in the literature but our findings present an enticing basis to further study this genetic interaction.

Deletion of YAP1, and deletion of BTN2 both caused a decrease in growth rate of yeast cell expressing parkin compared to wild-type cells, yet neither deletion caused a change in parkin localization. Yap1 encodes a transcription factor required for oxidative stress tolerance (117) and BTN2 encodes a v-SNARE binding protein that facilitates protein retrieval from the late endosome to the Golgi and contributes to prion curling (118). Decreased growth in the YAP1 deletion strain closely relates to the effects of the SOD2 deletion strain, in that an inadequate cellular response to oxidative stress causes parkin-related growth defects. This further supports the notion that oxidative stress is a major contributor to parkin modification.

Our data for the BTN2 deletion, however, suggests a role of parkin associated with inadequate protein quality control beyond oxidative stress. Yeast deficient in BTN2 show increased propensity to accumulate prions (149), and have altered protein trafficking and localization. Therefore parkin toxicity in the BTN2 deletion strain could imply that parkin's E3 activity is required to degrade accumulating prion proteins. Here, an increased burden on the protein quality control machinery caused by increased UPS activity of parkin could induce cellular stress and inhibit growth.

This may seem counter-intuitive as it is also plausible that parkin expression in these cells would eliminate prion accumulation, thus playing a protective role. The accumulation of potentially toxic proteins, such as prions, into benign aggregates has been suggested to prevent additional damage to the cell (33). It is possible that parkin ubiquitinates the sequestered prions and releases them into the cell, causing toxicity and inhibiting growth. This could be tested by assessing parkin ubiquitination activity on prion or prion-like proteins in the absence of BTN2 in future experiments.

Finally, deletion of SGT2, encoding a cytoplasmic HSP90 co-chaperone required to mediate post-translational insertion of tail-anchored proteins into the ER membrane (119), altered parkin localization. In this strain, we observed the formation of large puncta in addition to diffuse cytosolic parkin staining. Without SGT2, yeast cells may accumulate unprocessed proteins in the cytosol that normally require processing and insertion into the ER membrane. The observed change in parkin localization suggests that parkin is recruited to areas of the cell with an increased need for protein degradation, including JUNQ as described above, and may play a protective role to eliminate damaged or misfolded proteins and prevent cell damage. Notably, SGT2 deletion strains do not exhibit decreased growth in the absence of parkin, even though they have impaired insertion of tail-anchored proteins into the ER membrane. Apparently, the cellular protein quality control machinery adequately processes these mislocalized proteins and prevent growth defects. The expression of parkin in this strain may act as an additional support for UPS-mediated degradation of mislocalized proteins and therefore alters parkin localization without causing toxicity.

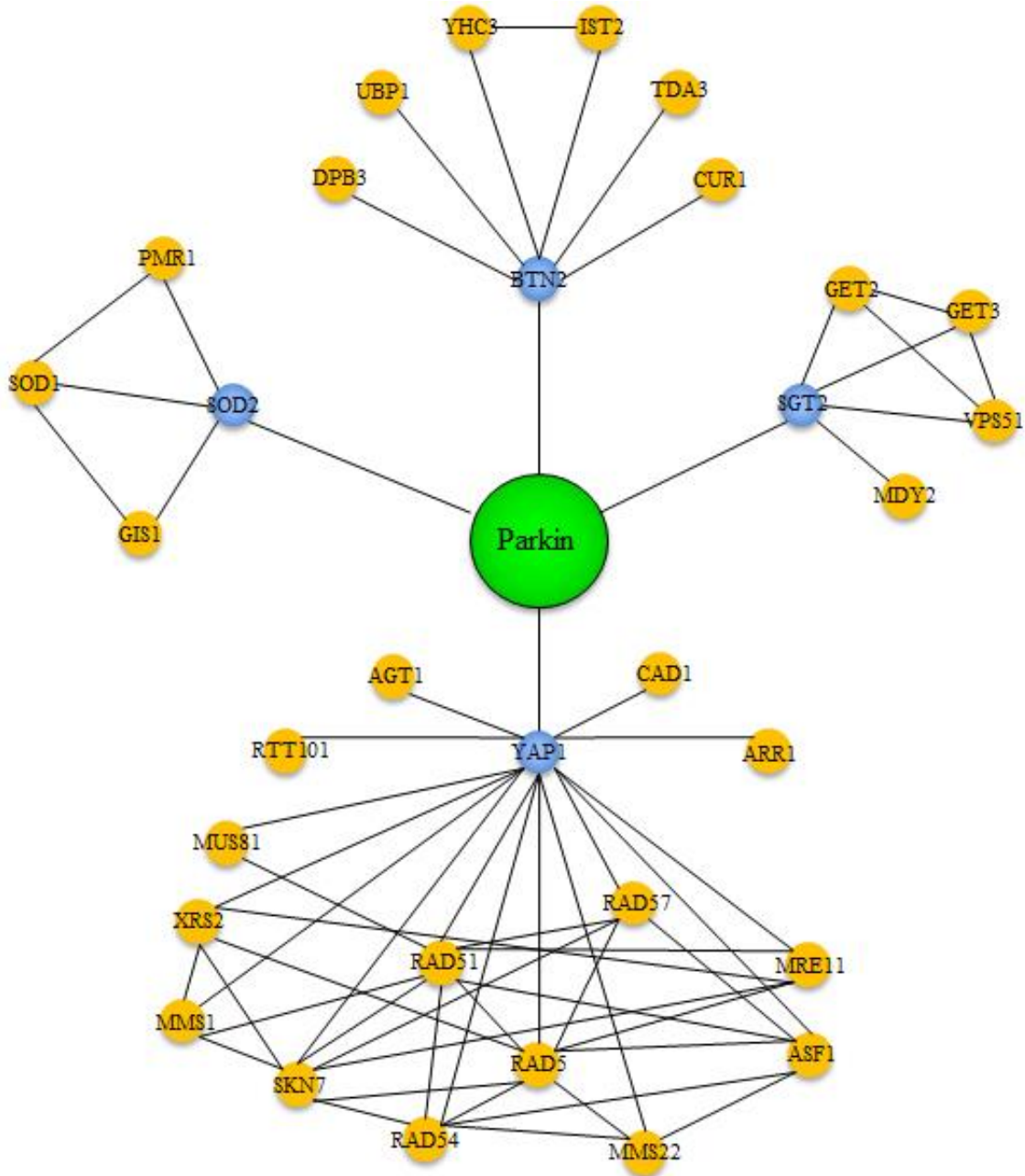


Figure 4-1. Parkin genetic interaction network. Network of genetic interactions of parkin showing two degrees of separation. Genetic interactions with parkin identified in this thesis are shown in blue and previously established genetic associations with interactors of parkin are shown in yellow.

To test this concept, we would need to examine parkin expression in a SGT2 deletion strain that has additional gene deletions of yeast E3 ligases or other genes involved in protein turnover and UPS. If parkin expression in these cells rescues growth defects caused by the buildup of misfolded proteins, it will support our claim that parkin is essential for protein folding homeostasis.

Overall, our pilot screen identified interesting and rather unexpected genetic interactions with parkin that implicate a role for parkin in both oxidative stress management and protein quality control as shown in **Figure 4-1**. Importantly, this provides a strong rationale to proceed with large scale genetic screens using deletion and over-expression libraries encompassing the entire yeast genome. This will further elucidate the parkin interaction network and identify previously unknown roles for parkin and potential therapeutic targets for treating PD. This is supported by previous findings from large scale genetic screens that identified toxic modifiers of mutant Htt and α -synuclein in yeast (150).

4.2.4 *Oxidative Damage to Parkin*

We next assessed the state of parkin oxidation. When performing Western blots on cellular protein lysates, the convention is to use reducing conditions (151). Although this often improves the quality and analyses of results, artificially reducing proteins eliminates oxidative modifications to proteins (151). In **Figure 3-4**, we compared protein lysates of yeast and mammalian cells prepared in reducing and non-reducing conditions by Western blot. We found that, under non-reducing conditions, parkin migrates in SDS-PAGE at a faster rate and produces a less defined signal. This suggests the presence of intramolecular disulfide formation between any of the 35 cysteine residues within parkin.

Furthermore, we observed a large shift in the apparent molecular weight of parkin expressed in HeLa and HEK293, and to a lesser extent in SH-SY5Y cells (**Figure 3-4 B**). In these experiments, unmodified SH-SY5Y cells were used to analyze endogenous levels of parkin, whereas HeLa and HEK293 cells used constitutively expressed transfected parkin at higher levels, as indicated by the strong signal intensity. Excess parkin accumulation caused by constitutive over-expression in HeLa and HEK293 cells may not be turned over as efficiently as lower levels of endogenous parkin in SH-SY5Y. As a result, excess parkin may be subjected to increased oxidative damage, thus increasing the number of disulfides formed and enhancing the shift in molecular weight seen in non-reducing Western blots for HeLa and HEK293 cells.

To further test the effects of parkin oxidation, we performed experiments in yeast with the addition of stress inducing chemicals to mimic the conditions potentially found in aging and PD patient cells (**Figures 3-5, 3-6 and 3-7**). We found that treatment with H₂O₂ and AZC elicited drastic changes in parkin localization causing the formation of multiple small puncta throughout cells. Treatment with these chemicals thus resembled aberrant parkin localization as observed in our pilot yeast deletion screen (**Figure 3-4**). H₂O₂ treatment is reminiscent of the oxidative stress in the SOD2 deletion strain as both caused the accumulation of parkin. Furthermore, impaired protein folding by AZC treatment and the ensuing induction of the heat shock response (152) mimic the effects of SGT2 deletion which lead to increased levels of damaged or misfolded proteins which also affects parkin localization.

Both AZC and H₂O₂ altered parkin localization, which suggests that different types of cellular stress conditions affect the cellular localization and accumulation of parkin. Also, treatment with H₂O₂ and AZC generally causes the accumulation and mislocalization of damaged and misfolded proteins, which may recruit a significant proportion of parkin. Alternatively, stress treatment could cause damage to parkin itself, leading to its sequestration for processing by molecular chaperones or the protein degradation machinery. However, Western blot analysis did not reveal any significant change in parkin migration patterns in the presence of H₂O₂ and other stress inducing chemicals (**Figure 3-6**), which does not clarify whether parkin is directly modified as a result of chemical stress. Further experiments will be required to decipher whether these chemicals are indeed modifying parkin itself or whether they indirectly affect parkin localization in yeast. The use of antibodies that specifically recognize oxidatively modified cysteine residues could clarify if parkin directly undergoes oxidative modification.

Growth curve assays in the presence of increasing concentrations H₂O₂ in yeast were used to elucidate a role of parkin under high levels of oxidative stress (**Figure 3-5 B**). Only at a concentration of 1 mM did the addition H₂O₂ have an effect on cell growth. At this concentration, H₂O₂ caused a delayed entry in logarithmic growth phase and caused slower growth during exponential growth phase. Although cell growth was affected by the increased H₂O₂ concentration, the difference between wild-type cells and cells expressing parkin was unaffected compared to untreated cells, suggesting that parkin is neither playing a protective nor a detrimental role in the presence of H₂O₂ in yeast.

We performed similar experiments in HeLa cells where H₂O₂, AZC, and other stress inducing chemicals were added before assessing parkin localization by immunofluorescence microscopy and parkin modification via Western blot (**Figure 3-7**). None of these stress treatments showed changes in parkin localization or migration compared to untreated cells. Although they are derived from human cells, the rapid rate of division of HeLa cells may act to effectively dilute toxic misfolded proteins induced by chemical stress, thus preventing changes to parkin localization or oxidative modification.

4.2.5 *Parkin Mutants and Truncations Alter Parkin Localization*

We used several truncation variants of parkin and specific parkin point mutants (**Figure 1-6**) to study the effect of parkin misfolding and map these effects to specific parkin domains. When expressed in wild-type yeast cells, none of the parkin variants or point mutants had any effect on cell growth. Furthermore, expression of the parkin S65A and S65E mutants as well as the 321C parkin variant did not alter parkin localization. Several parkin variants did, however, cause drastic changes in parkin localization and stability (**Figures 3-8, 3-9, 3-10, and 3-11**).

The AR-JP causing C289G and C418R mutants affecting residues required for Zn²⁺ coordination caused parkin to accumulate into subcellular foci (**Figure 3-10**) as shown previously (71). This change in parkin localization was similar to changes observed upon treatment with AZC and H₂O₂, and the SOD2 and SGT2 gene deletions from our pilot screen, where parkin formed multiple small inclusions while additionally maintaining some diffuse cytosolic localization. Expressing the overactive 141C mutant (**Figure 3-8**) also showed a similar localization pattern. The C289G and C418R mutants are structurally

unstable and misfold and thus may form aggregates. However, our Western blot analysis revealed that these mutants were expressed at the same level as wild-type parkin, which would suggest that they are not being degraded more than wild-type parkin. These mutants might simply relocate to specific subcellular locations, such as IPOD or JUNQ, to prevent their interference with normal cellular functions as discussed in section 4.2.3.

In contrast, the 141-409 mutant caused a more drastic change to parkin localization. Truncation of both the Ubl and Rcat/RING2 domains eliminated all diffused cytosolic parkin, and instead, caused parkin to form either two to three larger, or multiple smaller puncta. Evidently, the regulation of parkin by the Ubl domain and linker alters its localization as shown with the 141C variant. The additional truncation of the Rcat/RING2 domain in the 141-409 parkin variant, however, seems to further decrease parkin stability. This effect may be caused by the loss of the two structurally required Zn^{2+} ions found in the Rcat/RING2 domain, or destabilization of the entire C-terminus of parkin since Rcat/RING2 is adjacent to the RING0 domain when properly folded (63).

Our experiments did not directly test the solubility of these parkin aggregates. Future work should therefore include experiments that directly assess the solubility of parkin and its mutants, which could determine whether parkin mutations and truncations form insoluble protein aggregates or if they simply change parkin localization. These experiments will include Triton X-100 based solubility assays that can differentiate between soluble and insoluble fractions of cell lysates (153).

We selected only the 141C variant and the four point mutants for our experiments in HeLa cells (**Figure 3-12**). Localization studies showed that neither S65A nor S65E

parkin mutants altered parkin localization, but the AR-JP causing C289G and C418R mutants formed subcellular inclusions while maintaining some diffuse cytosolic localization. Western blots showed similar expression levels of the cysteine mutants compared to wild-type parkin. This supports our previous claim that these mutants are being sequestered to JUNQ-like compartments, and are not degraded as discussed in section 4.2.3.

In contrast to the results seen in yeast, the N-terminal truncation of the Ubl domain and linker region in the 141C variant did not alter parkin localization in HeLa cells. Also, experiments testing the stability of 141C in mammalian cells similarly did not resemble our result in yeast. In HeLa cells, 141C is expressed at approximately 50% of the level of wild-type parkin (**Figure 3-12 B and C**), whereas in yeast, 141C is expressed at nearly three times higher levels than wild-type parkin (**Figure 3-9 B, C, D and E**). Human cells endogenously express parkin, and likely contain pathways that require parkin activity. However, 141C is not normally expressed in mammalian cells and may therefore not be recognized and subsequently degraded. Alternatively, yeast cells do not endogenously express parkin or 141C, suggesting that they may be processed differently in yeast than in mammalian cells which could account for the difference in stability observed in these experiments. The discrepancies between our yeast and mammalian systems are further discussed below in section 4.3.1.

4.2.6 *PINK1 Modulates Parkin Localization and Toxicity*

The regulation of parkin by PINK1 has emerged as an important concept in parkin activation. Our next experiments addressed the PINK1-parkin interaction using our yeast

and mammalian cell models and we further characterized this interaction with parkin point mutants and parkin truncation variants.

4.2.6.1 Co-expression of PINK1 and Parkin Truncation Variants Cause Toxicity in Yeast

When expressed alone in yeast, human PINK1, containing a yeast-specific mitochondrial targeting sequence, exhibited a slightly more pronounced growth defect than that seen when expressing parkin alone (**Figure 3-13 A and B**). In contrast, the co-expression of PINK1 and wild-type parkin caused a severe growth inhibition. Experiments with a kinase dead mutant form of PINK1 showed that this effect is dependent on the kinase activity of PINK1. Of all variants used in this study, only the wild-type parkin and the two cysteine mutants contain intact S65 and thus can be phosphorylated by PINK1. It was therefore unexpected to find that the co-expression of PINK1 with 141C also exhibited a severe growth inhibition that was only slightly less toxic than the co-expression of PINK1 and wild-type parkin.

Our results suggest that the toxicity caused by the co-expression of PINK1 and parkin can at least partially be attributed to PINK1-mediated parkin phosphorylation. Yet the toxicity observed from co-expression of PINK1 cannot be attributed to phosphorylation of 141C, since it lacks the PINK1 phosphorylation site located in parkin's Ubl domain. Here, PINK1 may interact with and phosphorylate other proteins, which could be particularly toxic in yeast cells expressing 141C.

PINK1 has previously been shown to phosphorylate not only parkin (81, 142), but also mitochondrial proteins including TOM20 and mitofusin (86, 87) and, importantly, ubiquitin. Additionally, it has been postulated that phospho-ubiquitin strongly contributes

to parkin activation (154). Given that the 141C variant that lacks the auto-inhibitory Ubl domain, phosphorylation of ubiquitin in yeast by PINK1 may act to even further activate 141C. This may result in UPS overloading and cellular stress. **Figure 4-2** presents a model for PINK1 activity that involves phosphorylation of ubiquitin, mitochondrial, and cytoplasmic proteins causing increased activity of the 141C variant leading to increased UPS activity and degradation of essential cellular proteins. This can explain the observed growth inhibition that occurred independently of PINK1-mediated phosphorylation of parkin.

When co-expressing all of our parkin variants with PINK1, wild-type parkin, 141C and the independently expressed Ubl domain all exhibited PINK1-dependent changes in localization (**Figure 3-15 B**). Since PINK1 can phosphorylate ubiquitin and considering the structural similarity between the Ubl domain and ubiquitin, PINK1 may phosphorylate S65 of parkin's Ubl domain, even when it is detached from the rest of parkin. The Ubl domain might thus mimic phospho-ubiquitin and its function in the UPS. Only a fraction of the Ubl appears to be affected by PINK1 because the majority of the Ubl remains diffusely localized and small bright foci are formed in a small proportion of cells.

Figure 4-2. Model of PINK1-mediated increase of parkin ubiquitination activity in yeast causing toxicity. A) Under normal conditions, parkin or 141C is located in the cytosol and exhibits standard levels of ubiquitination activity. B) Following the introduction of PINK1 1) ubiquitin, 2) cytosolic proteins, or 3) mitochondrial proteins are phosphorylated by PINK1. 4) In response to 1, 2, or 3, parkin or 141C becomes overactive, which leads to 5) uncontrolled ubiquitination and 6) degradation of essential cellular proteins causing toxicity. 7) Alternatively, an increase in parkin activity increases parkin auto-ubiquitination leading to its degradation.

To test if parkin's Ubl domain can at least partially function as ubiquitin future experiments could use yeast strains expressing Ubl in place of the standard ubiquitin fusion genes and test their viability. Yeast cells contain four genes encoding ubiquitin, and yeast cells remain viable when up to three of these genes are deleted. By deleting these ubiquitin fusion genes while simultaneously expressing parkin's Ubl domain, we would be able to test cell viability and determine whether the Ubl domain can function in place of ubiquitin in yeast cells.

When independently expressed in yeast, the 141C parkin variant exhibited an altered localization compared to wild-type parkin as we have previously discussed in section 4.2.5. However, when we co-expressed 141C with PINK1, the formation of subcellular 141C puncta was exacerbated, causing a decrease in the amount of diffusely localized protein. This finding supports our model presented in **Figure 4-2** where PINK1 increases the activity of the already overactive 141C variant of parkin indirectly by phosphorylating ubiquitin or other cellular proteins.

Most parkin variants used here maintained some level of diffuse localization when expressed in yeast. The co-expression of PINK1, however, eliminated all diffuse wild-type parkin from the cytosol and formed similar puncta as seen with the 141-409 variant. In combination with the results from our growth assays, this could suggest that in the presence of PINK1, parkin is activated, as documented by several groups (142, 154–156). Yet parkin may also undergo a conformational change that causes its misfolding into a species that is toxic to the cell. Further testing would be required to determine the composition and structure of the parkin inclusions caused by its interaction with PINK1.

In addition, PINK1 expression could create phospho-ubiquitin in yeast. This could explain the toxicity associated with PINK1 expression, as yeast may not normally express a kinase that efficiently phosphorylates ubiquitin. Therefore phospho-ubiquitin may disturb UPS function and cause toxicity. In any case, the co-expression of parkin with PINK1 adds complexity to this scenario.

We did not assess the presence of phospho-parkin or phospho-ubiquitin in our yeast model, but future work could clarify the cause of these significant changes in parkin localization and toxicity. Experiments to test the presence of phospho-parkin or phospho-ubiquitin using phospho-specific antibodies in localization studies and Western blot could establish that PINK1 acts to phosphorylate parkin or ubiquitin in yeast. Co-immunoprecipitation of parkin substrates while inhibiting protein degradation with proteasome inhibitor would be followed by Western blot analysis probing for ubiquitin and phospho-ubiquitin in the presence and absence of PINK1. These experiments would indicate if parkin activity is increased in the presence of PINK1, if phospho-ubiquitin is created by PINK1, and if phospho-ubiquitin is incorporated into poly-ubiquitin chains built on parkin substrates.

Growth assays testing PINK1 co-expression with parkin-YFP supports our notion that PINK1 induces parkin misfolding. When co-expressing C-terminally YFP tagged wild-type parkin and parkin variants with PINK1, we observed similar toxicity as with untagged parkin and parkin variants co-expressed with PINK1. In all cases, the expression of YFP fusion forms of parkin reduced growth inhibition compared to untagged forms of the protein. Fluorescent protein fusions have been shown to increase the solubility of

normally insoluble proteins (157, 158) thus reducing the toxicity associated with protein misfolding. Our results suggest that PINK1 causes parkin to misfold and form a toxic insoluble species and subsequently the YFP fusion solubilizes parkin and reduces its toxicity.

We also tested if parkin formed amyloid-like aggregates in yeast using SDD-AGE (**Figure 3-16**), yet our experiments showed that parkin does not form amyloid-like conformers. This does not, however, disprove that parkin misfolds and forms soluble aggregates. Future experiments will include sedimentation assays to assess if parkin changes its three-dimensional conformation or misfolds when co-expressed with PINK1, when mutated, or when exposed to stress conditions.

4.2.6.2 Toxicity Associated with Co-expression of PINK1 and Parkin is Reduced by Parkin Point Mutations in Yeast

As discussed above, the co-expression of PINK1 with parkin induced severe growth inhibition in yeast. However, when co-expressing our four parkin point mutants with PINK1, we observed a significant decrease in PINK1-parkin dependent toxicity that only slightly differed depending on the parkin mutant being expressed (**Figure 3-17**).

The expression of all four point mutants caused similarly reduced levels of toxicity. However, the parkin S65E mutant, which to some extent mimics PINK1 phosphorylated parkin, caused a more severe growth defect than the other parkin point mutants, including the S65A mutant which cannot be phosphorylated by PINK1. This finding again may indicate that PINK1 alters parkin activity indirectly by phosphorylation of other cellular proteins including ubiquitin, which only additional experiments can clarify.

The increased toxicity caused by the phospho-mimic S65E parkin suggests that PINK1-mediated phosphorylation of parkin also contributes to parkin regulation. The use of aspartic and glutamic acid residues to mimic phosphorylation of proteins is a widely used technique but many studies have suggested that these substitutions can only partially recapitulate effects caused by phosphorylation (154, 159). The addition of a negatively charged residue mimics the effects of phosphate addition to a protein, but phosphate groups have a significantly a different shape than the carboxyl group of aspartic or glutamic acid residues. Additionally, phosphates carry two negative charges compared to the single negative charge on an acidic residue. These differences between phosphates and phospho-mimics may explain the decreased toxicity caused by the expression of the S65E parkin mutant compared to PINK1 co-expression with wild-type parkin.

The co-expression of the C289G and C418R parkin mutants with PINK1 also reduced toxicity compared to wild-type parkin. Although these parkin mutants still contain the S65 site of PINK1-directed phosphorylation and can be phosphorylated, they are structurally unstable (71). The misfolding of these parkin mutants caused by the loss of structurally required Zn^{2+} ions may cause a conformational shift that renders S65 partially inaccessible to PINK1 and prevent their phosphorylation. Alternatively, the structural instability of C289G and C418R may expose the Ubl domain to more efficient PINK-mediated phosphorylation. In any case, C289G and C418R are loss of function mutations (57), suggesting that PINK1-mediated phosphorylation of these mutants or other cellular proteins do not have the capacity to affect their already compromised functional state. Phosphorylation of parkin and C289G and C418R, may induce parkin misfolding, which is toxic to yeast cells. This would account for the toxicity observed in these experiments

co-expressing PINK1 with C289G and C418R parkin. Additionally, this would explain part of the toxicity caused by co-expression of PINK1 with wild-type parkin as discussed in section 4.2.6.1.

Co-expression of PINK1 (**Figure 3-18**) with C289G and C418R resulted in unaltered localization patterns. S65 parkin mutants exhibited slightly altered localization upon co-expression with PINK1, where both S65A and S65E parkin formed one or two small puncta in a small proportion of cells. Since neither of these S65 parkin mutants can be phosphorylated by PINK1, this suggests that the change in localization is due to the phosphorylation of ubiquitin to activate these parkin mutants and alter their localization.

4.2.6.3 *PINK1 Co-expression with Parkin in HeLa Cells Increases Viability*

Following these findings in yeast we performed similar localization and viability experiments in mammalian cells co-expressing wild-type parkin and PINK1. Neither toxicity associated with co-expression of PINK1 and parkin, nor changes in parkin localization were observed in HeLa cells. Viability assays showed an increase in cell viability by approximately 25% (**Figure 3-21 B**). These findings support the model currently accepted in the literature that parkin and its regulation by PINK1 are protective (88, 160, 161). As discussed in sections 4.2.5. and 4.3.1., the absence of endogenously expressed PINK1 and parkin and subsequent lack of processing or function in yeast may account for the discrepancies between our yeast and mammalian models.

4.2.7 *Parkin Turnover and Degradation*

In some of our experiments, we showed that parkin undergoes oxidative modification *in vivo*. Additionally, our results suggested that parkin undergoes proteolytic degradation (**Figure 3-22 B**). We also determined that parkin is degraded in yeast via degradation by the UPS (**Figure 3-23**). We propose that parkin misfolding under normal conditions and, by extension, conditions of oxidative stress, affect parkin activity, stability, and misfolding.

We also showed that when co-expressed with PINK1, parkin is less stable than when expressed alone in yeast (**Figure 3-19**). Similar experiments found that parkin stability was increased in HeLa cells following inhibition of the proteasome, albeit to a small extent. This suggests that parkin also undergoes proteasome-dependent degradation in mammalian cell but at a slower rate than in yeast. Future experiments could include testing the degradation and relative stability of the parkin point mutants and truncation variants used in this study to determine if AR-JP causing mutations can lead to altered parkin stability and potentially map which domains of parkin are essential for maintaining stability.

Ultimately, more work is required to further clarify the involvement of the protein quality control machinery in parkin degradation, and if this contributes to PD pathogenesis. Nevertheless, these results give an interesting basis for studying parkin post-translational processing and degradation and its effects on protein function and longevity.

4.3 Experimental Limitations

A thorough discussion of technical problems and limitations can be found in Appendix 1.

4.3 Modelling Parkinson's Disease in Yeast – Opportunities and Limitations

Studying human proteins and diseases in model organisms is a commonly used strategy in biomedical research, but there are inherent limitations with every model system. During our investigation, we discovered several interesting results regarding parkin misfolding, altered localization, toxicity, degradation, and oxidative modification in our yeast model. Notably, most of these findings did not replicate in mammalian cells. Unlike human cells, yeast cells do not endogenously express parkin, PINK1, or related orthologues of either protein. This allowed us to monitor the effects of co-expressing these proteins in yeast using it as a simple living test tube. Our approach to studying parkin and PINK1 in yeast relied mainly on analyzing phenotypic changes caused by the expression of one or both of these proteins; these phenotypic analyses included changes in growth rate, protein localization, and levels of protein expression.

One limitation of using yeast to study these proteins is that it is difficult to assess the functional state of parkin or PINK1 *in vivo* using these methods of analysis. It is possible that parkin expressed in yeast has altered function compared to parkin expressed in human cells. For example, parkin could have increased or decreased activity, or even be completely inactive. This could be due to differences in the subcellular environment of yeast cells, which may render parkin unable to recognize substrates for ubiquitination.

Alternatively, yeast E2s may not interact with parkin, rendering it unable to carry out ubiquitination and protein degradation.

It is also possible that the introduction of a non-native E3 to yeast disrupts normal cellular protein quality control and causes adverse effects. This circumstance seems unlikely, as expression of parkin alone did not noticeably affect yeast in any of our experiments. This could, however, occur upon co-expression of parkin with PINK which caused drastic changes to parkin toxicity, localization, stability, and potentially, activity. Nevertheless, without a bona fide parkin substrate, it is nearly impossible to definitively determine if parkin activity is altered in yeast.

Similarly, it is difficult to assess the phosphorylation activity of PINK1 in yeast. In attempts to ensure normal PINK1 localization, a modified mitochondrial targeting sequence was used in our experiments to direct PINK1 to yeast mitochondria. Most evidence suggests that PINK1 predominantly acts to phosphorylate parkin or ubiquitin (88, 142, 154, 155). PINK1 has also been shown to phosphorylate mitochondrial proteins such as TOM20 and mitofusin (86, 87). As discussed above, the foreign environment of yeast could expose PINK1 to different substrates and yeast mitochondrial proteins may not be recognized by PINK1, preventing their phosphorylation. All these scenarios may contribute to the toxic effects caused by the co-expression of PINK1 and parkin in yeast, which do not directly translate to human cells.

Additionally, results from our yeast model may not have been replicated in mammalian system due to poor transfection efficiency. When optimizing transfection protocols, a GFP expressing plasmid was used to determine transfection efficiency, which

was calculated to be 68.7% based on fluorescence. However, when examining cells transfected with parkin in the presence or absence of PINK1, immunofluorescence showed an estimated 20-25% of cells expressing transfected parkin. Based on this low transfection efficiency, the lack of change to parkin localization and toxicity in the presence of PINK1 could be due to an insufficient proportion of cells expressing the transfected proteins. As a result, any phenotypic changes potentially occurring would have been masked by the large majority of untransfected cells.

Generally, the discrepancy observed between yeast and mammalian cells suggests that our results may not directly address how dysfunction of parkin and PINK1 cause cell death in human brain cells in PD. Nevertheless, our findings lead to a better understanding of the interactions of parkin and PINK1 and cellular processing of parkin. In future, it would be advantageous to expand other conditions established in our yeast model into mammalian cells, using the truncation variants and point mutants in attempts to characterize and map the PINK1/parkin related effects and perform structure-function analyses to assess misfolding altered the activity of PINK1 or parkin.

4.4 Future Directions

We have outlined several experiments above that will be completed in the future to address questions directly raised from our results. These experiments include: 1) characterizing the genetic interaction of parkin and SOD2, 2) assessing the ability of parkin to ubiquitinate prions or prion-like proteins, 3) expression of parkin in an SGT2 deletion strain containing additional deletions of yeast E3s to determine if parkin acts to assist normal yeast UPS, 4) perform large scale genetic screens with the entire yeast deletion and

overexpression libraries to elucidate previously undescribed genetic interactions of parkin and potentially, cellular functions, 5) test for direct oxidative modification of parkin, 6) determine the solubility and conformation of parkin puncta caused by mutations, truncations, oxidative stress, or co-expression with PINK1, 7) determine if parkin's Ubl domain can function in place of ubiquitin in yeast, 8) perform assays to test the activity of PINK1 and parkin in yeast to determine their functional status, 9) test for the presence of phospho-ubiquitin in yeast and determine if it is incorporated into K63 poly-ubiquitin chains build on substrates of the UPS, and 10) pulse-chase experiments to assess the degradation of parkin in mammalian cells.

Looking beyond, expanding research on parkin oxidation, misfolding, and degradation into other model systems could be extremely advantageous for understanding these effects in humans. *C. elegans* has been used previously to study PD, in particular parkin (54–57), and their eight defined dopaminergic neurons present a simplistic system to study parkin activity in PD-relevant neuronal cell types. Fruit fly (*D. melanogaster*) models have also proven to be useful for studying PD given that there are several fruit fly models of PD genes, including parkin (166–170), and that the relationship of PINK1 and parkin was first studied in fruit flies (171). Rodent models may also be useful to study parkin degradation and altered localization in a complex brain system that can be used to study and compare different brain regions that have different levels of neuronal cell death in PD patients. Ultimately, studying these aspects of parkin regulation and modification in post mortem PD patient brain samples will help to determine if findings from these models translate into humans and can be attributed to parkin-mediated PD.

4.5 Significance

The implication of parkin in both familial and idiopathic PD and the limited understanding of the mechanisms underlying parkin dysfunction in PD present a strong rationale for continued research on parkin oxidation, misfolding, and degradation. This thesis repeatedly provides evidence that oxidative stress, regulation by PINK1, protein misfolding, UPS-mediated degradation, and the protein quality control machinery work in tandem to regulate both parkin function and dysfunction. Future research based upon our findings and using our yeast model will further determine the underlying genetic, cellular, and molecular mechanisms by which parkin contributes to PD and may also establish parkin misfolding as a promising therapeutic target for PD treatment.

References

1. Smythies, J. (1999) The neurotoxicity of glutamate, dopamine, iron and reactive oxygen species: functional interrelationships in health and disease: a review-discussion. *Neurotox. Res.* **1**, 27–39
2. Stone, J. R., and Yang, S. (2006) Hydrogen peroxide: a signaling messenger. *Antioxid. Redox Signal.* **8**, 243–270
3. Rapoport, R., Hanukoglu, I., and Sklan, D. (1994) A fluorimetric assay for hydrogen peroxide, suitable for NAD(P)H-dependent superoxide generating redox systems. *Anal. Biochem.* **218**, 309–313
4. Kodydková, J., Vávrová, L., Kocík, M., and Žák, A. (2014) Human catalase, its polymorphisms, regulation and changes of its activity in different diseases. *Folia Biol. (Praha)*. **60**, 153–167
5. Dasuri, K., Zhang, L., and Keller, J. N. (2013) Oxidative stress, neurodegeneration, and the balance of protein degradation and protein synthesis. *Free Radic. Biol. Med.* **62**, 170–185
6. Miller, M. W., and Sadeh, N. (2014) Traumatic stress, oxidative stress and post-traumatic stress disorder: neurodegeneration and the accelerated-aging hypothesis. *Mol. Psychiatry*. **19**, 1156–1162
7. Chung, H. S., Wang, S.-B., Venkatraman, V., Murray, C. I., and Van Eyk, J. E. (2013) Cysteine oxidative posttranslational modifications: emerging regulation in the cardiovascular system. *Circ. Res.* **112**, 382–392
8. Miseta, A., and Csutora, P. (2000) Relationship Between the Occurrence of Cysteine in Proteins and the Complexity of Organisms. *Mol. Biol. Evol.* **17**, 1232–1239
9. Hartl, F. U., and Hayer-Hartl, M. (2002) Molecular chaperones in the cytosol: from nascent chain to folded protein. *Science*. **295**, 1852–1858
10. Cortez, L., and Sim, V. (2014) The therapeutic potential of chemical chaperones in protein folding diseases. *Prion*
11. Malinowska, L., Kroschwald, S., Munder, M. C., Richter, D., and Alberti, S. (2012) Molecular chaperones and stress-inducible protein-sorting factors coordinate the spatiotemporal distribution of protein aggregates. *Mol. Biol. Cell.* **23**, 3041–3056
12. Kozutsumi, Y., Segal, M., Normington, K., Gething, M. J., and Sambrook, J. (1988) The presence of malfolded proteins in the endoplasmic reticulum signals the induction of glucose-regulated proteins. *Nature*. **332**, 462–464

13. Lindberg, I., Shorter, J., Wiseman, R. L., Chiti, F., Dickey, C. A., and McLean, P. J. (2015) Chaperones in Neurodegeneration. *J. Neurosci. Off. J. Soc. Neurosci.* **35**, 13853–13859
14. Chhangani, D., and Mishra, A. (2013) Protein quality control system in neurodegeneration: a healing company hard to beat but failure is fatal. *Mol. Neurobiol.* **48**, 141–156
15. Ebrahimi-Fakhari, D., Saidi, L.-J., and Wahlster, L. (2013) Molecular chaperones and protein folding as therapeutic targets in Parkinson's disease and other synucleinopathies. *Acta Neuropathol. Commun.* **1**, 79
16. Inden, M., Kitamura, Y., Takeuchi, H., Yanagida, T., Takata, K., Kobayashi, Y., Taniguchi, T., Yoshimoto, K., Kaneko, M., Okuma, Y., Taira, T., Ariga, H., and Shimohama, S. (2007) Neurodegeneration of mouse nigrostriatal dopaminergic system induced by repeated oral administration of rotenone is prevented by 4-phenylbutyrate, a chemical chaperone. *J. Neurochem.* **101**, 1491–1504
17. Giasson, B. I., and Lee, V. M.-Y. (2003) Are ubiquitination pathways central to Parkinson's disease? *Cell.* **114**, 1–8
18. Correale, S., de Paola, I., Morgillo, C. M., Federico, A., Zaccaro, L., Pallante, P., Galeone, A., Fusco, A., Pedone, E., Luque, F. J., and Catalanotti, B. (2014) Structural model of the hUba1-UbcH10 quaternary complex: in silico and experimental analysis of the protein-protein interactions between E1, E2 and ubiquitin. *PLoS One.* **9**, e112082
19. Ungermannova, D., Parker, S. J., Nasveschuk, C. G., Wang, W., Quade, B., Zhang, G., Kuchta, R. D., Phillips, A. J., and Liu, X. (2012) Largazole and its derivatives selectively inhibit ubiquitin activating enzyme (e1). *PLoS One.* **7**, e29208
20. Moudry, P., Lukas, C., Macurek, L., Hanzlikova, H., Hodny, Z., Lukas, J., and Bartek, J. (2012) Ubiquitin-activating enzyme UBA1 is required for cellular response to DNA damage. *Cell Cycle Georget. Tex.* **11**, 1573–1582
21. Li, W., Bengtson, M. H., Ulbrich, A., Matsuda, A., Reddy, V. A., Orth, A., Chanda, S. K., Batalov, S., and Joazeiro, C. A. P. (2008) Genome-wide and functional annotation of human E3 ubiquitin ligases identifies MULAN, a mitochondrial E3 that regulates the organelle's dynamics and signaling. *PLoS One.* **3**, e1487
22. Jara, J. H., Frank, D. D., and Özdinler, P. H. (2013) Could dysregulation of UPS be a common underlying mechanism for cancer and neurodegeneration? Lessons from UCHL1. *Cell Biochem. Biophys.* **67**, 45–53
23. Qi, J., and Ronai, Z. A. (2015) Dysregulation of ubiquitin ligases in cancer. *Drug Resist. Updat. Rev. Comment. Antimicrob. Anticancer Chemother.* **23**, 1–11

24. Reyskens, K. M. S. E., and Essop, M. F. (2014) HIV protease inhibitors and onset of cardiovascular diseases: a central role for oxidative stress and dysregulation of the ubiquitin-proteasome system. *Biochim. Biophys. Acta.* **1842**, 256–268
25. Willis, M. S., Bevilacqua, A., Pulinilkunnil, T., Kienesberger, P., Tannu, M., and Patterson, C. (2014) The role of ubiquitin ligases in cardiac disease. *J. Mol. Cell. Cardiol.* **71**, 43–53
26. Ciechanover, A., and Brundin, P. (2003) The Ubiquitin Proteasome System in Neurodegenerative Diseases: Sometimes the Chicken, Sometimes the Egg. *Neuron.* **40**, 427–446
27. Zheng, C., Geetha, T., and Babu, J. R. (2014) Failure of ubiquitin proteasome system: risk for neurodegenerative diseases. *Neurodegener. Dis.* **14**, 161–175
28. Lim, L., Lee, X., and Song, J. (2015) Mechanism for transforming cytosolic SOD1 into integral membrane proteins of organelles by ALS-causing mutations. *Biochim. Biophys. Acta.* **1848**, 1–7
29. Lesage, S., and Brice, A. (2009) Parkinson's disease: from monogenic forms to genetic susceptibility factors. *Hum. Mol. Genet.* **18**, R48-59
30. Duennwald, M. L. (2013) Yeast as a platform to explore polyglutamine toxicity and aggregation. *Methods Mol. Biol. Clifton NJ.* **1017**, 153–161
31. Roberts, R. F., Wade-Martins, R., and Alegre-Abarategui, J. (2015) Direct visualization of alpha-synuclein oligomers reveals previously undetected pathology in Parkinson's disease brain. *Brain J. Neurol.* **138**, 1642–1657
32. Osterberg, V. R., Spinelli, K. J., Weston, L. J., Luk, K. C., Woltjer, R. L., and Unni, V. K. (2015) Progressive aggregation of alpha-synuclein and selective degeneration of lewy inclusion-bearing neurons in a mouse model of parkinsonism. *Cell Rep.* **10**, 1252–1260
33. Kaganovich, D., Kopito, R., and Frydman, J. (2008) Misfolded proteins partition between two distinct quality control compartments. *Nature.* **454**, 1088–1095
34. Lloret, A., Fuchsberger, T., Giraldo, E., and Viña, J. (2015) Molecular mechanisms linking amyloid β toxicity and Tau hyperphosphorylation in Alzheimer's disease. *Free Radic. Biol. Med.* **83**, 186–191
35. Kumar, A., Singh, A., and Ekavali (2015) A review on Alzheimer's disease pathophysiology and its management: an update. *Pharmacol. Rep.* **67**, 195–203
36. Trepte, P., Stempel, N., and Wanker, E. E. (2014) Spontaneous self-assembly of pathogenic huntingtin exon 1 protein into amyloid structures. *Essays Biochem.* **56**, 167–180

37. Park, S. M., and Kim, K. S. (2013) Proteolytic clearance of extracellular α -synuclein as a new therapeutic approach against Parkinson disease. *Prion*. **7**, 121–126
38. Burns, A., and Iliffe, S. (2009) Alzheimer's disease. *BMJ*. **338**, b158
39. Kawas, C. H. (2006) Medications and diet: protective factors for AD? *Alzheimer Dis. Assoc. Disord.* **20**, S89-96
40. Patterson, C., Feightner, J. W., Garcia, A., Hsiung, G.-Y. R., MacKnight, C., and Sadochnik, A. D. (2008) Diagnosis and treatment of dementia: 1. Risk assessment and primary prevention of Alzheimer disease. *CMAJ Can. Med. Assoc. J. J. Assoc. Medicale Can.* **178**, 548–556
41. Pohanka, M. (2011) Cholinesterases, a target of pharmacology and toxicology. *Biomed. Pap. Med. Fac. Univ. Palacký Olomouc Czechoslov.* **155**, 219–229
42. Walker, F. O. (2007) Huntington's disease. *Lancet Lond. Engl.* **369**, 218–228
43. Silverman, J. M., Fernando, S. M., Grad, L. I., Hill, A. F., Turner, B. J., Yerbury, J. J., and Cashman, N. R. (2016) Disease Mechanisms in ALS: Misfolded SOD1 Transferred Through Exosome-Dependent and Exosome-Independent Pathways. *Cell. Mol. Neurobiol.* **36**, 377–381
44. Aulas, A., and Vande Velde, C. (2015) Alterations in stress granule dynamics driven by TDP-43 and FUS: a link to pathological inclusions in ALS? *Front. Cell. Neurosci.* **9**, 423
45. Bury, J. J., Highley, J. R., Cooper-Knock, J., Goodall, E. F., Higginbottom, A., McDermott, C. J., Ince, P. G., Shaw, P. J., and Kirby, J. (2016) Oligogenic inheritance of optineurin (OPTN) and C9ORF72 mutations in ALS highlights localisation of OPTN in the TDP-43-negative inclusions of C9ORF72-ALS. *Neuropathol. Off. J. Jpn. Soc. Neuropathol.* **36**, 125–134
46. Keller, B. A., Volkening, K., Droppelmann, C. A., Ang, L. C., Rademakers, R., and Strong, M. J. (2012) Co-aggregation of RNA binding proteins in ALS spinal motor neurons: evidence of a common pathogenic mechanism. *Acta Neuropathol. (Berl.)*. **124**, 733–747
47. Droppelmann, C. A., Campos-Melo, D., Volkening, K., and Strong, M. J. (2014) The emerging role of guanine nucleotide exchange factors in ALS and other neurodegenerative diseases. *Front. Cell. Neurosci.* **8**, 282
48. Parkinson Society Fact Sheet (2015)
49. Kim, H. J., Kim, H. J., Lee, J. Y., Yun, J. Y., Kim, S. Y., Park, S. S., and Jeon, B. S. (2011) Phenotype analysis in patients with early onset Parkinson's disease with and without parkin mutations. *J Neurol.* **258**, 2260–7

50. Uversky, V. N., and Eliezer, D. (2009) Biophysics of Parkinson's disease: structure and aggregation of alpha-synuclein. *Curr Protein Pept Sci.* **10**, 483–99
51. Nuytemans, K., Theuns, J., Cruts, M., and Van Broeckhoven, C. (2010) Genetic etiology of Parkinson disease associated with mutations in the SNCA, PARK2, PINK1, PARK7, and LRRK2 genes: a mutation update. *Hum Mutat.* **31**, 763–80
52. Schiesling, C., Kieper, N., Seidel, K., and Krüger, R. (2008) Review: Familial Parkinson's disease – genetics, clinical phenotype and neuropathology in relation to the common sporadic form of the disease. *Neuropathol. Appl. Neurobiol.* **34**, 255–271
53. Shimura, H., Schlossmacher, M. G., Hattori, N., Frosch, M. P., Trockenbacher, A., Schneider, R., Mizuno, Y., Kosik, K. S., and Selkoe, D. J. (2001) Ubiquitination of a new form of alpha-synuclein by parkin from human brain: implications for Parkinson's disease. *Science.* **293**, 263–9
54. Chung, K. K., Zhang, Y., Lim, K. L., Tanaka, Y., Huang, H., Gao, J., Ross, C. A., Dawson, V. L., and Dawson, T. M. (2001) Parkin ubiquitinates the alpha-synuclein-interacting protein, synphilin-1: implications for Lewy-body formation in Parkinson disease. *Nat Med.* **7**, 1144–50
55. Kitada, T., Asakawa, S., Hattori, N., Matsumine, H., Yamamura, Y., Minoshima, S., Yokochi, M., Mizuno, Y., and Shimizu, N. (1998) Mutations in the parkin gene cause autosomal recessive juvenile parkinsonism. *Nature.* **392**, 605–8
56. Terreni, L., Calabrese, E., Calella, A. M., Forloni, G., and Mariani, C. (2001) New mutation (R42P) of the parkin gene in the ubiquitinlike domain associated with parkinsonism. *Neurology.* **56**, 463–466
57. Corti, O., Lesage, S., and Brice, A. (2011) What Genetics Tells us About the Causes and Mechanisms of Parkinson's Disease. *Physiol. Rev.* **91**, 1161–1218
58. Morett, E., and Bork, P. (1999) A novel transactivation domain in parkin. *Trends Biochem. Sci.* **24**, 229–231
59. Hristova, V. A., Beasley, S. A., Rylett, R. J., and Shaw, G. S. (2009) Identification of a novel Zn²⁺-binding domain in the autosomal recessive juvenile Parkinson-related E3 ligase parkin. *J Biol Chem.* **284**, 14978–86
60. Spratt, D. E., Walden, H., and Shaw, G. S. (2014) RBR E3 ubiquitin ligases: new structures, new insights, new questions. *Biochem. J.* **458**, 421–437
61. Buetow, L., Gabrielsen, M., Anthony, N. G., Dou, H., Patel, A., Aitkenhead, H., Sibbet, G. J., Smith, B. O., and Huang, D. T. (2015) Activation of a primed RING E3-E2-ubiquitin complex by non-covalent ubiquitin. *Mol. Cell.* **58**, 297–310

62. Kamadurai, H. B., Qiu, Y., Deng, A., Harrison, J. S., Macdonald, C., Actis, M., Rodrigues, P., Miller, D. J., Souphron, J., Lewis, S. M., Kurinov, I., Fujii, N., Hammel, M., Piper, R., Kuhlman, B., and Schulman, B. A. (2013) Mechanism of ubiquitin ligation and lysine prioritization by a HECT E3. *Elife*. **2**, e00828
63. Kumar, A., Aguirre, J. D., Condos, T. E. C., Martinez-Torres, R. J., Chaugule, V. K., Toth, R., Sundaramoorthy, R., Mercier, P., Knebel, A., Spratt, D. E., Barber, K. R., Shaw, G. S., and Walden, H. (2015) Disruption of the autoinhibited state primes the E3 ligase parkin for activation and catalysis. *EMBO J*. **34**, 2506–2521
64. Spratt, D. E., Julio Martinez-Torres, R., Noh, Y. J., Mercier, P., Manczyk, N., Barber, K. R., Aguirre, J. D., Burchell, L., Purkiss, A., Walden, H., and Shaw, G. S. (2013) A molecular explanation for the recessive nature of parkin-linked Parkinson's disease. *Nat Commun*. **4**, 1983
65. Chaugule, V. K., Burchell, L., Barber, K. R., Sidhu, A., Leslie, S. J., Shaw, G. S., and Walden, H. (2011) Autoregulation of Parkin activity through its ubiquitin-like domain. *Embo J*. **30**, 2853–67
66. West, A., Periquet, M., Lincoln, S., Lucking, C. B., Nicholl, D., Bonifati, V., Rawal, N., Gasser, T., Lohmann, E., Deleuze, J. F., Maraganore, D., Levey, A., Wood, N., Durr, A., Hardy, J., Brice, A., and Farrer, M. (2002) Complex relationship between Parkin mutations and Parkinson disease. *Am J Med Genet*. **114**, 584–91
67. Mata, I. F., Lockhart, P. J., and Farrer, M. J. (2004) Parkin genetics: one model for Parkinson's disease. *Hum. Mol. Genet*. **13 Spec No 1**, R127-133
68. Sarraf, S. A., Raman, M., Guarani-Pereira, V., Sowa, M. E., Huttlin, E. L., Gygi, S. P., and Harper, J. W. (2013) Landscape of the PARKIN-dependent ubiquitylome in response to mitochondrial depolarization. *Nature*. **496**, 372–6
69. Kazlauskaitė, A., Kelly, V., Johnson, C., Baillie, C., Hastie, C. J., Peggie, M., Macartney, T., Woodroof, H. I., Alessi, D. R., Pedrioli, P. G. A., and Muqit, M. M. K. (2014) Phosphorylation of Parkin at Serine65 is essential for activation: elaboration of a Miro1 substrate-based assay of Parkin E3 ligase activity. *Open Biol*. **4**, 130213
70. Schlehe, J. S., Lutz, A. K., Pilsl, A., Lammermann, K., Grgur, K., Henn, I. H., Tatzelt, J., and Winklhofer, K. F. (2008) Aberrant folding of pathogenic Parkin mutants: aggregation versus degradation. *J Biol Chem*. **283**, 13771–9
71. Gu, W. J., Corti, O., Araujo, F., Hampe, C., Jacquier, S., Lucking, C. B., Abbas, N., Duyckaerts, C., Rooney, T., Pradier, L., Ruberg, M., and Brice, A. (2003) The C289G and C418R missense mutations cause rapid sequestration of human Parkin into insoluble aggregates. *Neurobiol Dis*. **14**, 357–64
72. Meng, F., Yao, D., Shi, Y., Kabakoff, J., Wu, W., Reicher, J., Ma, Y., Moosmann, B., Masliah, E., Lipton, S. A., and Gu, Z. (2011) Oxidation of the cysteine-rich

regions of parkin perturbs its E3 ligase activity and contributes to protein aggregation. *Mol. Neurodegener.* **6**, 34

73. Choi, P., Golts, N., Snyder, H., Chong, M., Petrucelli, L., Hardy, J., Sparkman, D., Cochran, E., Lee, J. M., and Wolozin, B. (2001) Co-association of parkin and alpha-synuclein. *Neuroreport.* **12**, 2839–2843
74. Schlossmacher, M. G., Frosch, M. P., Gai, W. P., Medina, M., Sharma, N., Forno, L., Ochiishi, T., Shimura, H., Sharon, R., Hattori, N., Langston, J. W., Mizuno, Y., Hyman, B. T., Selkoe, D. J., and Kosik, K. S. (2002) Parkin localizes to the Lewy bodies of Parkinson disease and dementia with Lewy bodies. *Am. J. Pathol.* **160**, 1655–1667
75. Chan, N. C., Salazar, A. M., Pham, A. H., Sweredoski, M. J., Kolawa, N. J., Graham, R. L., Hess, S., and Chan, D. C. (2011) Broad activation of the ubiquitin-proteasome system by Parkin is critical for mitophagy. *Hum Mol Genet.* **20**, 1726–37
76. Narendra, D., Tanaka, A., Suen, D.-F., and Youle, R. J. (2009) Parkin-induced mitophagy in the pathogenesis of Parkinson disease. *Autophagy.* **5**, 706–708
77. Okatsu, K., Kimura, M., Oka, T., Tanaka, K., and Matsuda, N. (2015) Unconventional PINK1 localization to the outer membrane of depolarized mitochondria drives Parkin recruitment. *J. Cell Sci.* **128**, 964–978
78. Matsuda, N., and Tanaka, K. (2010) Uncovering the roles of PINK1 and parkin in mitophagy. *Autophagy.* **6**, 952–4
79. Sim, C. H., Gabriel, K., Mills, R. D., Culvenor, J. G., and Cheng, H.-C. (2012) Analysis of the regulatory and catalytic domains of PTEN-induced kinase-1 (PINK1). *Hum. Mutat.* **33**, 1408–1422
80. Greene, A. W., Grenier, K., Aguilera, M. A., Muise, S., Farazifard, R., Haque, M. E., McBride, H. M., Park, D. S., and Fon, E. A. (2012) Mitochondrial processing peptidase regulates PINK1 processing, import and Parkin recruitment. *EMBO Rep.* **13**, 378–385
81. Matsuda, N., Sato, S., Shiba, K., Okatsu, K., Saisho, K., Gautier, C. A., Sou, Y.-S., Saiki, S., Kawajiri, S., Sato, F., Kimura, M., Komatsu, M., Hattori, N., and Tanaka, K. (2010) PINK1 stabilized by mitochondrial depolarization recruits Parkin to damaged mitochondria and activates latent Parkin for mitophagy. *J. Cell Biol.* **189**, 211–221
82. Song, S., Jang, S., Park, J., Bang, S., Choi, S., Kwon, K.-Y., Zhuang, X., Kim, E., and Chung, J. (2013) Characterization of PINK1 (PTEN-induced putative kinase 1) mutations associated with Parkinson disease in mammalian cells and *Drosophila*. *J. Biol. Chem.* **288**, 5660–5672

83. Park, J. W., Lee, S. Y., Yang, J. Y., Rho, H. W., Park, B. H., Lim, S. N., Kim, J. S., and Kim, H. R. (1997) Effect of carbonyl cyanide m-chlorophenylhydrazone (CCCP) on the dimerization of lipoprotein lipase. *Biochim. Biophys. Acta.* **1344**, 132–138
84. Narendra, D. P., Jin, S. M., Tanaka, A., Suen, D.-F., Gautier, C. A., Shen, J., Cookson, M. R., and Youle, R. J. (2010) PINK1 Is Selectively Stabilized on Impaired Mitochondria to Activate Parkin. *PLoS Biol.* 10.1371/journal.pbio.1000298
85. Koyano, F., Okatsu, K., Kosako, H., Tamura, Y., Go, E., Kimura, M., Kimura, Y., Tsuchiya, H., Yoshihara, H., Hirokawa, T., Endo, T., Fon, E. A., Trempe, J.-F., Saeki, Y., Tanaka, K., and Matsuda, N. (2014) Ubiquitin is phosphorylated by PINK1 to activate parkin. *Nature.* **510**, 162–166
86. Bertolin, G., Ferrando-Miguel, R., Jacoupy, M., Traver, S., Grenier, K., Greene, A. W., Dauphin, A., Waharte, F., Bayot, A., Salamero, J., Lombes, A., Bulteau, A. L., Fon, E. A., Brice, A., and Corti, O. (2013) The TOMM machinery is a molecular switch in PINK1 and PARK2/PARKIN-dependent mitochondrial clearance. *Autophagy.* **9**, 1801–17
87. Gegg, M. E., Cooper, J. M., Chau, K. Y., Rojo, M., Schapira, A. H., and Taanman, J. W. (2010) Mitofusin 1 and mitofusin 2 are ubiquitinated in a PINK1/parkin-dependent manner upon induction of mitophagy. *Hum Mol Genet.* **19**, 4861–70
88. Shiba-Fukushima, K., Imai, Y., Yoshida, S., Ishihama, Y., Kanao, T., Sato, S., and Hattori, N. (2012) PINK1-mediated phosphorylation of the Parkin ubiquitin-like domain primes mitochondrial translocation of Parkin and regulates mitophagy. *Sci Rep.* **2**, 1002
89. Botstein, D., Chervitz, S. A., and Cherry, J. M. (1997) Yeast as a model organism. *Science.* **277**, 1259–1260
90. Duennwald, M. L. (2011) Monitoring polyglutamine toxicity in yeast. *Methods San Diego Calif.* **53**, 232–237
91. Duennwald, M. L. (2011) Polyglutamine misfolding in yeast: toxic and protective aggregation. *Prion.* **5**, 285–290
92. Chafekar, S. M., Wisén, S., Thompson, A. D., Echeverria, A., Walter, G. M., Evans, C. G., Makley, L. N., Gestwicki, J. E., and Duennwald, M. L. (2012) Pharmacological tuning of heat shock protein 70 modulates polyglutamine toxicity and aggregation. *ACS Chem. Biol.* **7**, 1556–1564
93. Repalli, J., and Meruelo, D. (2015) Screening strategies to identify HSP70 modulators to treat Alzheimer's disease. *Drug Des. Devel. Ther.* **9**, 321–331

94. Chen, X., and Petranovic, D. (2015) Amyloid- β peptide-induced cytotoxicity and mitochondrial dysfunction in yeast. *FEMS Yeast Res.* 10.1093/femsyr/fov061
95. Nair, S., Traini, M., Dawes, I. W., and Perrone, G. G. (2014) Genome-wide analysis of *Saccharomyces cerevisiae* identifies cellular processes affecting intracellular aggregation of Alzheimer's amyloid- β 42: importance of lipid homeostasis. *Mol. Biol. Cell.* **25**, 2235–2249
96. D'Angelo, F., Vignaud, H., Di Martino, J., Salin, B., Devin, A., Cullin, C., and Marchal, C. (2013) A yeast model for amyloid- β aggregation exemplifies the role of membrane trafficking and PICALM in cytotoxicity. *Dis. Model. Mech.* **6**, 206–216
97. Martins, D., and English, A. M. (2014) SOD1 oxidation and formation of soluble aggregates in yeast: relevance to sporadic ALS development. *Redox Biol.* **2**, 632–639
98. Kryndushkin, D., Wickner, R. B., and Shewmaker, F. (2011) FUS/TLS forms cytoplasmic aggregates, inhibits cell growth and interacts with TDP-43 in a yeast model of amyotrophic lateral sclerosis. *Protein Cell.* **2**, 223–236
99. Gade, V. R., Kardani, J., and Roy, I. (2014) Effect of endogenous Hsp104 chaperone in yeast models of sporadic and familial Parkinson's disease. *Int. J. Biochem. Cell Biol.* **55**, 87–92
100. Mbefo, M. K., Fares, M.-B., Paleologou, K., Oueslati, A., Yin, G., Tenreiro, S., Pinto, M., Outeiro, T., Zweckstetter, M., Masliah, E., and Lashuel, H. A. (2015) Parkinson disease mutant E46K enhances α -synuclein phosphorylation in mammalian cell lines, in yeast, and in vivo. *J. Biol. Chem.* **290**, 9412–9427
101. Wang, S., Zhang, S., Liou, L.-C., Ren, Q., Zhang, Z., Caldwell, G. A., Caldwell, K. A., and Witt, S. N. (2014) Phosphatidylethanolamine deficiency disrupts α -synuclein homeostasis in yeast and worm models of Parkinson disease. *Proc. Natl. Acad. Sci. U. S. A.* **111**, E3976-3985
102. Dixon, C., Mathias, N., Zweig, R. M., Davis, D. A., and Gross, D. S. (2005) Alpha-synuclein targets the plasma membrane via the secretory pathway and induces toxicity in yeast. *Genetics.* **170**, 47–59
103. Popova, B., Kleinknecht, A., and Braus, G. H. (2015) Posttranslational Modifications and Clearing of α -Synuclein Aggregates in Yeast. *Biomolecules.* **5**, 617–634
104. Petroi, D., Popova, B., Taheri-Talesh, N., Irniger, S., Shahpasandzadeh, H., Zweckstetter, M., Outeiro, T. F., and Braus, G. H. (2012) Aggregate clearance of α -synuclein in *Saccharomyces cerevisiae* depends more on autophagosome and vacuole function than on the proteasome. *J. Biol. Chem.* **287**, 27567–27579

105. De Graeve, S., Marinelli, S., Stolz, F., Hendrix, J., Vandamme, J., Engelborghs, Y., Van Dijck, P., and Thevelein, J. M. (2013) Mammalian ribosomal and chaperone protein RPS3A counteracts α -synuclein aggregation and toxicity in a yeast model system. *Biochem. J.* **455**, 295–306
106. Shendelman, S., Jonason, A., Martinat, C., Leete, T., and Abeliovich, A. (2004) DJ-1 is a redox-dependent molecular chaperone that inhibits alpha-synuclein aggregate formation. *PLoS Biol.* **2**, e362
107. Zhou, W., Zhu, M., Wilson, M. A., Petsko, G. A., and Fink, A. L. (2006) The oxidation state of DJ-1 regulates its chaperone activity toward alpha-synuclein. *J. Mol. Biol.* **356**, 1036–1048
108. Skoneczna, A., Miciałkiewicz, A., and Skoneczny, M. (2007) *Saccharomyces cerevisiae* Hsp31p, a stress response protein conferring protection against reactive oxygen species. *Free Radic. Biol. Med.* **42**, 1409–1420
109. Pereira, C., Costa, V., Martins, L. M., and Saraiva, L. (2015) A yeast model of the Parkinson's disease-associated protein Parkin. *Exp. Cell Res.* **333**, 73–79
110. Alberti, S., Gitler, A. D., and Lindquist, S. (2007) A suite of Gateway® cloning vectors for high-throughput genetic analysis in *Saccharomyces cerevisiae*. *Yeast Chichester Engl.* **24**, 913–919
111. von der Haar, T. (2007) Optimized Protein Extraction for Quantitative Proteomics of Yeasts. *PLoS ONE*. 10.1371/journal.pone.0001078
112. Wauer, T., and Komander, D. (2013) Structure of the human Parkin ligase domain in an autoinhibited state. *EMBO J.* 10.1038/emboj.2013.125
113. Narendra, D., Tanaka, A., Suen, D.-F., and Youle, R. J. (2008) Parkin is recruited selectively to impaired mitochondria and promotes their autophagy. *J. Cell Biol.* **183**, 795–803
114. Winklhofer, K. F., Henn, I. H., Kay-Jackson, P. C., Heller, U., and Tatzelt, J. (2003) Inactivation of Parkin by Oxidative Stress and C-terminal Truncations A PROTECTIVE ROLE OF MOLECULAR CHAPERONES. *J. Biol. Chem.* **278**, 47199–47208
115. Saffi, J., Sonego, L., Varela, Q. D., and Salvador, M. (2006) Antioxidant activity of L-ascorbic acid in wild-type and superoxide dismutase deficient strains of *Saccharomyces cerevisiae*. *Redox Rep. Commun. Free Radic. Res.* **11**, 179–184
116. van Loon, A. P., Pesold-Hurt, B., and Schatz, G. (1986) A yeast mutant lacking mitochondrial manganese-superoxide dismutase is hypersensitive to oxygen. *Proc. Natl. Acad. Sci. U. S. A.* **83**, 3820–3824

117. Okazaki, S., Tachibana, T., Naganuma, A., Mano, N., and Kuge, S. (2007) Multistep disulfide bond formation in Yap1 is required for sensing and transduction of H₂O₂ stress signal. *Mol. Cell.* **27**, 675–688
118. Kama, R., Robinson, M., and Gerst, J. E. (2007) Btn2, a Hook1 Ortholog and Potential Batten Disease-Related Protein, Mediates Late Endosome-Golgi Protein Sorting in Yeast. *Mol. Cell. Biol.* **27**, 605–621
119. Kiktev, D. A., Patterson, J. C., Müller, S., Bariar, B., Pan, T., and Chernoff, Y. O. (2012) Regulation of chaperone effects on a yeast prion by cochaperone Sgt2. *Mol. Cell. Biol.* **32**, 4960–4970
120. Praekelt, U. M., and Meacock, P. A. (1990) HSP12, a new small heat shock gene of *Saccharomyces cerevisiae*: analysis of structure, regulation and function. *Mol. Gen. Genet. MGG.* **223**, 97–106
121. Tkach, J. M., Yimit, A., Lee, A. Y., Riffle, M., Costanzo, M., Jaschob, D., Hendry, J. A., Ou, J., Moffat, J., Boone, C., Davis, T. N., Nislow, C., and Brown, G. W. (2012) Dissecting DNA damage response pathways by analysing protein localization and abundance changes during DNA replication stress. *Nat. Cell Biol.* **14**, 966–976
122. Panaretou, B., and Piper, P. W. (1992) The plasma membrane of yeast acquires a novel heat-shock protein (hsp30) and displays a decline in proton-pumping ATPase levels in response to both heat shock and the entry to stationary phase. *Eur. J. Biochem. FEBS.* **206**, 635–640
123. Muller, E. G. (1991) Thioredoxin deficiency in yeast prolongs S phase and shortens the G1 interval of the cell cycle. *J. Biol. Chem.* **266**, 9194–9202
124. Garrido, E. O., and Grant, C. M. (2002) Role of thioredoxins in the response of *Saccharomyces cerevisiae* to oxidative stress induced by hydroperoxides. *Mol. Microbiol.* **43**, 993–1003
125. Ozkaynak, E., Finley, D., Solomon, M. J., and Varshavsky, A. (1987) The yeast ubiquitin genes: a family of natural gene fusions. *EMBO J.* **6**, 1429–1439
126. Finley, D., Sadis, S., Monia, B. P., Boucher, P., Ecker, D. J., Crooke, S. T., and Chau, V. (1994) Inhibition of proteolysis and cell cycle progression in a multiubiquitination-deficient yeast mutant. *Mol. Cell. Biol.* **14**, 5501–5509
127. Trotter, E. W., Rand, J. D., Vickerstaff, J., and Grant, C. M. (2008) The yeast Tsa1 peroxiredoxin is a ribosome-associated antioxidant. *Biochem. J.* **412**, 73–80
128. Wong, C.-M., Siu, K.-L., and Jin, D.-Y. (2004) Peroxiredoxin-null yeast cells are hypersensitive to oxidative stress and are genomically unstable. *J. Biol. Chem.* **279**, 23207–23213

129. Wong, C.-M., Zhou, Y., Ng, R. W. M., Kung Hf, H., and Jin, D.-Y. (2002) Cooperation of yeast peroxiredoxins Tsa1p and Tsa2p in the cellular defense against oxidative and nitrosative stress. *J. Biol. Chem.* **277**, 5385–5394
130. Munhoz, D. C., and Netto, L. E. S. (2004) Cytosolic thioredoxin peroxidase I and II are important defenses of yeast against organic hydroperoxide insult: catalases and peroxiredoxins cooperate in the decomposition of H₂O₂ by yeast. *J. Biol. Chem.* **279**, 35219–35227
131. Kryndushkin, D. S., Shewmaker, F., and Wickner, R. B. (2008) Curing of the [URE3] prion by Btn2p, a Batten disease-related protein. *EMBO J.* **27**, 2725–2735
132. Hiltunen, J. K., Mursula, A. M., Rottensteiner, H., Wierenga, R. K., Kastaniotis, A. J., and Gurvitz, A. (2003) The biochemistry of peroxisomal beta-oxidation in the yeast *Saccharomyces cerevisiae*. *FEMS Microbiol. Rev.* **27**, 35–64
133. Jamieson, D. J. (1998) Oxidative stress responses of the yeast *Saccharomyces cerevisiae*. *Yeast Chichester Engl.* **14**, 1511–1527
134. Biteau, B., Labarre, J., and Toledano, M. B. (2003) ATP-dependent reduction of cysteine-sulphinic acid by *S. cerevisiae* sulphiredoxin. *Nature.* **425**, 980–984
135. Pedrajas, J. R., Miranda-Vizuete, A., Javanmardy, N., Gustafsson, J. A., and Spyrou, G. (2000) Mitochondria of *Saccharomyces cerevisiae* contain one-conserved cysteine type peroxiredoxin with thioredoxin peroxidase activity. *J. Biol. Chem.* **275**, 16296–16301
136. Sakaki, K., Tashiro, K., Kuhara, S., and Mihara, K. (2003) Response of genes associated with mitochondrial function to mild heat stress in yeast *Saccharomyces cerevisiae*. *J. Biochem. (Tokyo).* **134**, 373–384
137. Dröge, W. (2002) Free radicals in the physiological control of cell function. *Physiol. Rev.* **82**, 47–95
138. Pauly, N., Pucciariello, C., Mandon, K., Innocenti, G., Jamet, A., Baudouin, E., Hérouart, D., Frendo, P., and Puppo, A. (2006) Reactive oxygen and nitrogen species and glutathione: key players in the legume-Rhizobium symbiosis. *J. Exp. Bot.* **57**, 1769–1776
139. Spatola, M., and Wider, C. (2014) Genetics of Parkinson's disease: the yield. *Parkinsonism Relat. Disord.* **20 Suppl 1**, S35-38
140. Watanabe, M., Funakoshi, T., Unuma, K., Aki, T., and Uemura, K. (2014) Activation of the ubiquitin-proteasome system against arsenic trioxide cardiotoxicity involves ubiquitin ligase Parkin for mitochondrial homeostasis. *Toxicology.* **322**, 43–50

141. Wang, C., Ko, H. S., Thomas, B., Tsang, F., Chew, K. C. M., Tay, S.-P., Ho, M. W. L., Lim, T.-M., Soong, T.-W., Pletnikova, O., Troncoso, J., Dawson, V. L., Dawson, T. M., and Lim, K.-L. (2005) Stress-induced alterations in parkin solubility promote parkin aggregation and compromise parkin's protective function. *Hum. Mol. Genet.* **14**, 3885–3897
142. Iguchi, M., Kujuro, Y., Okatsu, K., Koyano, F., Kosako, H., Kimura, M., Suzuki, N., Uchiyama, S., Tanaka, K., and Matsuda, N. (2013) Parkin-catalyzed Ubiquitin-Ester Transfer Is Triggered by PINK1-dependent Phosphorylation. *J. Biol. Chem.* **288**, 22019–22032
143. Shibata, T., Ohta, T., Tong, K. I., Kokubu, A., Odogawa, R., Tsuta, K., Asamura, H., Yamamoto, M., and Hirohashi, S. (2008) Cancer related mutations in NRF2 impair its recognition by Keap1-Cul3 E3 ligase and promote malignancy. *Proc. Natl. Acad. Sci. U. S. A.* **105**, 13568–13573
144. Perfeito, R., Cunha-Oliveira, T., and Rego, A. C. (2013) Reprint of: revisiting oxidative stress and mitochondrial dysfunction in the pathogenesis of Parkinson disease-resemblance to the effect of amphetamine drugs of abuse. *Free Radic. Biol. Med.* **62**, 186–201
145. Bolner, A., Micciolo, R., Bosello, O., and Nordera, G. P. (2016) A Panel of Oxidative Stress Markers in Parkinson's Disease. *Clin. Lab.* **62**, 105–112
146. Chung, K. K., Thomas, B., Li, X., Pletnikova, O., Troncoso, J. C., Marsh, L., Dawson, V. L., and Dawson, T. M. (2004) S-nitrosylation of parkin regulates ubiquitination and compromises parkin's protective function. *Science.* **304**, 1328–31
147. Van Laar, V. S., Roy, N., Liu, A., Rajprohat, S., Arnold, B., Dukes, A. A., Holbein, C. D., and Berman, S. B. (2015) Glutamate excitotoxicity in neurons triggers mitochondrial and endoplasmic reticulum accumulation of Parkin, and, in the presence of N-acetyl cysteine, mitophagy. *Neurobiol. Dis.* **74**, 180–193
148. Flynn, J. M., and Melov, S. (2013) SOD2 in Mitochondrial Dysfunction and Neurodegeneration. *Free Radic. Biol. Med.* 10.1016/j.freeradbiomed.2013.05.027
149. Wickner, R. B., Bezsonov, E., and Bateman, D. A. (2014) Normal levels of the antiprion proteins Btn2 and Cur1 cure most newly formed [URE3] prion variants. *Proc. Natl. Acad. Sci.* **111**, E2711–E2720
150. Willingham, S., Outeiro, T. F., DeVit, M. J., Lindquist, S. L., and Muchowski, P. J. (2003) Yeast genes that enhance the toxicity of a mutant huntingtin fragment or alpha-synuclein. *Science.* **302**, 1769–1772
151. Gorr, T. A., and Vogel, J. (2015) Western blotting revisited: critical perusal of underappreciated technical issues. *Proteomics Clin. Appl.* **9**, 396–405

152. Morano, K. A., Grant, C. M., and Moye-Rowley, W. S. (2012) The response to heat shock and oxidative stress in *Saccharomyces cerevisiae*. *Genetics*. **190**, 1157–1195
153. Theodoraki, M. A., Nillegoda, N. B., Saini, J., and Caplan, A. J. (2012) A network of ubiquitin ligases is important for the dynamics of misfolded protein aggregates in yeast. *J. Biol. Chem.* **287**, 23911–23922
154. Kane, L. A., Lazarou, M., Fogel, A. I., Li, Y., Yamano, K., Sarraf, S. A., Banerjee, S., and Youle, R. J. (2014) PINK1 phosphorylates ubiquitin to activate Parkin E3 ubiquitin ligase activity. *J. Cell Biol.* **205**, 143–153
155. Kazlauskaitė, A., Kondapalli, C., Gourlay, R., Campbell, D. G., Ritorto, M. S., Hofmann, K., Alessi, D. R., Knebel, A., Trost, M., and Muqit, M. M. K. (2014) Parkin is activated by PINK1-dependent phosphorylation of ubiquitin at Ser65. *Biochem. J.* **460**, 127–139
156. Kondapalli, C., Kazlauskaitė, A., Zhang, N., Woodroof, H. I., Campbell, D. G., Gourlay, R., Burchell, L., Walden, H., Macartney, T. J., Deak, M., Knebel, A., Alessi, D. R., and Muqit, M. M. (2012) PINK1 is activated by mitochondrial membrane potential depolarization and stimulates Parkin E3 ligase activity by phosphorylating Serine 65. *Open Biol.* **2**, 120080
157. Janczak, M., Bukowski, M., Górecki, A., Dubin, G., Dubin, A., and Wladyka, B. (2015) A systematic investigation of the stability of green fluorescent protein fusion proteins. *Acta Biochim. Pol.* **62**, 407–411
158. Duennwald, M. L., Jagadish, S., Muchowski, P. J., and Lindquist, S. (2006) Flanking sequences profoundly alter polyglutamine toxicity in yeast. *Proc. Natl. Acad. Sci. U. S. A.* **103**, 11045–11050
159. Wagner, L. E., Li, W.-H., Joseph, S. K., and Yule, D. I. (2004) Functional consequences of phosphomimetic mutations at key cAMP-dependent protein kinase phosphorylation sites in the type 1 inositol 1,4,5-trisphosphate receptor. *J. Biol. Chem.* **279**, 46242–46252
160. Zhang, H.-T., Mi, L., Wang, T., Yuan, L., Li, X.-H., Dong, L.-S., Zhao, P., Fu, J.-L., Yao, B.-Y., and Zhou, Z.-C. (2016) PINK1/Parkin-mediated mitophagy play a protective role in manganese induced apoptosis in SH-SY5Y cells. *Toxicol. Vitro Int. J. Publ. Assoc. BIBRA.* **34**, 212–219
161. Dai, H., Deng, Y., Zhang, J., Han, H., Zhao, M., Li, Y., Zhang, C., Tian, J., Bing, G., and Zhao, L. (2015) PINK1/Parkin-mediated mitophagy alleviates chlorpyrifos-induced apoptosis in SH-SY5Y cells. *Toxicology.* **334**, 72–80
162. Springer, W., Hoppe, T., Schmidt, E., and Baumeister, R. (2005) A *Caenorhabditis elegans* Parkin mutant with altered solubility couples alpha-synuclein aggregation to proteotoxic stress. *Hum. Mol. Genet.* **14**, 3407–3423

163. Valenci, I., Yonai, L., Bar-Yaacov, D., Mishmar, D., and Ben-Zvi, A. (2015) Parkin modulates heteroplasmy of truncated mtDNA in *Caenorhabditis elegans*. *Mitochondrion*. **20**, 64–70
164. Vistbakka, J., VanDuyn, N., Wong, G., and Nass, R. (2012) *C. elegans* as a genetic model system to identify Parkinson's disease-associated therapeutic targets. *CNS Neurol. Disord. Drug Targets*. **11**, 957–964
165. Chakraborty, S., Bornhorst, J., Nguyen, T. T., and Aschner, M. (2013) Oxidative stress mechanisms underlying Parkinson's disease-associated neurodegeneration in *C. elegans*. *Int. J. Mol. Sci.* **14**, 23103–23128
166. Bhandari, P., Song, M., Chen, Y., Burelle, Y., and Dorn, G. W. (2014) Mitochondrial contagion induced by Parkin deficiency in *Drosophila* hearts and its containment by suppressing mitofusin. *Circ. Res.* **114**, 257–265
167. Botella, J. A., Bayersdorfer, F., Gmeiner, F., and Schneuwly, S. (2009) Modelling Parkinson's disease in *Drosophila*. *Neuromolecular Med.* **11**, 268–80
168. Cha, G. H., Kim, S., Park, J., Lee, E., Kim, M., Lee, S. B., Kim, J. M., Chung, J., and Cho, K. S. (2005) Parkin negatively regulates JNK pathway in the dopaminergic neurons of *Drosophila*. *Proc Natl Acad Sci U A.* **102**, 10345–50
169. de Castro, I. P., Costa, A. C., Celardo, I., Tufi, R., Dinsdale, D., Loh, S. H. Y., and Martins, L. M. (2013) *Drosophila* ref(2)P is required for the parkin-mediated suppression of mitochondrial dysfunction in pink1 mutants. *Cell Death Dis.* **4**, e873
170. Thomas, R. E., Andrews, L. A., Burman, J. L., Lin, W.-Y., and Pallanck, L. J. (2014) PINK1-Parkin pathway activity is regulated by degradation of PINK1 in the mitochondrial matrix. *PLoS Genet.* **10**, e1004279
171. Park, J., Lee, S. B., Lee, S., Kim, Y., Song, S., Kim, S., Bae, E., Kim, J., Shong, M., Kim, J. M., and Chung, J. (2006) Mitochondrial dysfunction in *Drosophila* PINK1 mutants is complemented by parkin. *Nature.* **441**, 1157–61
172. Gill, G. (2004) SUMO and ubiquitin in the nucleus: different functions, similar mechanisms? *Genes Dev.* **18**, 2046–2059

Appendices

Appendix 1. Discussion of technical limitations.

Immunofluorescence Microscopy

The use of immunofluorescence microscopy to visualize subcellular localization of proteins is a powerful tool that eliminates the need to genetically modify the cells or cellular proteins with fluorescent protein fusions. One limitation of immunofluorescence microscopy is the availability of specific and effective antibodies required for proper protein recognition. Parkin is a widely studied protein and there are several commercially available antibodies recognizing different epitopes within parkin. In this study, four different parkin antibodies were used that mapped to three different domains of the protein.

HeLa cells were chosen to transfect wild-type human parkin as the literature suggests that they do not express any endogenous parkin. Untransfected HeLa cells were used to test the specificity of these four parkin antibodies. These experiments showed that all four of these parkin antibodies resulted in significant background staining. (**Appendix 3**). While the RING1 and Rcat/RING2 specific antibodies caused diffuse staining throughout the cytosol of HeLa cells with varying degrees of intensity, the Ubl specific antibody caused strong staining in the nucleus and weaker staining in the cytosol. It is possible that the Ubl specific antibody, given the structural similarities of the Ubl domain to ubiquitin, could be binding to ubiquitin or the ubiquitin-like protein SUMO in HeLa cells which would account for the strong nuclear and weaker cytosolic staining (172). Alternatively, HeLa cells might express parkin-like proteins or proteins with structurally

similar epitopes to parkin, which may include other E3s. This would result in non-specific binding of parkin antibodies in fixed HeLa cells. This speculation is supported by the fact that Western blots performed with these antibodies did not elicit non-specific staining, suggesting that these antibodies are not suitable for immunofluorescence microscopy.

Several attempts were made to decrease or eliminate non-specific signals. These strategies included increasing blocking periods, increasing concentrations of BSA in the blocking solution, adding goat serum to blocking solutions to prevent non-specific binding of the secondary goat-derived antibodies, and decreasing primary and secondary antibody incubation times. Despite all these efforts, the non-specific staining persisted even when using all of the techniques described above in combination. This could bring into question the specificity of these antibodies when probing for non-denatured proteins. Due to time constraints, we were unable to rectify this problem and immunofluorescent images were taken of cells expressing parkin at high enough levels to overcome the background staining. To address this problem in the future, our protocol would need to be further optimized. Additionally, the use of other commercially available parkin antibodies or a home-made parkin antibody would be tested to determine if this issue was due to the specific antibodies used in this study.

Parkin Protein Fusions

The use of fluorescent fusions or peptide epitope tags is an invaluable technique that enables simple and easy identification of protein localization. Protein fusions can be cloned onto proteins onto either the N- or C-terminus.

Fluorescent protein fusions are used to visualize proteins in living cells. A concern regarding using recombinant proteins with fluorescent fusions is the effects the fluorescent fusion has on protein folding and stability. GFP is significantly larger than most peptide epitope tags as it is a 238 amino acid protein and must adopt a proper three dimensional fold in order to function. The beta barrel fold of GFP is also an extremely stable conformation and can remain in cells for extensive periods of time after translation, even if it is cleaved from a recombinant protein. The addition of stable fluorescent fusions like GFP can also affect the stability of recombinant proteins. For these reasons the use of fluorescent fusion proteins can raise concerns regarding the validity of results acquired using these recombinant proteins when assessing protein function, folding and stability.

These concerns are particularly important when studying parkin. Structural studies have shown that the C-terminal residue of parkin is buried within the hydrophobic core of the Rcat/RING2 domain (60, 112) and the addition of large protein fusions at the C-terminal end of the protein may likely disrupt the fold of the Rcat/RING2 domain that is required for parkin's E3 ligase function. For this reason, many groups have chosen N-terminal fluorescent fusions when studying parkin localization in order prevent misfolding and subsequent loss of function of the C-terminal domain. However, recently structural findings have shown that the N-terminal Ubl domain of parkin is highly mobile and plays a major role in regulating parkin activity (63) rendering N-terminal fusions problematic regarding effects on parkin function.

For these reasons, in this study, we used unmodified parkin wherever possible to avoid concerns regarding effects of protein fusions. All of our growth experiments were

performed using both wild-type parkin and parkin-YFP which showed no difference in growth with the exception of co-expression of PINK1 and parkin discussed in section 4.2.6.1. Although immunofluorescence can be done in yeast, due to time constraints of this project, we chose to use fluorescently fused parkin, parkin point mutants, and parkin truncation variants for localization studies in yeast. In our experiments, we observed drastic changes in parkin localization caused by various parkin point mutations, truncations and PINK1 co-expression. Notably, when assessing parkin localization using parkin point mutants and truncation variants with C-terminal YFP fusions, our results were always compared to a C-terminally YFP fused wild-type parkin as a control to ensure all changes were due to changes to parkin itself or co-expression with PINK1. However, we cannot definitively rule out that the fluorescent tags did not have an effect on parkin localization, and may have stabilized mutant or truncated forms of the protein. To validate these results, immunofluorescence would need to be performed to assess if point mutants, truncations, and PINK1 co-expression have the same effects on untagged parkin.

Inhibiting Protein Degradation in Mammalian Cells

Before treating yeast cells with the proteasome inhibitor MG132 to test parkin degradation and stability we first had to quench parkin expression. In yeast, this was achieved by engineering parkin expression constructs under control of the galactose-inducible GAL1 promoter. Thus, by switching yeast cells to a glucose based media, parkin transcription was attenuated. In mammalian cells however, inhibiting transcription of parkin using cycloheximide also prevents translation of other cellular proteins. Therefore, experiments testing parkin stability in mammalian cells probably did not yield the same

results as those performed in yeast, which are likely due to alterations to many cellular processes and potential cell death following prolonged exposure to cycloheximide. It is also possible that the treatment with cycloheximide alters general cellular protein expression so severely that the protein degradation machinery is stressed to a point that it can no longer facilitate the same rate of parkin degradation that would occur under normal conditions. This concern could be addressed by performing pulse chase experiments using radio-labelled atoms that would eliminate the need to inhibit protein production while still allowing the assessment of parkin degradation.

Appendix 2. Comprehensive parkin sequence alignment.

```

SP|O60260|PRKN2_HUMAN -----MIVFVRFNSSHGFPVEVSDTSI 23
TR|Q7KTX7|Q7KTX7_DROME ----MSFIKFIATFVRKMLELLQFGGKT---LTHTLSIYVKTNTGKTLTVNLEPQWDI 52
SP|Q9WVS6|PRKN2_MOUSE -----MIVFVRFNSSYGFPPVEVSDTSI 23
SP|Q9JK66|PRKN2_RAT -----MIVFVRFNSSYGFPPVEVSDTSI 23
TR|F1NWU0|F1NWU0_CHICK -----MIVFVRFNSSHGFPVELGLDASI 23
TR|H2QU08|H2QU08_PANTR -----MIVFVRFNSSHGFPVEVSDTSI 23
TR|F6U1L3|F6U1L3_MACMU -----SVFVRFNSSHGFPVEVSDTSI 22
TR|I3N341|I3N341_ICTTR -----VFVRFNSSHGFPVEVSDTSI 21
TR|U3KCF7|U3KCF7_FICAL -----VFVRFNSSHGFPVEVGLDSSI 21
TR|Q561U2|Q561U2_DANRE -----MIVFVRFNSSHGFPVELEQGASV 23
TR|W4YQE2|W4YQE2_STRPU -----MTVHINPSQNG 11
TR|Q7Q591|Q7Q591_ANOGA ----MFDLFGFIRQLIGSMLAIFSGKKT---LSNSLSVYVKTNTGNTLAVDLEPHMDI 52
TR|C3Z502|C3Z502_BRAFL -----MSTFQVMVRFNSNHSFLVTVHTSWTI 26
TR|H3D789|H3D789_TETNG -----VPVIVRYNLGPEVVVEVQEEATV 23
TR|M3ZNV3|M3ZNV3_XIPMA -----AAVFVRFNRGPGVAMELSAAARV 23
TR|AOA087XI83|AOA087XI83_POEFO -----VAVFVRFNRGPGVAVELSAAAHV 23
TR|AOA0A9XSY6|AOA0A9XSY6_LYGHE ----MFLDFFFWSLWESLVHIMTFSRNP---QNNKLSIHVKSNTGNSVDVLDLPQWDI 51
TR|E0VIU9|E0VIU9_PEDHC ----MSILEWFWNILCGMAQYLTFSKNL--TNDNLVNIYVKS NVGGTISVNLDPKSDI 52
TR|T1H7C6|T1H7C6_MEGSC ----MEFIFEFFRSFLNAMLALLSFGKKT---VKNTLNINVKTNDQ-VLNIELQKSRNL 51
TR|L7M1N2|L7M1N2_9ACAR -MAGALRSFLDALALFLWRRLAFLSFRLRQPETPMNEITINVRFSADLVIPLRLERDATA 59
TR|V5GZV6|V5GZV6_IXORI MAASFLRWLLYVLASTFQRPLAFLRRGWPPPHVAMDEVTINVQFSTNLAISVTVKRDCVT 60
TR|V5IIZ0|V5IIZ0_IXORI MAASFLRWLLYVLASTFQRPLAFLRRGWPPPHVAMDEVTINVQFSTNLAISVTVKRDCVT 60
TR|H0ZGE3|H0ZGE3_TAEGU -----VFVRFNSSHGFPVEVGSDDSI 21
TR|Q1WDP3|Q1WDP3_PIG -----MIVFVRFNSSHGFPVEVSDTSI 23
TR|H0X3U6|H0X3U6_OTOGA -----VFVRFNSSHGFPVEVSDTSI 21
TR|I3JJF6|I3JJF6_ORENI -----FLPFLQFNLGPGVPVELQEEASV 23
TR|B8YGJ6|B8YGJ6_MACFA -----MIVFVRFNSSHGFPVEVSDTSI 23
TR|Q5J4W3|Q5J4W3_TAKRU -----MIVFVRYNLGPEVVVELQEEATV 23
TR|U3FQA1|U3FQA1_CALJA -----MLVFVRFNSSHGFPVEVSDTSI 23
TR|G3N0R1|G3N0R1_BOVIN -----MKVFVRFNSNHGFPVEVSDTSI 23
TR|Q17DC3|Q17DC3_AEDAE ----MFDIVNFFKNLIYNMLAIFSGRKK---LSNTLSIYVKTNTGNTLSVDLEPHMDI 52
TR|G3PFJ2|G3PFJ2_GASAC -----MIIVRYNLGPCVPVELQEEASV 23
TR|E2BWM9|E2BWM9_HARSA -----
TR|AOA067RG71|AOA067RG71_ZOONE ----MSFIINFIRKILQTMLQLVSVGKRT---ISNSLNVYIKTNTGCTLSVDLDPKWI 52
TR|AOA0L0CIZ3|AOA0L0CIZ3_LUCCU ----MSFLINLIKAFIDKMLALLSFGSKT---ITNTLSIYVKTNTGRTLSVNLEPKWDI 52
TR|AOA0F7Z269|AOA0F7Z269_CROAD -----MIVFVRFNSSHGFPVEVSDTSI 23
TR|AOA0B2UTN0|AOA0B2UTN0_TOXCA -----M-QLLVSVRNR-----SQKHYAHLDRSMNLHIDVPSEGTI 34
TR|Q9XUS3|Q9XUS3_CAEEEL -----MSDEI-SILIQDRKT-----G-----QRRNLTLNINITGNI 30

```

```

SP|O60260|PRKN2_HUMAN      FQLKEVVAKRQGV PADQLRVI FAGKELRNDWTVQNC DL DQQSIVHIVQRPWRKGQEMNAT 83
TR|Q7KTX7|Q7KTX7_DROME    KNVKELVAPQLGLQPDDLKIIFAGKELSDATTIEQCDLGQQSVLHAI RLRPPVQR----- 107
SP|Q9WVS6|PRKN2_MOUSE     LQLKEVVAKRQGV PADQLRVI FAGKELPNHLTVQNC DL EQQSIVHIVQRP RRRSHETNAS 83
SP|Q9JK66|PRKN2_RAT       FQLKEVVAKRQGV PADQLRVI FAGKELQNLHTVQNC DL EQQSIVHIVQRPQRKSHETNAS 83
TR|F1NWU0|F1NWU0_CHICK    LQLKEAVAQRQGV PADQLRVI FAGRELSNDLTLQNC DLVQQSIVHIVQNLQKNSD-KDET 82
TR|H2QU08|H2QU08_PANTR    FQLKEVVAKRQGV PADQLRVI FAGKELRNDWTVQHCDL DQQSIVHIVQRPWRKGQEMNAT 83
TR|F6U1L3|F6U1L3_MACMU   FQLKEVVAKRQGV PTDQLRVI FAGKELRNDWTVQNC DL DQQSIVHIVQRP RRRKGQEMNAT 82
TR|I3N341|I3N341 ICTTR    FQLKEVVAKRQGV PAGQLRVI FAGKELQNDLTVQNC DL EQQSIVHIVQRP RRGPEADAP 80
TR|U3KCF7|U3KCF7_FICAL   LQLKEAVAQRQGV PADQLRVI FAGRELSNDLTLQNC DL AQQSIVHIVQSPQ-NSQNKEKT 80
TR|Q561U2|Q561U2_DANRE   SELKEAVGRLQGV PSDQLRVI FAGRELCNESTLQGC DLPEQSTVHV VLPSTSAHRSELI 83
TR|W4YQE2|W4YQE2_STRPU   GELRSEVARLSGQSPADIRLVFAGKLI DDVQIMEDLRICENTMIHAVPAQRIQCHSDGPK 71
TR|Q7Q591|Q7Q591_ANOGA   KDVKEMVAPRLGLEPQELKII FAGRELSDTTTI SECDLGQQSIIHVVKSRPTAITTPQKR 112
TR|C3Z502|C3Z502_BRAFL   ARFKQEVGRTQGVPSGQIHI L FAGRDLSDSLRIEDCQLGQQTVIHAISGLPQLSVDA--- 83
TR|H3D789|H3D789_TETNG   AELKEVVARQQGVQPERLRVLFAGRELKSTSTLQDC DLPEQSTVHV VLP PPAASSSSKVHL 83
TR|M3ZNV3|M3ZNV3_XIPMA   AELKEIVASQQGVPAQELRVLFAGRELQSSASLQGC DLPEHSTVHV VLP PPGSLHLPPPQ 83
TR|A0A087XI83|A0A087XI83_POEFO AELKEIVGRQGVPAQALRVLFAGRELSNDLTLQNC DL PDQSTVHV VLP PPGSIHLLPL- 82
TR|A0A0A9XSY6|A0A0A9XSY6_LYGHE GTLKEAIA PKI GLPADDMEI ILAGKSLDDSTT IADC DLGEQSVLHAVKSHGQRRRSRL 111
TR|E0VIU9|E0VIU9_PEDHC   KNVKELVAPKLGLEPDDVKIIFAGKELLDSTVIEVLDFFS-DILHAVKVNKKI----- 104
TR|T1H7C6|T1H7C6_MEGSC   KK----SLLLLGITVEEIKIIFAGKELTDSTTIAECD LGNMSFLHAIKPRRN VQGG--- 104
TR|L7M1N2|L7M1N2_9ACAR   KDVKERLAEQLSLPVQEIRIIFAGKELLDHIAIKDYNVEEQTTVHAVRSANDGA-----Y 114
TR|V5GZV6|V5GZV6_IXORI   KAMKERLASQLDVPVQELRVI FAGKELRDDAYFKDCNIEEYTTVHAVRSAACATPGAEPV 120
TR|V5IIZ0|V5IIZ0_IXORI   KAMKERLASQLDVPVQELRVI FAGKELRDDAYFKDCNIEEYTTVHAVRSAACATPGAEPV 120
TR|H0ZGE3|H0ZGE3_TAEGU   LQLKEAVAQRQGV PADQLRVI FAGRELSNDLTLQNC DL AQQSIVHIVES PQKNSQDKEKT 81
TR|Q1WDP3|Q1WDP3_PIG     FQLKEVVAKRQGV PADQLRVI FAGKELRNDLTVQRCDL DQQSIVHV VLRPQRNGQERGVA 83
TR|H0X3U6|H0X3U6_OTOGA   FQLKEVVAKRQGV PADQLRVI FAGKELRNDWTVQNC DL DQQSIVHIVQKPWRKGHEMAAT 81
TR|I3JF6|I3JF6_ORENI     AQLKEVVG SQQGV RPERLRVLFAGRELQSTATLQGS DLPEQSTVHV VLP PPGASSFQQLM 83
TR|B8YGJ6|B8YGJ6_MACFA   FQLKEVVAKRQGV PTDQLRVI FAGKELRNDWTVQNC DL DQQSIVHIVQRP RRRKGQEMNAT 83
TR|Q5J4W3|Q5J4W3_TAKRU   AELKEVVGQQQGVQPDLLRVLFAGRELKSTSTLQGC DLPEQSTVHIIVPSPASSSYKTLL 83
TR|U3FQA1|U3FQA1_CALJA   FQLKEVVAKRQGV PADQLRVI FAGKELRNDWTVQNC DL DQQSIVHIVQRPWRKGQESNAT 83
TR|G3N0R1|G3N0R1_BOVIN   FQLKEVVARRQGV PADQLCVI FAGKELRNDWTVQSC DL DQQSIVHIVL RPRRKGPE---- 79
TR|Q17DC3|Q17DC3_AEDAE   KDVKEIVAPQLGLPAGELKII FAGKELSDTITITISECDLGQQSIIHAVKARTIPKKVN--- 109
TR|G3PFJ2|G3PFJ2_GASAC   ADLQQLVGSQQGVHAE LLRVLFAGRELKSSFTLQGC DLPEQSTVHV VLPKSAPTPGHLLL 83
TR|E2BWM9|E2BWM9_HARSA   -----MGMAAEDIKII FAGKELHNSIVIEECDLGQQSTLHAVRNPHK KLNQC-- 48
TR|A0A067RG71|A0A067RG71_ZOONE KDVKELVAPRLGLSP EEVKII FAGKELHDSIVIEECDLGQQSILHAVRSHASHRKKP--- 109
TR|A0A0L0CIZ3|A0A0L0CIZ3_LUCCU KNVKEIVAPQLGLQPEEVKII FAGKELSDATTIEECDLGQQSILHAIQARPVQQR----- 107
TR|A0A0F7Z269|A0A0F7Z269_CROAD FQLKEAVAKRQGV PADQLHVI FAGKELRNDLTLKNC DL LPQQSIVHIVQNRQKSENENPR- 82
TR|A0A0B2UTN0|A0A0B2UTN0_TOXCA SDVIEVLARRIKVSPNSFKI ILCGKVLGGATSLHSL LLLGPQTS LAAVVVDVSASDDKSAN 94
TR|Q9XUS3|Q9XUS3_CAEEEL  EDLTKDVEKLTEIPSELEVVFCGKKLSKSTIMRDL SLTPATQIMLLR PKFN SHN-ENGA 89

```

. : : : . * : : . . : :

```

SP|O60260|PRKN2_HUMAN          GGDDPRNAAGGCERE PQSLTRVDLSSSVLPGDSVGLAVILHTDSRKDSPP----- 133
TR|Q7KTX7|Q7KTX7_DROME        ---QKI---QSATLEEEEP SLSDEASKPLNETLLDLQLESEER-L----- 145
SP|Q9WVS6|PRKN2_MOUSE          GGDEPQSTSEGSIWESRSLTRVDLSSHTLPVDSVGLAVILDTDSKRDSEA----- 133
SP|Q9JK66|PRKN2_RAT            GGDKPQSTPEGSIWEP RSLTRVDLSSSILPADSVGLAVILDTDSKSDSEA----- 133
TR|F1NWU0|F1NWU0_CHICK        EDNHAGGILKTLERVPESLTRIDLSSSILPSLSAGLAVILDTKEPNISPP----- 132
TR|H2QU08|H2QU08_PANTR        GGDDPRNAAGGCERE PQSLTRVDLSSSVLPGDSVGLAVILHTDSRKDSPP----- 133
TR|F6U1L3|F6U1L3_MACMU        GGDNARNTAGGCERE PQSLTRVDLSSSVLPGDSVGLAVILHTDSRNDSP----- 132
TR|I3N341|I3N341 ICTTR        GGDEPRTVLGGPERE PRSLTRVDLSSSVLPADSVGLAVVLDTGSRRDSTA----- 130
TR|U3KCF7|U3KCF7_FICAL        EDSCIGGVPKTLKREPESLTRIDLST SILPSVSAGLAVILDPGKNSVSLP----- 130
TR|Q561U2|Q561U2_DANRE        Q-----QRRLGSGMESLTRL DLSSSRQTTASEGLAVILETEASRREDT----- 126
TR|W4YQE2|W4YQE2_STRPU        -----T-IKDEGVKPPQPVH-----VLMESRIIDEDQ RSPET----- 101
TR|Q7Q591|Q7Q591_ANOGA        QAKPAL---NATISEEPSPEEQQH NKPLSETMSELTVLDERN----- 152
TR|C3Z502|C3Z502_BRAFL        -----RSSAAAPRSLSDVQLNVRP----- 102
TR|H3D789|H3D789_TETNG        L---QEHQARGEEDHDSLTRL DLSSSRLTTTTSGLAVILERNGLGGVGATAGGGEAG-- 138
TR|M3ZNV3|M3ZNV3_XIPMA        E-----H----LAASVTRLRL DLSSSRLA AVATAAVQTT-----VLEGGGGDED- 124
TR|A0A087XI83|A0A087XI83_POEFO -----AARGTRLRLDLSSSRLAVLEG-----GRGGGGDED- 112
TR|A0A0A9XSY6|A0A0A9XSY6_LYGHE ---NQI---MSDLVEE-----NDALPATVSEIDEN-HDT-VQ----- 140
TR|E0VIU9|E0VIU9_PEDHC        -----KNVIPDKPLCETLEELHQLNDQK-NV----- 129
TR|T1H7C6|T1H7C6_MEGSC        -----I-----STLTKKEDQPSKPLCETLPDLKLVNM----- 131
TR|L7M1N2|L7M1N2_9ACAR        M-----DAEVQC-PLGEGII--TSQ----- 131
TR|V5GZV6|V5GZV6_IXORI        V-----SAEMCCAPLGGSLAKGTRG----- 140
TR|V5IIZ0|V5IIZ0_IXORI        V-----SAEMCCAPLGGSLAKA--Q----- 138
TR|H0ZGE3|H0ZGE3_TAEGU        EYSCVGGVPKALKREPESLTRIDLST SILPSVSAGLAVILDPGKNSVSLP----- 131
TR|Q1WDP3|Q1WDP3_PIG          AGHR----PGRAGREPASLTRVDL SSVLPGDAVGLAVILQDDSADGAAP----- 129
TR|H0X3U6|H0X3U6_OTOGA        GGDGPRSTGGPGREPQSLTRVDL SSSLLPADSVGLAVILDTESRSDDPP----- 131
TR|I3JF66|I3JF66_ORENI        Q-----E----H-RAEGLSRLRL DLSSSRLPASSE-----GGGGGAEG- 115
TR|B8YGJ6|B8YGJ6_MACFA        GGDNARNTAGGCERE PQSLTRVDLSSSVLPGDSVGLAVILHTDSRNDSP----- 133
TR|Q5J4W3|Q5J4W3_TAKRU        L---PEHLSQGEENHDSLTRL DL SASRLPTTSSTLGVILERN DSEG V GATAGGGGAEAA 140
TR|U3FQA1|U3FQA1_CALJA        GGDNPRNAAGGCERE PQSLTRVDL SSVLPGDSVGLAVILHTESRDSDSP----- 133
TR|G3N0R1|G3N0R1_BOVIN        -GHSRPAWGRSDREPESLTRVDL SSSMLPADSVGLAVILQDGEESGASS----- 128
TR|Q17DC3|Q17DC3_AEDAE        NGKTL L---ESP ISEETL--EESTSTKPLCETLTDLQMTVEVNE----- 147
TR|G3PFJ2|G3PFJ2_GASAC        L---RERLAGGQEEGNSLARLDI SSSRFPCTPPGLDGS-----NGGGG-EGA 127
TR|E2BWM9|E2BWM9_HARSA        -ASSSI---EE--YKSESSDLNESGSKPMNETLTDLSLSDSSDQ-H----- 86
TR|A0A067RG71|A0A067RG71_ZOONE -----GSESPSEGSKPLNETLMDLQLSDHER-RS----- 137
TR|A0A0L0CIZ3|A0A0L0CIZ3_LUCCU ---KRL---YSTVAEE-EP-SEEQPSKPLCETLVDLQLLSEER-S----- 143
TR|A0A0F7Z269|A0A0F7Z269_CROAD -----LLLSSNGREPTSLTRVDLSTNLLPSDSLGLAVILDNRIP I----- 122
TR|A0A0B2UTN0|A0A0B2UTN0_TOXCA A----- 95
TR|Q9XUS3|Q9XUS3_CAEL        T----- 90

```

```

SP|O60260|PRKN2_HUMAN -----AGSPAGRSIYNSFFVYCKGPCQ-----RVQPGKLRVQCS 167
TR|Q7KTX7|Q7KTX7_DROME -----NITDEERVRAKAHFFVHCS-QCD-----KLCNGKLRVRCA 179
SP|Q9WVS6|PRKN2_MOUSE -----ARGP-VKPTYNSFFIYCKGPCH-----KVQPGKLRVQCG 166
SP|Q9JK66|PRKN2_RAT -----ARGPEAKPTYHSFFVYCKGPCH-----KVQPGKLRVQCG 167
TR|F1NWX0|F1NWX0_CHICK -----SEK-SGAASYNSFFVYCKNFCQ-----AVKPGKLRVRCN 165
TR|H2QU08|H2QU08_PANTR -----AGSPAGRSIYNSFFVYCKGPCQ-----RVQPGKLRVQCS 167
TR|F6U1L3|F6U1L3_MACMU -----AGSPADRPIYNSFFVYCKGPCQ-----RVQPGKLRVQCS 166
TR|I3N341|I3N341 ICTTR -----ARGP-GRPTYNSFFVYCKGPCQ-----GVQPGKLRVRCG 163
TR|U3KCF7|U3KCF7_FICAL -----SEKSAGAASYNSFFVYCKNFCQ-----AVKPGKLRVRCN 164
TR|Q561U2|Q561U2_DANRE -----A-GHTGAKAHSSFFVYCKTVCK-----AIQPGKLRVRCR 159
TR|W4YQE2|W4YQE2_STRPU -----PDVDLASSLHPSFFVYCKSHCR-----SVQPGKLRVCCQ 135
TR|Q7Q591|Q7Q591_ANOGA -----GDQSIPIGRTKAHFFVYCS-QCE-----KVCTGKLRVRCG 186
TR|C3Z502|C3Z502_BRAFL -----EGADTAAGSLPSYFVYCKRPFCK-----AVRPGKLRVRCG 136
TR|H3D789|H3D789_TETNG NDGATPESGGEVQAAGVKGHSVHPRSTFFVYCKS-CK-----SIQPGKLRVRCR 186
TR|M3ZNV3|M3ZNV3_XIPMA -----QR--T---EQQAAPKGV CSTFFVYCKR-CS-----SIQSGKLRVRCR 161
TR|A0A087XI83|A0A087XI83_POEFO -----QR--T---EQQAAPKGV---TFFVYCKR-CS-----SIQSGKLRVRCR 146
TR|A0A0A9XSY6|A0A0A9XSY6_LYGHE -----PSPADSDGKPKQKQQAHFVYCA-TCMTNNLGNPTLPLKPKKEGKLRVRCN 189
TR|E0VIU9|E0VIU9_PEDHC -----ESIEESNLKNEGKNAHFFIYCANPCK-----KINTGKLRVCCS 168
TR|T1H7C6|T1H7C6_MEGSC -----RKAHFFVYCS--QCK-----KLCKGKLRVRCF 155
TR|L7M1N2|L7M1N2_9ACAR -----LTEEEHLARKTEADKALFFVYCKQPCD-----RVLPKGLRVCCA 170
TR|V5GZV6|V5GZV6_IXORI -----YTEEERLASTAEVDKTLFFVYCKSPCG-----RVEPGKLRVRCN 179
TR|V5IIZ0|V5IIZ0_IXORI -----LTEEERLASTAEVDKTLFFVYCKSPCG-----RVEPGKLRVRCN 177
TR|H0ZGE3|H0ZGE3_TAEGU -----SEKSAGAASYNSFFVYCKNFCQ-----AVKPGKLRVRCN 165
TR|Q1WDP3|Q1WDP3_PIG -----AGRPADRPTNKSFFVYCKGPCQ-----RVQPGKLRVRCN 163
TR|H0X3U6|H0X3U6_OTOGA -----AAGPAGRPVYNSFFVYCKGPCH-----RVQPGKLRVQCN 165
TR|I3JF6|I3JF6_ORENI -----ES--LEEVAHSSVRACSTFFVYCKS-CC-----SIEPGKLRARCQ 155
TR|B8YGJ6|B8YGJ6_MACFA -----AGSPADRPIYNSFFVYCKGPCQ-----RVQPGKLRVQCS 167
TR|Q5J4W3|Q5J4W3_TAKRU LGGDSADDRAVLQSAGAKDHSVRPRSTFFVYCKS-CK-----LVQPGKLRVRCR 188
TR|U3FQA1|U3FQA1_CALJA -----AGSAAGRPVYNSFFVYCKGPCQ-----KVQPGKLRVQCG 167
TR|G3N0R1|G3N0R1_BOVIN -----ARRPAGRPTYNSFFVYCKGPCQ-----GVQPGKLRVRCN 162
TR|Q17DC3|Q17DC3_AEDAE -----KPGSPARERRKAHFFVYCS-QCE-----KVCTGKLRVRCG 181
TR|G3PFJ2|G3PFJ2_GASAC EGG----DREQVQAASLKVLCVRTCSTFFVYCKR-CK-----SIQPGKLRVCCS 171
TR|E2BWM9|E2BWM9_HARSA -----NLSTEEQQDNRAHFYIYCPGPCK-----IVTAGKLRVKCA 121
TR|A0A067RG71|A0A067RG71_ZOONE -----VRTDEDREKRKAHFFVYCAWPCCK-----EMKLGKLRVRCN 172
TR|A0A0L0CIZ3|A0A0L0CIZ3_LUCCU -----NIPEENRERSKAHFFVHCS-QCN-----KLCKGKLRVRCN 177
TR|A0A0F7Z269|A0A0F7Z269_CROAD -----PPNNSEVKYSSFFVYCKSFCQ-----AVKPGKLRVRCR 155
TR|A0A0B2UTN0|A0A0B2UTN0_TOXCA -----SSSIDSNRTDVPSFHVYCKG-CN-----SLAKGKLRVYCA 129
TR|Q9XUS3|Q9XUS3_CAEEEL -----TAKITDSSILGSFYVWCKN-CD-----DVKRGLRVYCA 124
::: * * ****. *

```

```

SP|O60260|PRKN2_HUMAN          TCRQATLTLTQGPSCWDDVLIIPNRMSGECQSPHC-----PGTSA-EFFFKCGAHP 216
TR|Q7KTX7|Q7KTX7_DROME        LCKGGAFTVHRDPECWDDVLKSRRI PGHCESLEVACV--DNAAGDPPFA-EFFFKCAEHV 236
SP|Q9WVS6|PRKN2_MOUSE         TCKQATLTLAQGPSCWDDVLIIPNRMSGECQSPDC-----PGTRA-EFFFKCGAHP 215
SP|Q9JK66|PRKN2_RAT           TCRQATLTLAQGPSCWDDVLIIPNRMSGECQSPDC-----PGTRA-EFFFKCGAHP 216
TR|F1NWX0|F1NWX0_CHICK        ECKQGTTLARGPSCWDDVLIIPNRITGVCQSPDC-----SGNVA-EFYFKCGAHP 214
TR|H2QU08|H2QU08_PANTR        TCGQATLTLTQGPSCWDDVLIIPNRMSGECQSPHC-----PGTSA-EFFFKCGAHP 216
TR|F6U1L3|F6U1L3_MACMU        TCRQATLTLTQGPSCWDDVLIIPNRMSGECQSPHC-----PGTTAVRFFLRCGEHG 216
TR|I3N341|I3N341_ICTTR        TCRQATLTLAQGPSCWDDVLIIPNRMSGKQSPGC-----PGTRA-EFFFKCGAHP 212
TR|U3KCF7|U3KCF7_FICAL        VCKQGTTLARGPSCWDDVLIIPNRIGGVCQSRGC-----TGNVA-EFYFKCGAHP 213
TR|Q561U2|Q561U2_DANRE        DCKQGTTLTLRGPSCWDDVLLPNRIHGVCQSQGC-----NGRLA-EFYLKASHP 208
TR|W4YQE2|W4YQE2_STRPU        TCKDNAFIVKEDPVCWDDVILSNRISGSCFVPGC-----QGQKA-EFFFKCSSHA 184
TR|Q7Q591|Q7Q591_ANOGA        ICGSGAFTVHRDPTCWDVLLKRRITGHCENYEVPCV--ENDEGEPPFT-EFYFKCSEHS 243
TR|C3Z502|C3Z502_BRAFL        TCRQTTLTLRSDPNCWEDVLPVPGKI QGRCLSRGC-----PGTVA-EFYFKCADHH 185
TR|H3D789|H3D789_TETNG        SCRQTTLTLRGPSCWDDVLLRNLHGVCHSDGC-----HGTEA-EFYMKCARHP 235
TR|M3ZNV3|M3ZNV3_XIPMA        RCRQMTLTLRCRGPSCWDDVLLPGRIHGVCQFEGC-----HGNEA-EFYMKCASHP 210
TR|A0A087XI83|A0A087XI83_POEFO RCRQMALTLRGPSCWDDVLLPGRIHGVCQFEGC-----HGNEA-EFYMKCASHP 195
TR|A0A0A9XSY6|A0A0A9XSY6_LYGHE SCKSGAIQLDSDPASWSDVLERTRITGDCQEGCS-----DGPVAVA-EFYFKCAEHV 241
TR|E0VIU9|E0VIU9_PEDHC        ECKHGAFTVYKDPWCWDDVLDKNRITGVCNNVG-----CEGLYA-KFYFKCAHP 217
TR|T1H7C6|T1H7C6_MEGSC        KCKSGAFTVYKDPWCWDDVLDKNRITGVCNNVG-----CEGLYA-KFYFKCAEHV 212
TR|L7M1N2|L7M1N2_9ACAR        SCGEGSFILQKDPSCWKDVLPEPGRLLGQCQICH-----QVRAA-RFFFKCTG-- 216
TR|V5GZV6|V5GZV6_IXORI        TCGQGCFLLDREPCWPDVLERGRLGGRCEQEG-----CGGRLA-DFFFKASSN 228
TR|V5IIZ0|V5IIZ0_IXORI        TCGQGCFLLDREPCWPDVLERGRLGGRCEQEG-----CGGRLA-DFFFKASSN 226
TR|H0ZGE3|H0ZGE3_TAEGU        VCKQGTTLARGPSCWDDVLIIPNRIGGVCQSQGC-----NGNVA-EFYFKCGAHP 214
TR|Q1WDP3|Q1WDP3_PIG          TCQQATLTLTQGPSCWDDVLIIPNRMSGECQSPNC-----PGTTA-EFFFKCGAHP 212
TR|H0X3U6|H0X3U6_OTOGA        TCKQATLTLAQGPSCWDDVLIIPNRMSGECQSPNC-----PGTTA-EFFFKCGAHP 214
TR|I3JF6|I3JF6_ORENI          SCKQTTLTLRGPSCWDDVLLPGRIHGICQSEGC-----QGNEA-EFYMKCASHP 204
TR|B8YGJ6|B8YGJ6_MACFA        TCRQATLTLTQGPSCWDDVLIIPNRMSGECQSPHC-----PGTTA-EFFFKCGAHP 216
TR|Q5J4W3|Q5J4W3_TAKRU        SCRQATLTLRGPSCWDDVLLQSRVHGVCCHSDGC-----HGTEA-EFYMKCASHP 237
TR|U3FQA1|U3FQA1_CALJA        TCRQATLTLTQGPSCWDDVLIIPNRMSGECQSPNC-----PGTSA-EFFFKCGAHP 216
TR|G3N0R1|G3N0R1_BOVIN        TCQQATLTLAQGPSCWDDVLIIPNRMSGECQSPNC-----PGTRA-EFFFKCGAHP 211
TR|Q17DC3|Q17DC3_AEDAE        ICKSGAFTVHRDPACWDDVLLKRRITGHCENYEIPCV--ENELGDPPT-EFYFKCSEHS 238
TR|G3PFJ2|G3PFJ2_GASAC        SRETTFTTLRGPSCWDDVLLPGRVHGFCQSDAC-----VGNEA-EFYMKCASHP 220
TR|E2BWM9|E2BWM9_HARSA        KCNSGAVTVDRDPQCWSDILEPNRITVHCENDFCPASSLSEEEFQVTYA-HFYFKCTRHV 180
TR|A0A067RG71|A0A067RG71_ZOONE SCRSGAFTVDRDPQCWDDVLEGRITGDCQNDSD---C---IGSDDGPKFA-EFYFKCFEHT 226
TR|A0A0L0CIZ3|A0A0L0CIZ3_LUCCU LCKGGAFTVHRDPECWDDVLKSRRI RGHCESLEIACV--DNDIGDPPFA-EFYFKCAEHI 234
TR|A0A0F7Z269|A0A0F7Z269_CROAD TCKQGTTLTLARDPSCWEDVLIIPNSILGVCHYQNC-----SGEIA-EFYFKCGAHP 204
TR|A0A0B2UTN0|A0A0B2UTN0_TOXCA RCLSSSVVLKRDPEKWSVDLSSRAINAECEDCE-----EETFA-KFCFKVICD 177
TR|Q9XUS3|Q9XUS3_CAEEEL        KCSSTSVLVKSEPQNSVDLKSRI PAVCEECCT-----PGLFA-EFKFKCLACN 173
* . : * * * : : * : * : *

```

```

SP|O60260|PRKN2_HUMAN          T--SDKE-TSVALHLIATNSRNITCITCTDVRSPVLVVFQCNHRHVICLDCFHLYCVTRLN 273
TR|Q7KTX7|Q7KTX7_DROME        S-GGEKD-FAAPLNLIKNNIKNVPCIACTDVSDTVLVFPCASQHVTCIDCFRHYCRSRLG 294
SP|Q9WVS6|PRKN2_MOUSE          T--SDKD-TSVALNLIITSNRRSIPCIACDVRSPVLVVFQCNHRHVICLDCFHLYCVTRLN 272
SP|Q9JK66|PRKN2_RAT            T--SDKD-TSVALNLIITNSRSIPCIACDVRNPVLVVFQCNHRHVICLDCFHLYCVTRLN 273
TR|F1NWU0|F1NWU0_CHICK        T--TDSE-TSVALNLIITNSRGITCITCTDIRSPVLVVFQCMHRHVICLDCFHLYCVTMLN 271
TR|H2QU08|H2QU08_PANTR        T--SDKE-TSVALHLIATNSRNITCITCTDVRSPVLVVFQCNHRHVICLDCFHLYCVTRLN 273
TR|F6U1L3|F6U1L3_MACMU        A--EDKS-LGHGLHLLPTKLRNVRNIFLSLCRSPVLVVFQCNHRHVICLDCFHLYCVTRLN 273
TR|I3N341|I3N341 ICTTR        T--SDKE-TSVALNLIITNSRDISCITCTDTRSPVLVVFQCTHRHVICLDCFHLYCVTRLN 269
TR|U3KCF7|U3KCF7_FICAL        T--ADSE-TSVALNLIITNSRCITCITCTDIRSPVLVVFQCVHRHVICLDCFHLYCVTMLN 270
TR|Q561U2|Q561U2_DANRE        T--CDND-TSVALDLIMPNTRRVPCIACTDIMTPVLVVFQCAERHVICLECFHLYCVSRLN 265
TR|W4YQE2|W4YQE2_STRPU        S--SVND-QFTVPLPVKTNTRRVICITCADILTSVLVVFPCASQHVTCIDCFRHYCRSRLG 241
TR|Q7Q591|Q7Q591_ANOGA        S-GGEKD-FAAPLSLIKTNHKNIPCIACDVTSETILVVFPCVAGHVSCLDLDCFQRYCVTRLN 301
TR|C3Z502|C3Z502_BRAFL        T--SEDD-TSVALPLVKSNTQSVDCGCTDVRTPVMVFECADGHVMCLDCFARYCVTKLN 242
TR|H3D789|H3D789_TETNG        T--SDSD-HSVALDLIMTNSRDVPCIAADVVDVVLVVFQCLERHVICLECFRHYCQVRVN 292
TR|M3ZNV3|M3ZNV3_XIPMA        T--SEDD-VSVALDLVLSNTRSVPCIGCTDIRDVVLVVFQCSDRHVICLDCFQRYCQTRLN 267
TR|A0A087XI83|A0A087XI83_POEFO T--SEDD-VSVALDLVLSNTRGVPCIGCTDIRDVVLVVFQCSDRHVICLDCFQRYCQTRLN 252
TR|A0A0A9XSY6|A0A0A9XSY6_LYGHE P-KSENESEAVPLYLIRANSRTPCLACMDIMDTVIVFSCA--HTICLDCFNDYITSKIR 298
TR|E0VIU9|E0VIU9_PEDHC        S-QGEND-TAVPLNLIKRNHKKIPCLACTDICDPVLVVFPCSDNRHVICLECFRHYCQVRVN 275
TR|T1H7C6|T1H7C6_MEGSC        L-GMEDD-FAAPLKLIRINEQNVPCIACTDVTSETILVVFPCVAGHVSCLDLDCFQRYCQTRLN 270
TR|L7M1N2|L7M1N2_9ACAR        KIGSHDDQVPIVQLIRYNYLQVPCIACTDVRSPVLVVFQCNHRHVICLDCFHLYCVTRLN 274
TR|V5GZV6|V5GZV6_IXORI        RLEGHQDQRGSTVPLVRCNFLGVPCLSDTDSRIVLVFVPCVAGHVSCLDLDCFQRYCQTRLN 288
TR|V5IIZ0|V5IIZ0_IXORI        RLEGHQDQRGSTVPLVRCNFLGVPCLSDTDSRIVLVFVPCVAGHVSCLDLDCFQRYCQTRLN 286
TR|H0ZGE3|H0ZGE3_TAEGU        T--TDSE-TSVALNLIITNSRCITCITCTDIRSPVLVVFQCVHRHVICLDCFHLYCVTMLN 271
TR|Q1WDP3|Q1WDP3_PIG          T--SDKE-TSVALNLIITNSRDITCITCTDIRSPILVVFQCNHRHVICLDCFHLYCVTRLN 269
TR|H0X3U6|H0X3U6_OTOGA        T--SNKD-TSVALNLIITNSRDISCITCTDVRSPVLVVFQCNHRHVICLDCFHLYCVTRLN 271
TR|I3JF6|I3JF6_ORENI          T--SDDD-FSVALDLIMTNTGRVPCIACTDVMGVVLVVFQCLERHVICLDCFQRYCQTRLN 261
TR|B8YGJ6|B8YGJ6_MACFA        T--SDKE-TSVALHLIATNSRNITCITCTDVRSPVLVVFQCNHRHVICLDCFHLYCVTRLN 273
TR|Q5J4W3|Q5J4W3_TAKRU        T--SDND-HSVALDLIMTNSRDVPCIACTDVMGVVLVVFQCLERHVICLECFRHYCQVRVN 294
TR|U3FQA1|U3FQA1_CALJA        T--SDKE-TSIALHLIATNSRNITCITCTDVRSPVLVVFQCNHRHVICLDCFHLYCVTRLN 273
TR|G3N0R1|G3N0R1_BOVIN        T--SDKE-TSVALNLIITNSRDISCITCTDIRSPVLVVFQCTHRHVICLDCFHLYCVTRLN 268
TR|Q17DC3|Q17DC3_AEDAE        S-GGEKD-FAAPLNLIKTNHKDIPCIACDVTSDTVLVFPCVAGHVTCIDCFRHYCVSRLN 296
TR|G3PFJ2|G3PFJ2_GASAC        T--PEDE-VSVALDLIMTNSREVPMACSDTTELVLVVFQCAERHVICLHCFHRYCQTRLN 277
TR|E2BWM9|E2BWM9_HARSA        S-LGEDD-KVIPLYLIRANLRNVPCIACTDVRETVLVVFPCVAGHVTCIDCFCEYCVIRLQ 238
TR|A0A067RG71|A0A067RG71_ZOONE S-QGEDD-QAVPLYLIKSNVRDVPCLACTDVSDPVLVVFPCDLAHVTCLECFRHYCVARLR 284
TR|A0A0L0CIZ3|A0A0L0CIZ3_LUCCU S-GGEKD-FAAPLNLIKINIKDIPCLACTDVSDTVLVFPCVAGHVTCIECFRHYCVSRLM 292
TR|A0A0F7Z269|A0A0F7Z269_CROAD T--SDSE-TSVPLNLIITNTRYISCITCTDVRSPVLVVFPCVAGHVTCIDCFHLYCVTMLN 261
TR|A0A0B2UTN0|A0A0B2UTN0_TOXCA E-----VAVPLTHVGRYRGECECSICGETALR-AVVDVGCHEHETCVDCFTAYMETAFT 229
TR|Q9XUS3|Q9XUS3_CAEEEL        D-----PAAALTHVRGNWQMETECVCDGK-EK-VIFDLGCNHITCQFCFRDYLLSQLE 224

```

* : * * * * *

SP O60260 PRKN2_HUMAN	CPRPGCGAGLLP-----EPD--QRKVTCEGG-NLGGCGFAFCRECKEAYHEGEC	378
TR Q7KTX7 Q7KTX7_DROME	CPQPGCGMGLLV-----EPD--CRKVTTCQ-----NGCGYVFCRNCLQGYHIGEC	395
SP Q9WVS6 PRKN2_MOUSE	CPRPGCGAGLLP-----EQG--QRKVTCEGG-NLGGCGFVFCRDCKEAYHEGDC	377
SP Q9JK66 PRKN2_RAT	CPRPGCGAGLLP-----EQG--QKKVTCEGG-NLGGCGFVFCRDCKEAYHEGEC	378
TR F1NWU0 F1NWU0_CHICK	CPTPGCGAGLLP-----EPE--VRKIVCEPG-NGIGCGFVFCRECKEAYHEGEC	376
TR H2QU08 H2QU08_PANTR	CPRPGCGAGLLP-----EPD--QRKVTCEGG-NLGGCGFAFCRECKEAYHEGEC	378
TR F6U1L3 F6U1L3_MACMU	CPRPGCGAGLLP-----ESD--QRKVTCEGG-NLGGCGFAFCRECKEAYHEGEC	378
TR I3N341 I3N341 ICTTR	CPRPGCGAGLLP-----EAG--QRKVTCEAG-NLGGCGFVFCRDCKEEHHEGSC	373
TR U3KCF7 U3KCF7_FICAL	CPSPGCGAGLLP-----EPG--LRRIVCEPG-NGIGCGSVFCRECKEEFHHEGEC	375
TR Q561U2 Q561U2_DANRE	CPAPGCGAGLLP-----PDE--ERRVCCEPGNGLGGCGFVFCRDCKEEFHHEGPC	371
TR W4YQE2 W4YQE2_STRPU	CPSPGCGAGLLP-----ESD--GESRVCEIQE-EGFGCGFVFCRNCHAYHEGEC	347
TR Q7Q591 Q7Q591_ANOGA	CPQPGCGMGLLV-----DPE--CRRIQCQ-----NGCGYVFCRSCLQGYHIGEC	402
TR C3Z502 C3Z502_BRAFL	CPGRGCGVGLLP-----EGS--SNMVECVRQ-AGSGCGFVFCRCLCKEAYHNGPC	347
TR H3D789 H3D789_TETNG	CPSPGCGAGLVP-----PDG--ARRVECDRQ---VGGCGFVFCRNCREGYHEGVCP	395
TR M3ZNV3 M3ZNV3_XIPMA	CPSPGCGAGLLP-----PEG--SRKVECDRR--LLGGCGFVFCRDCREGFHEGPCE	371
TR A0A087XI83 A0A087XI83_POEFO	CPSPGCGAGLLP-----PEG--SRRVECDRR---LGCGFVFCRDCREGFHEGPCE	355
TR A0A0A9XSY6 A0A0A9XSY6_LYGHE	CPHPCMGMIY-----DDD--CDAVRC-----TCGYVFCRCLQGNHIGDC	397
TR E0VIU9 E0VIU9_PEDHC	CPQPGCGQILV-----DQN--CNRVQC-----SCGYVFCRCLQGYHIGEC	374
TR T1H7C6 T1H7C6_MEGSC	CPRPDCMGMLLI-----EPD--CKKVVQC-----NGCGFVFCRDCLQGYHIGEC	371
TR L7M1N2 L7M1N2_9ACAR	CPRPGCGQGLLP-----EPG--CDRVKCD----RGCGFVFCRCLQGHHLGPCT	375
TR V5GZV6 V5GZV6_IXORI	CPQPGCGQILV-----DLG--CTRVTCEAA--TQGGCGFVFCRCLQGHHLGPCI	392
TR V5IIZ0 V5IIZ0_IXORI	CPQPGCGQILV-----DLG--CTRVTCEAA--TQGGCGFVFCRCLQGHHLGPCI	390
TR H0ZGE3 H0ZGE3_TAEGU	CPTPGCGAGLLP-----EPD--LRRIVCEPG-NGIGCGSVFCRECKEEFHHEGEC	376
TR Q1WDP3 Q1WDP3_PIG	CPRPGCGAGLLP-----EPG--QRKVTCEGG-NSLGGGLVFCRDCKESYHEGEC	374
TR H0X3U6 H0X3U6_OTOGA	CPRPGCGAGLLP-----EPG--QRRVACERD-SGLGGCGFVFCRECKEADHDGEC	376
TR I3JF6 I3JF6_ORENI	CPSPGCGAGLVP-----PDG--SRKVECDRR---LGCGFVFCRCLCRGEYHEGPCQ	364
TR B8YGJ6 B8YGJ6_MACFA	CPRPGCGAGLLP-----ESD--QRKVTCEGG-NLGGCGFAFCRECKEAYHEGEC	378
TR Q5J4W3 Q5J4W3_TAKRU	CPSPGCGAGLVP-----PDD--SRRVECDRQ---IGCGFVFCRICREGYHEGGCL	397
TR U3FQA1 U3FQA1_CALJA	CPRPGCGAGLLP-----EPD--QRKVTCEGG-NLGGCGFAFCRECKEAYHEGEC	378
TR G3N0R1 G3N0R1_BOVIN	CPGPGCGAGLLP-----EPG--QRKVSCEPG-HLGGCGFVFCRDCKEAYHEGDCG	373
TR Q17DC3 Q17DC3_AEDAE	CPQPGCGMGLLV-----DPE--CKRVQCQ-----NGCGFVFCRNCLQGYHIGEC	397
TR G3PFJ2 G3PFJ2_GASAC	CPSPGCGAGLIP-----PDD--SRRVTCDRH---LGCGFVFCRCLQGYHIGEC	380
TR E2BWM9 E2BWM9_HARSA	CPMPDCMGMIIPPTIEEQAEDDDQ--RRRIQCI----GGCGYVFCRCLQGYHTGKCE	350
TR A0A067RG71 A0A067RG71_ZOONE	CPQPGCGMIIA-----EPE--CRRITCT-----NGCGFVFCRCLQGYHIGECV	385
TR A0A0L0CIZ3 A0A0L0CIZ3_LUCCU	CPQPGCGMGLLV-----EPD--CKKVTTCQ-----NGCGYVFCRNCLQGYHLGDCL	393
TR A0A0F7Z269 A0A0F7Z269_CROAD	CPTPGCGAGLLP-----ESE--MRKIVCEPR-NLGGCGFVFCRECKEAYHEGEC	366
TR A0A0B2UTN0 A0A0B2UTN0_TOXCA	CPYSGCGAFLW-----EQDVTSPKVLCP-----ECHRFLFCGVCRREHCVV---	329
TR Q9XUS3 Q9XUS3_CAEEEL	CPNVSCGQFFW-----EPYDDDGSRQCP-----DCFFSFCRCKFERNCVC---	324
	** * * * *	

SP O60260 PRKN2_HUMAN	AVFEAS---GTTT-QAYRVDERAAEQARWEA-AS-KETIKKTTKPCPRCHVPVEKNGGCM	432
TR Q7KTX7 Q7KTX7_DROME	PEGTGA---SATNSCEYTVDPNRAAEARWDE-AS-NVTIKVSTKPCPKCRTPTTERDGGCM	450
SP Q9WVS6 PRKN2_MOUSE	SLLEPS---GATS-QAYRVDKRAAEQARWEE-AS-KETIKKTTKPCPRCNVPIEKNGGCM	431
SP Q9JK66 PRKN2_RAT	SMFEAS---GATS-QAYRVDQRAAEQARWEE-AS-KETIKKTTKPCPRCNVPIEKNGGCM	432
TR F1NWX0 F1NWX0_CHICK	SFLSTQ---GAVAQKGYVVDENAAQARWEE-AS-KETIKKTTKPCPNCHIPVEKNGGCM	431
TR H2QU08 H2QU08_PANTR	ALFEAS---GTTT-QAYRVDERAAEQARWEA-AS-KETIKKTTKPCPRCHVPVEKNGGCM	432
TR F6U1L3 F6U1L3_MACMU	ALFEAS---GTTT-QAYRVDERAAEQARWEE-AS-KETIKKTTKPCPRCHVPVEKNGGCM	432
TR I3N341 I3N341 ICTTR	TLLEAS---AAAK-QAYRVDERAAEHARWEE-AS-KETIKRTTKPCPHCGVPVEKNGGCM	427
TR U3KCF7 U3KCF7_FICAL	SLLSPQ---GAVA-QGYAVDEHAAMQARWEE-AS-RETIKKTTPCPCPNCHIPVEKNGGCM	429
TR Q561U2 Q561U2_DANRE	HTTSTA---SAGALQGYVVDDEEAALRARWEQ-AS-QETITKTTTHPCPKCQVPVEKNGGCM	426
TR W4YQE2 W4YQE2_STRPU	QRIEFP---HGPRGSGSEVDMERERRARWESEES-KRTIGETSKPCPNCKVPVERNGGCM	403
TR Q7Q591 Q7Q591_ANOGA	ETPTPS---TPGNEQGYAIDPLRASEARWDE-AT-KIAIKVTTKPCPCRTATERDGGCM	457
TR C3Z502 C3Z502_BRAFL	QTAPQP---SAPA-NNYRVDRRARRARWER-RT-AATIERTTKACPGCKVRTEKNDGCM	401
TR H3D789 H3D789_TETNG	TTQSQT---TAEASQDFVVDEEATLRARWDQ-AS-LLLLQESTKPCPKCSVPVERNGGCM	450
TR M3ZNV3 M3ZNV3_XIPMA	GPAAPP---PADACQGFVVEDEASQRGRWDR-AS-LQLILESTRRCPRCLVPVERNGGCM	426
TR A0A087XI83 A0A087XI83_POEFO	GPAAPP---PGDACQGFVVGDEASQRGRWDL-AS-LQLIQESTRRCPRCLVPVERNGGCM	410
TR A0A0A9XSY6 A0A0A9XSY6_LYGHE	NAVDIL---TGLSPTYTIDPSRAAQSKWDE-AS-HRSIRAGTKPCPKCRTATERAGGCM	451
TR E0VIU9 E0VIU9_PEDHC	NPTDVP---FLSNCDYPLDPEKLEKARWED-AS-STVIKVLTKPCPKRTSTERAGGCM	429
TR T1H7C6 T1H7C6_MEGSC	PEVNQI---DTTRSCEYSVNPNNAAEARWED-VSTAVTIKVSTKPCPKCRTPTTERDGGCM	427
TR L7M1N2 L7M1N2_9ACAR	SSREAGEERAAGPRF-----LAAQGSWDE-AS-RLTVQATTKPCPKCRTPTERSGGCM	427
TR V5GZV6 V5GZV6_IXORI	RDEEDEASAAALGSVWAYPVDEAQARGSRWDE-AS-RLTVRSTTKPCPMCRTPTTERDGGCM	450
TR V5IIZ0 V5IIZ0_IXORI	RDEEDEASAAALGSVWAYPVDEAQARGSRWDE-AS-RLTVRSTTKPCPMCRTPTTERDGGCM	448
TR H0ZGE3 H0ZGE3_TAEGU	SLLSPP---GAMA-QGYVVDDEHAAMQARWEE-AS-RETIKKTTPCPCPNCHIPVEKNGGCM	430
TR Q1WDP3 Q1WDP3_PIG	ALFEAS---AAVA-QAYRVDQKAAEQARWEE-AS-KETIRKTTKPCPRCHVPVEKNGGCM	428
TR H0X3U6 H0X3U6_OTOGA	ALFEAS---GTVA-QAYRVDERAAEQARWEE-AS-KETIKQTTKPCPRCHVPVEKNGGCM	430
TR I3JF6 I3JF6_ORENI	AVTAPP---TGEEAQGFVVGEEASLRGRWER-AS-LLVIAELTRRCPTCSVPVERNGGCM	419
TR B8YGJ6 B8YGJ6_MACFA	ALFEAS---GTTT-QAYRVDERAAEQARWEE-AS-KETIKKTTKPCPRCHVPVEKNGGCM	432
TR Q5J4W3 Q5J4W3_TAKRU	ATQSQT---TAEGSQDFVVDEGASLRGRWDR-AS-LLLLQESTKPCPKCSAPVERNGGCM	452
TR U3FQA1 U3FQA1_CALJA	ALSEAS---GTIP-QAYRVDERAAEQARWEE-AS-KETIKKTTKPCPRCHVPVEKNGGCM	432
TR G3N0R1 G3N0R1_BOVIN	AVIEAS---GTVT-QAYRVNEKAAEQARWEE-AS-KETIKKTTKPCPRCHVPVEKNGESG	427
TR Q17DC3 Q17DC3_AEDAE	ETPQPN---A-GAAPNYTIDPLRASEARWDE-AS-KIAIKVTTKPCPCRTATERDGGCM	451
TR G3PFJ2 G3PFJ2_GASAC	TEQAPP---IAESSQGFVVEEASVKGRWDQ-AS-LLLLQETTTRCPCQCSVPVERDGGCM	435
TR E2BWM9 E2BWM9_HARSA	FQPLGAST-DVSSLRNYSDVPLRAKDAKWE-AS-RKTIQVSTKPCPLCRTPTTERDGGCM	407
TR A0A067RG71 A0A067RG71_ZOONE	HEGDGSGTSASTGDCQYNVDPGRAAQARWDE-AT-KVAIKVTTKPCPKCRTPTTERAGGCM	443
TR A0A0L0CIZ3 A0A0L0CIZ3_LUCCU	PENGTG---NTTGSCEYAVDPNRAAEARWDE-AS-NVTIKVSTKPCPKCRTPTTERDGGCM	448
TR A0A0F7Z269 A0A0F7Z269_CROAD	SFFKCP---GATAQMGFEIDEHAAVRRARWEG-AS-KETIKRTTKPCPKCHVPVEKDDGGCM	421
TR A0A0B2UTN0 A0A0B2UTN0_TOXCA	-EEND-----AT-ELTIKTTCHSCPTCGVPPTERNGGCA	360
TR Q9XUS3 Q9XUS3_CAEEEL	-QSED-----D-LT-RTTIDATTRRCPKCHVATERNGGCA	356

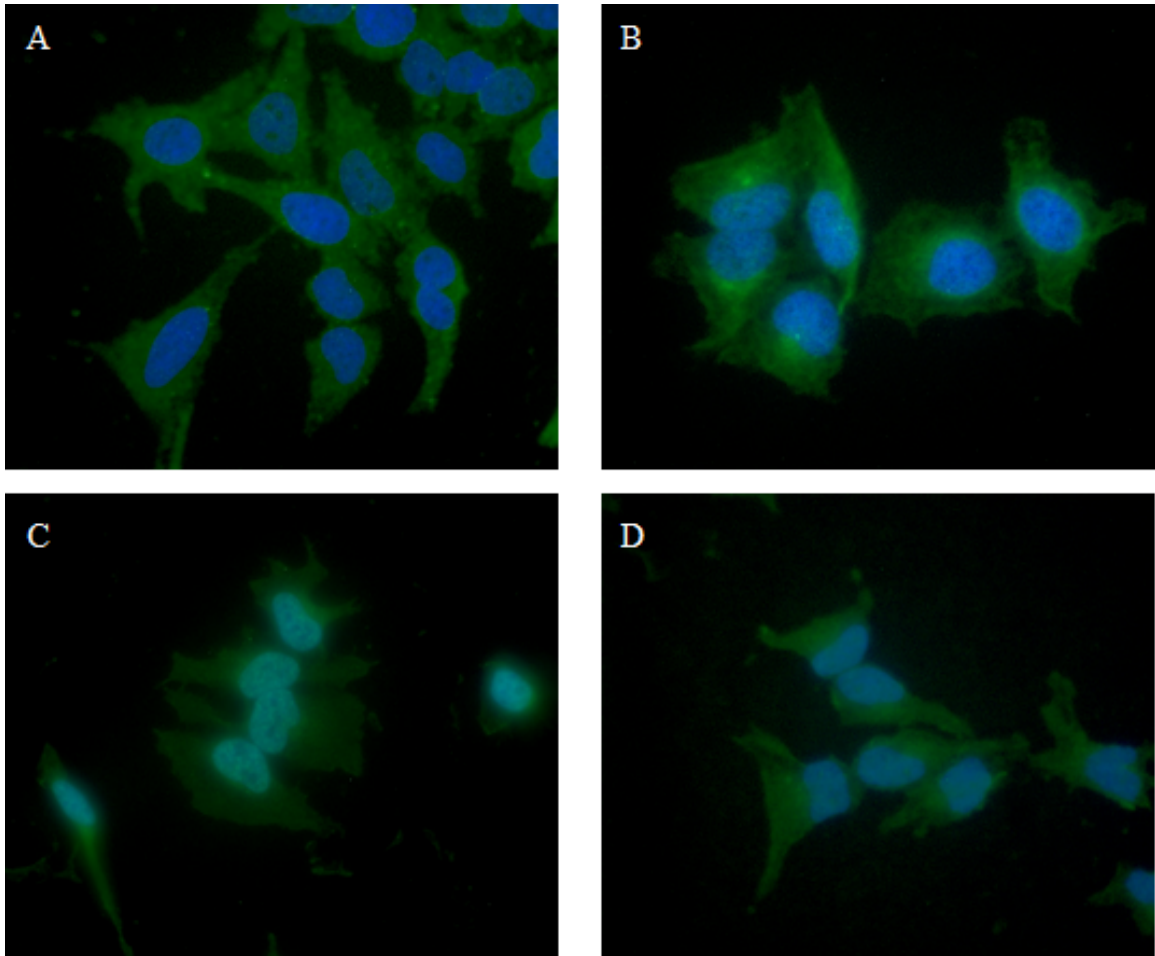
: : : * * * * :

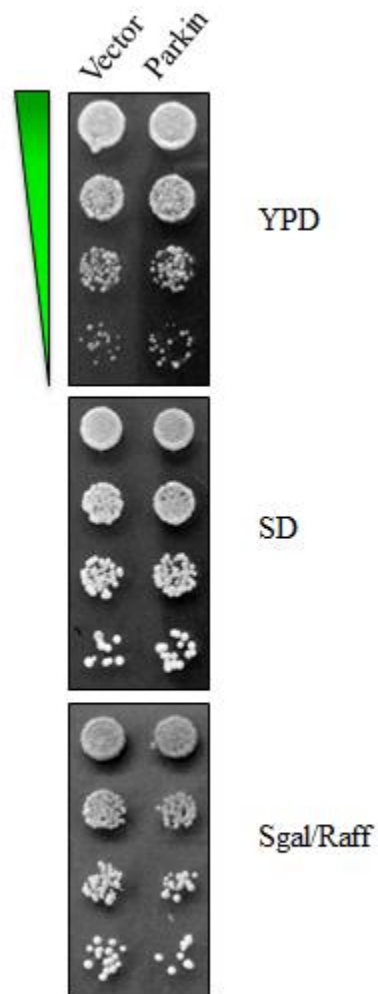
SP O60260 PRKN2_HUMAN	HMKCPQPQCRLEWCWNCGCEWNRVCMGDHWFVDV-----	465
TR Q7KTX7 Q7KTX7_DROME	HMVCTRAGCGFEWCWVCQTEWTRDCMGAHWFG-----	482
SP Q9WVS6 PRKN2_MOUSE	HMKCPQPQCKLEWCWNCGCEWNRACMGDHWFDV-----	464
SP Q9JK66 PRKN2_RAT	HMKCPQPQCKLEWCWNCGCEWNRACMGDHWFDV-----	465
TR F1NWX0 F1NWX0_CHICK	HMKCPRPQCRFEWCWNCGLEWNRTCMGNHWFD-----	463
TR H2QU08 H2QU08_PANTR	HMKCPQPQCRLEWCWNCGCEWNRVCMGDHWFVDV-----	465
TR F6U1L3 F6U1L3_MACMU	HMKCPQPQCRLEWCWNCGCEWNRVCMGDHWFVDV-----	465
TR I3N341 I3N341 ICTTR	HMKCPQPQCRLEWCWNCGCEWNRTCMGDHWFVDV-----	460
TR U3KCF7 U3KCF7_FICAL	HMKCPRPQCRFEWCWNCGLEWNRTCMGDHWFDD-----	461
TR Q561U2 Q561U2_DANRE	HMVCPRPQCKFEWCWLCRVEWNRDCMGNHWFE-----	458
TR W4YQE2 W4YQE2_STRPU	HMICSRTOCKYEWCIWCGIEWNMGCLEDHWFAGFLL-----	440
TR Q7Q591 Q7Q591_ANOGA	HMVCTRSGCGFEWCWVCQTPWTRDCMAAHWFG-----	489
TR C3Z502 C3Z502_BRAFL	HMTCP--RCGFHWCWLCEREWGRNCQDRHWFGEGR-----	434
TR H3D789 H3D789_TETNG	HMQCP--LCKAEWCWLCGVFWNRRCMGDHWFG-----	480
TR M3ZNV3 M3ZNV3_XIPMA	HMQCT--QCRAEWCWLCGAPWNRRCMGNHWFG-----	456
TR A0A087XI83 A0A087XI83_POEFO	HMQCT--QCRAEWCWLCGAPWNRRCMGNHWFG-----	440
TR A0A0A9XSY6 A0A0A9XSY6_LYGHE	HMVCTR--CNFEWCWVCQISWTRSCMGSHWFG-----	481
TR E0VIU9 E0VIU9_PEDHC	HMICSTRANCGFHCWVCQTEWTRDCMASHWFG-----	461
TR T1H7C6 T1H7C6_MEGSC	HMVCTRSGCDFEWCWVCQTEWTRDCMGAHWFG-----	459
TR L7M1N2 L7M1N2_9ACAR	HMVCSRSQCGFQWCWLCQDEWTRQCMGAHWFG-----	459
TR V5GZV6 V5GZV6_IXORI	HMICSRSQCGFQWCWLCQTEWSRNCMGAHWFG-----	482
TR V5IIZ0 V5IIZ0_IXORI	HMICSRSQCGFQWCWLCQTEWSRNCMGAHWFG-----	480
TR H0ZGE3 H0ZGE3_TAEGU	HMKCPHPQCRFEWCWNCGLEWNRTCMGDHWFE-----	462
TR Q1WDP3 Q1WDP3_PIG	HMKCPQPQCQLEWCWNCGWEWNRDCMGDHWFDV-----	461
TR H0X3U6 H0X3U6_OTOGA	HMKCPQPQCRLEWCWNCGCEWNRVCMGDHWFDV-----	463
TR I3JF6 I3JF6_ORENI	HMHCP--LCKAEWCWLCGVFWNRRCMGNHWFG-----	450
TR B8YGJ6 B8YGJ6_MACFA	HMKCPQPQCRLEWCWNCGCEWNRVCMGDHWFVDV-----	465
TR Q5J4W3 Q5J4W3_TAKRU	HMLCP--LCKAEWCWLCGVFWNRRCMGDHWFG-----	482
TR U3FQA1 U3FQA1_CALJA	HMKCPQPQCRLEWCWNCGCEWNRVCMGDHWFVDV-----	465
TR G3N0R1 G3N0R1_BOVIN	LTEE-----RCGGLSS---EGGREVGIYKGFFLAGELSAGALGPSGQGLNLSTHV	474
TR Q17DC3 Q17DC3_AEDAE	HMVCTRSGCGFEWCWVCQTPWTRDCMAAHWFG-----	483
TR G3PFJ2 G3PFJ2_GASAC	HMQCP--LCRAEWCWLCGVSWNRDCMGNHWFG-----	465
TR E2BWM9 E2BWM9_HARSA	HMVCMRAGCGYHWCWVCQMWTRECMANHWFG-----	439
TR A0A067RG71 A0A067RG71_ZOONE	HMVCTRQPQCNFHCWVCQTEWSRDCMGSHWFG-----	475
TR A0A0L0CIZ3 A0A0L0CIZ3_LUCCU	HMVCTRAGCGFEWCWVCQTEWTRDCMGAHWFG-----	480
TR A0A0F7Z269 A0A0F7Z269_CROAD	HMKCPQSQCKFEWCWKCWLEWNRTCMGDHWFDD-----	453
TR A0A0B2UTN0 A0A0B2UTN0_TOXCA	HMHCA--HCGTHWCFCVKPWTEECQWDHWFDD-----	390
TR Q9XUS3 Q9XUS3_CAEEEL	HIHCT--SCGMDWCFKCKTEWKEECQWDHWFN-----	386

* : .

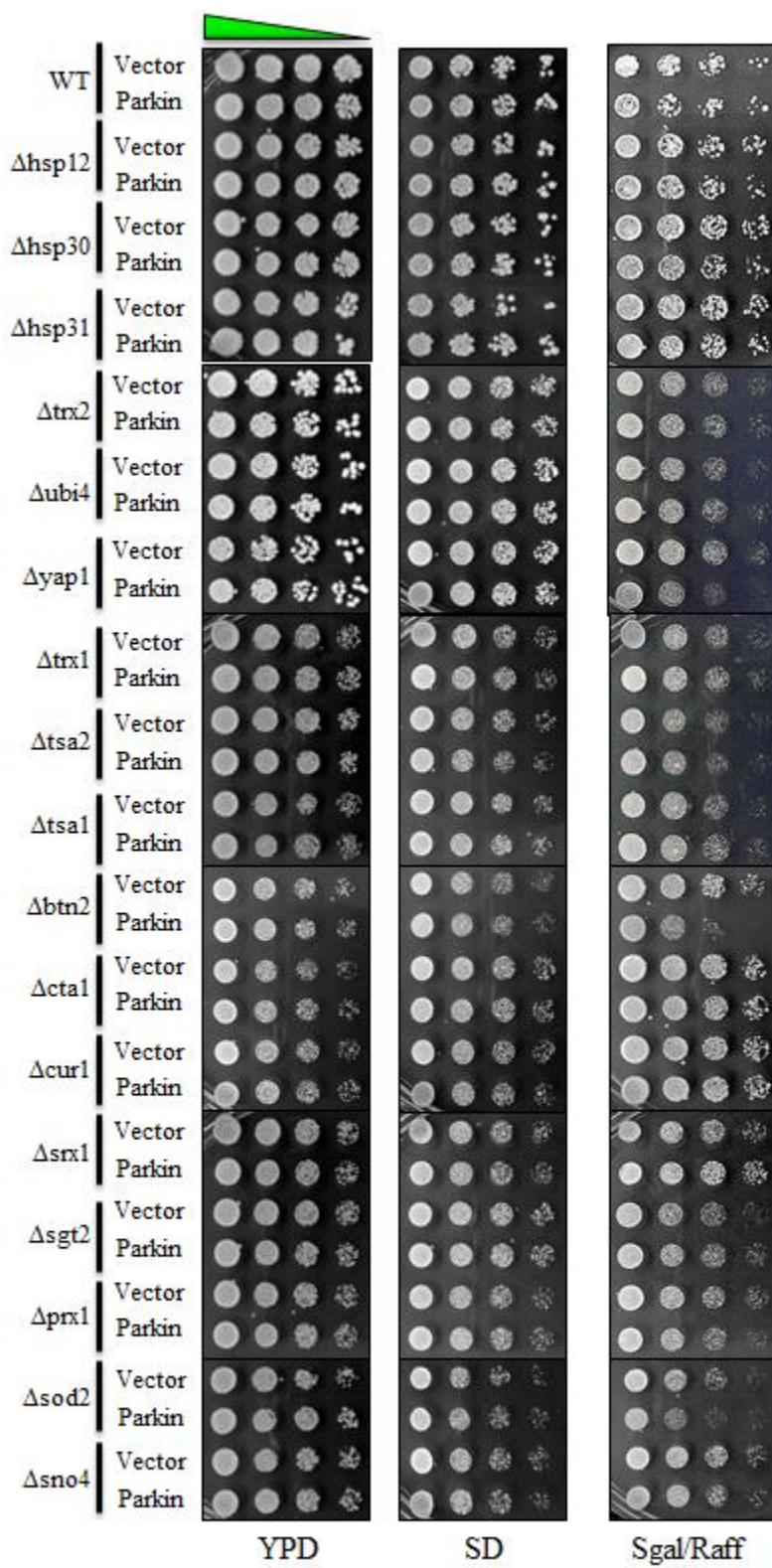
SP O60260 PRKN2_HUMAN	-----
TR Q7KTX7 Q7KTX7_DROME	-----
SP Q9WVS6 PRKN2_MOUSE	-----
SP Q9JK66 PRKN2_RAT	-----
TR F1NWU0 F1NWU0_CHICK	-----
TR H2QU08 H2QU08_PANTR	-----
TR F6U1L3 F6U1L3_MACMU	-----
TR I3N341 I3N341_ICTTR	-----
TR U3KCF7 U3KCF7_FICAL	-----
TR Q561U2 Q561U2_DANRE	-----
TR W4YQE2 W4YQE2_STRPU	-----
TR Q7Q591 Q7Q591_ANOGA	-----
TR C3Z502 C3Z502_BRAFL	-----
TR H3D789 H3D789_TETNG	-----
TR M3ZNV3 M3ZNV3_XIPMA	-----
TR A0A087XI83 A0A087XI83_POEFO	-----
TR A0A0A9XSY6 A0A0A9XSY6_LYGHE	-----
TR E0VIU9 E0VIU9_PEDHC	-----
TR T1H7C6 T1H7C6_MEGSC	-----
TR L7M1N2 L7M1N2_9ACAR	-----
TR V5GZV6 V5GZV6_IXORI	-----
TR V5IIZ0 V5IIZ0_IXORI	-----
TR H0ZGE3 H0ZGE3_TAEGU	-----
TR Q1WDP3 Q1WDP3_PIG	-----
TR H0X3U6 H0X3U6_OTOGA	-----
TR I3JF6 I3JF6_ORENI	-----
TR B8YGJ6 B8YGJ6_MACFA	-----
TR Q5J4W3 Q5J4W3_TAKRU	-----
TR U3FQA1 U3FQA1_CALJA	-----
TR G3N0R1 G3N0R1_BOVIN	KLLNLLNRKSSSVK 488
TR Q17DC3 Q17DC3_AEDAE	-----
TR G3PFJ2 G3PFJ2_GASAC	-----
TR E2BWM9 E2BWM9_HARSA	-----
TR A0A067RG71 A0A067RG71_ZOONE	-----
TR A0A0L0CIZ3 A0A0L0CIZ3_LUCCU	-----
TR A0A0F7Z269 A0A0F7Z269_CROAD	-----
TR A0A0B2UTN0 A0A0B2UTN0_TOXCA	-----
TR Q9XUS3 Q9XUS3_CAEEEL	-----

Appendix 3. Non-specific immunofluorescence signal in HeLa cells with parkin antibodies. Untransfected HeLa cells were fixed and used for immunofluorescence with A) a Cell Signaling parkin antibody B) an Abcam parkin antibody C) a Novus parkin antibody or D) a Santa Cruz parkin antibody.

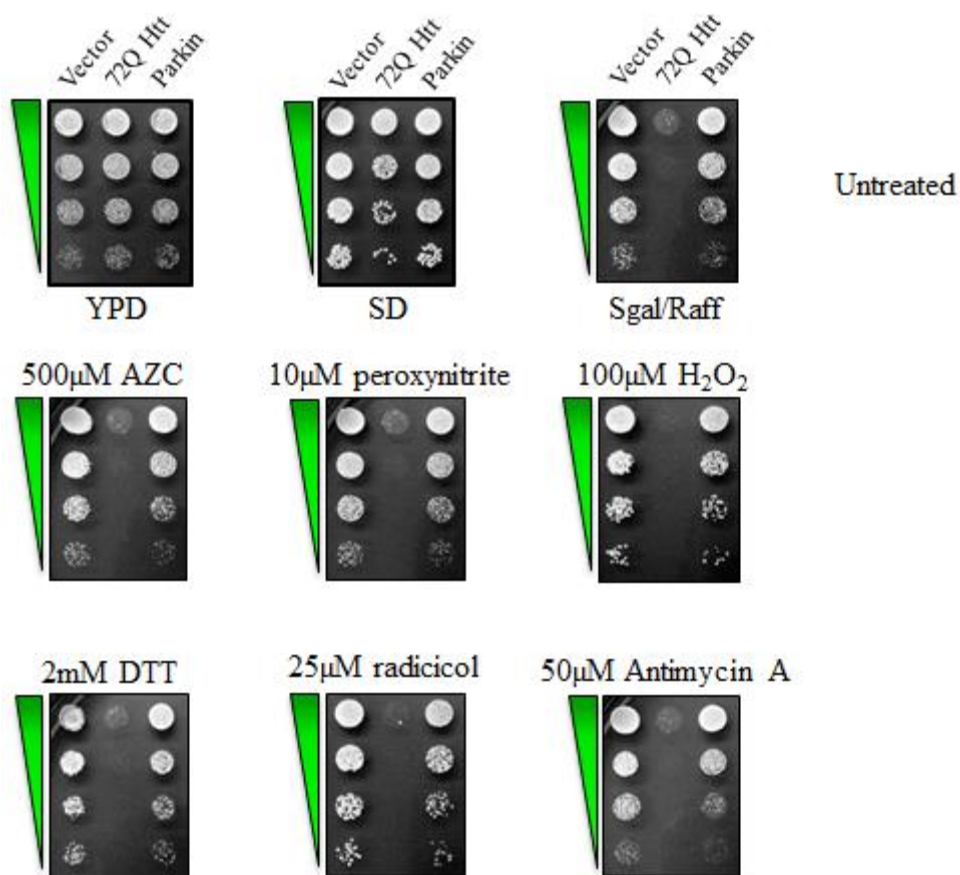


Appendix 4. Supplementary figure data.

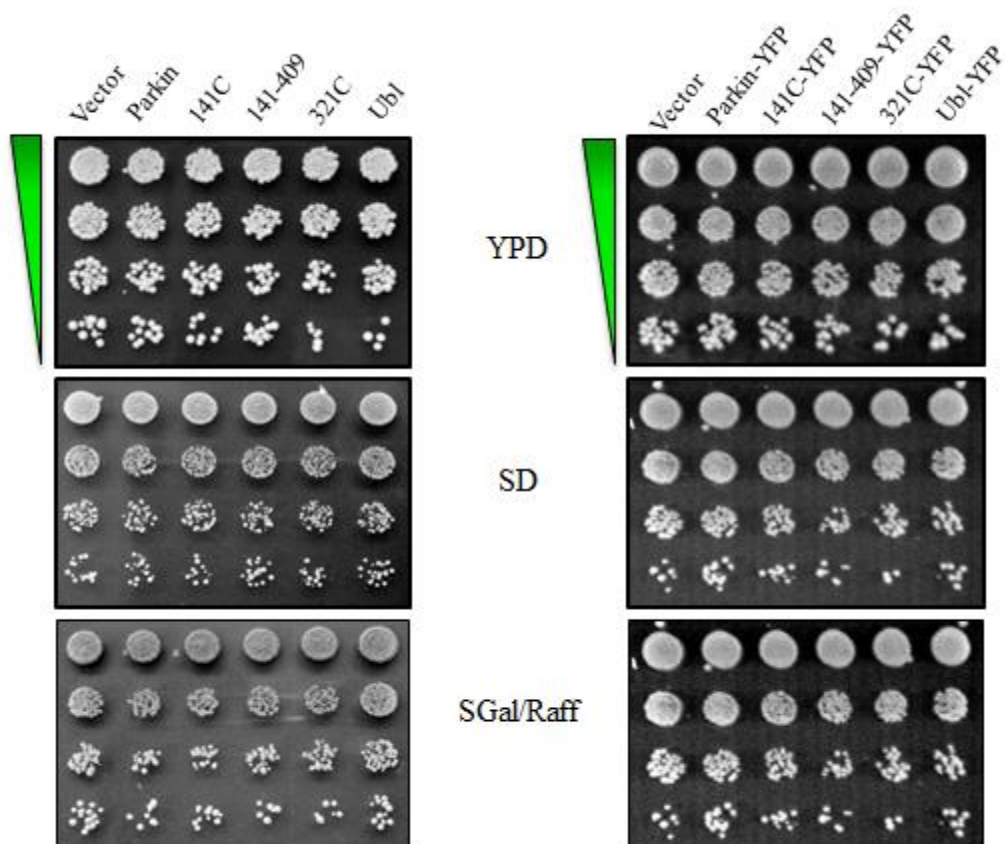
Supplement to Figure 3-2



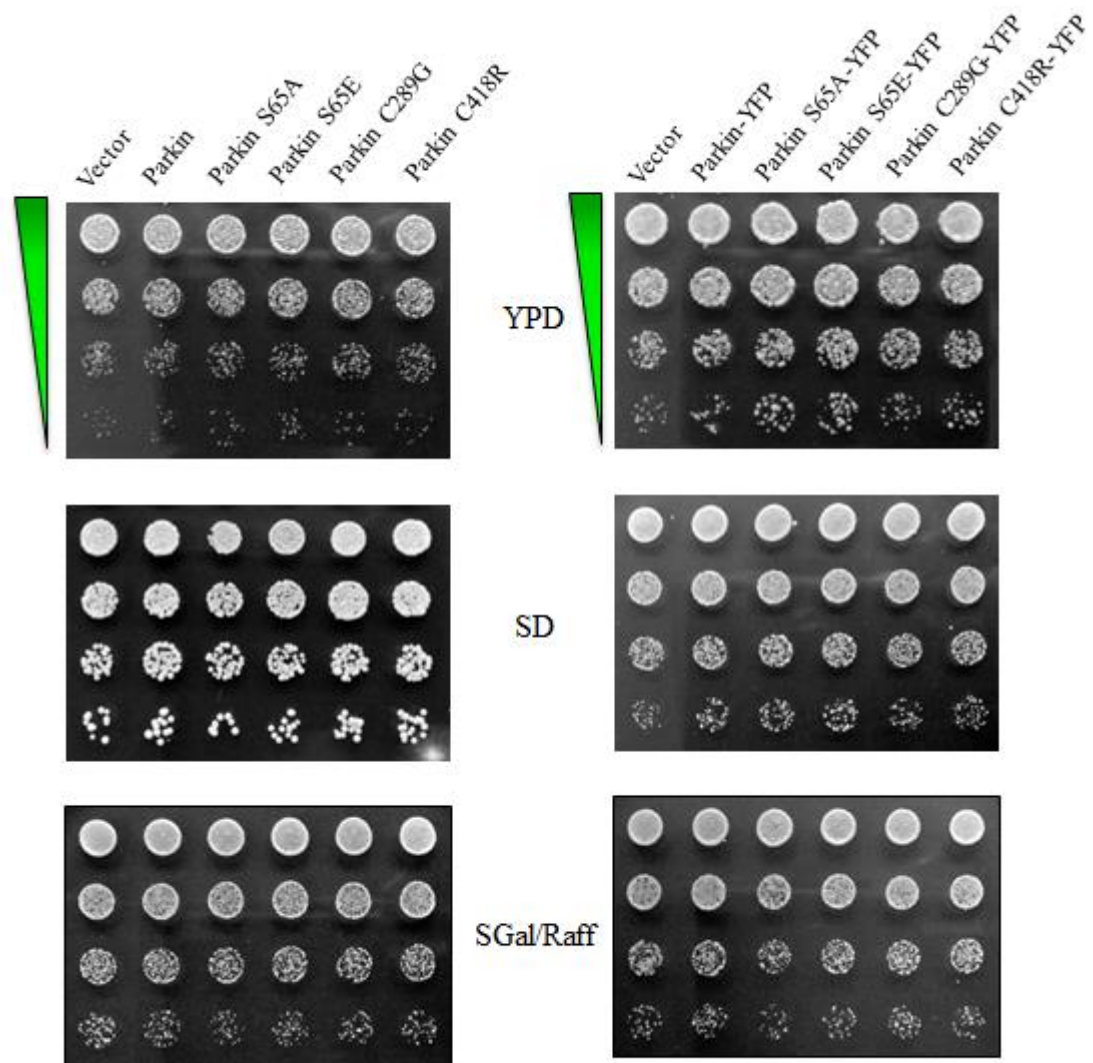
Supplement to Figure 3-3



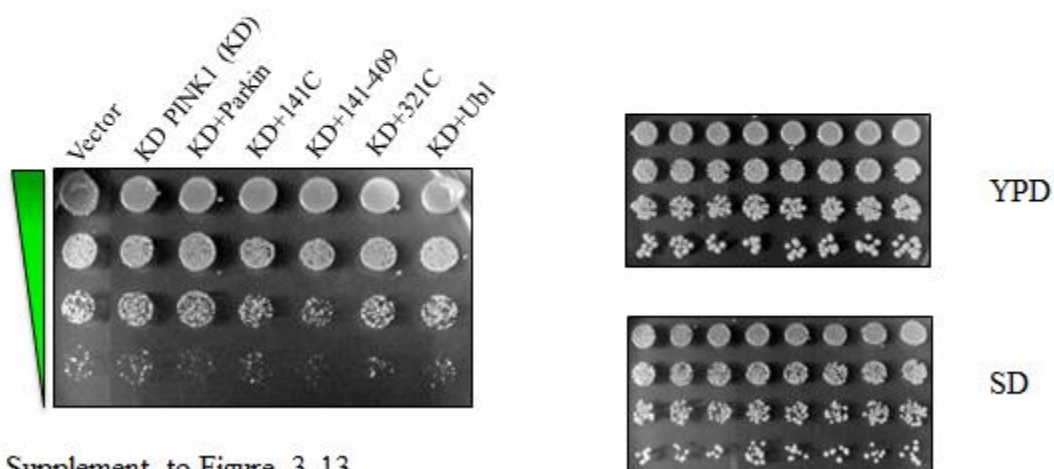
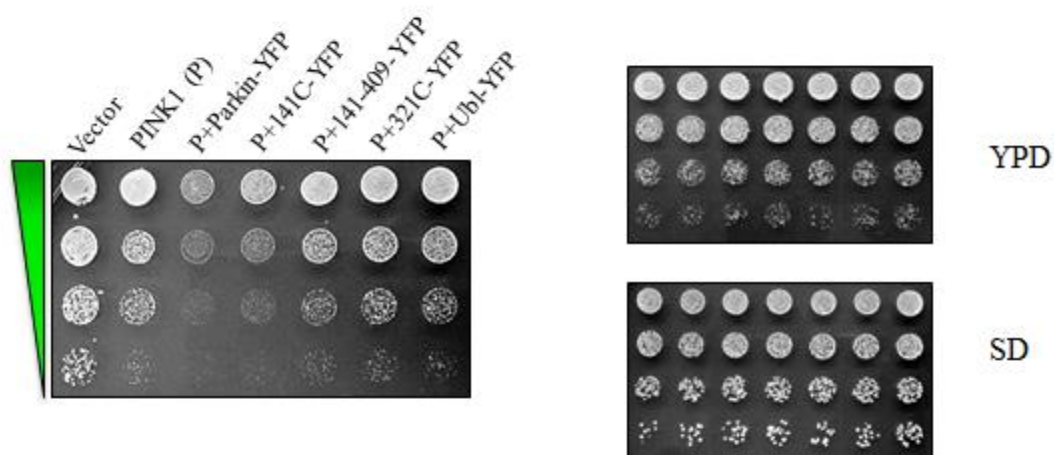
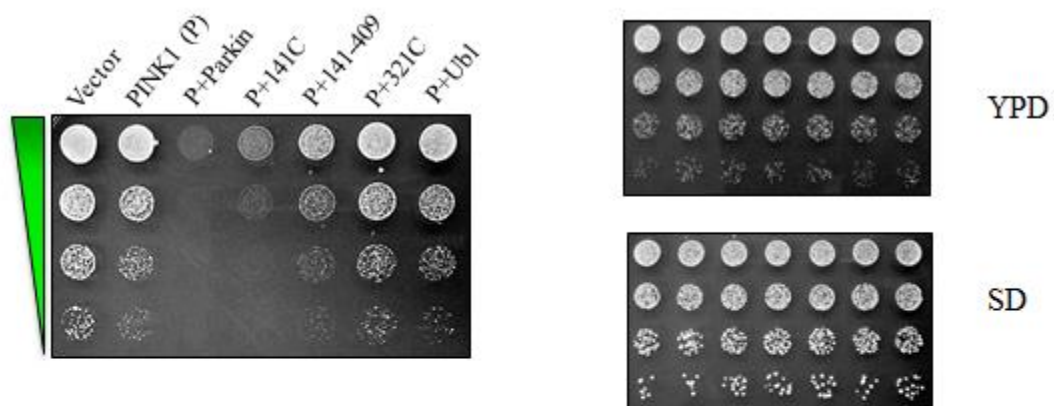
Supplement to Figure 3-5



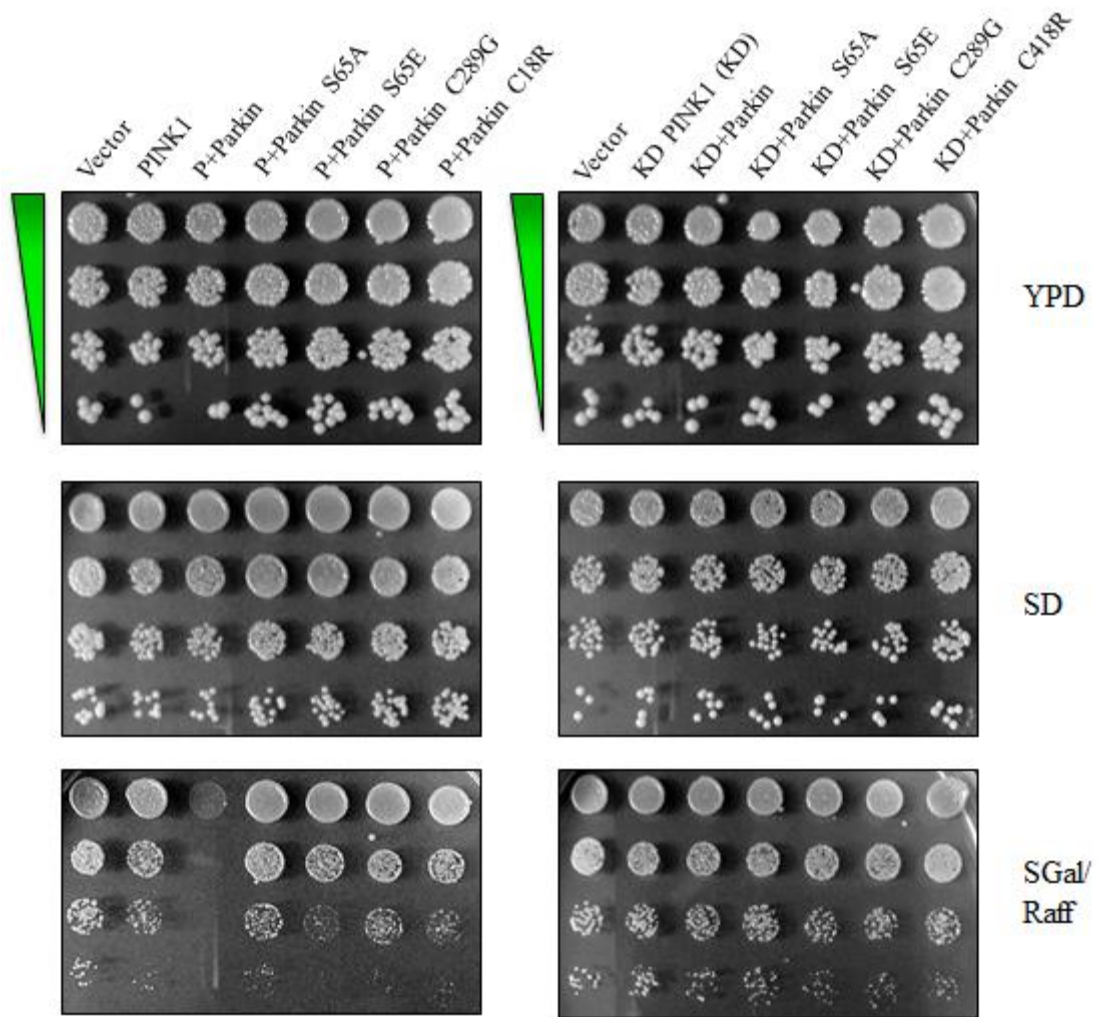
Supplement to Figure 3-8



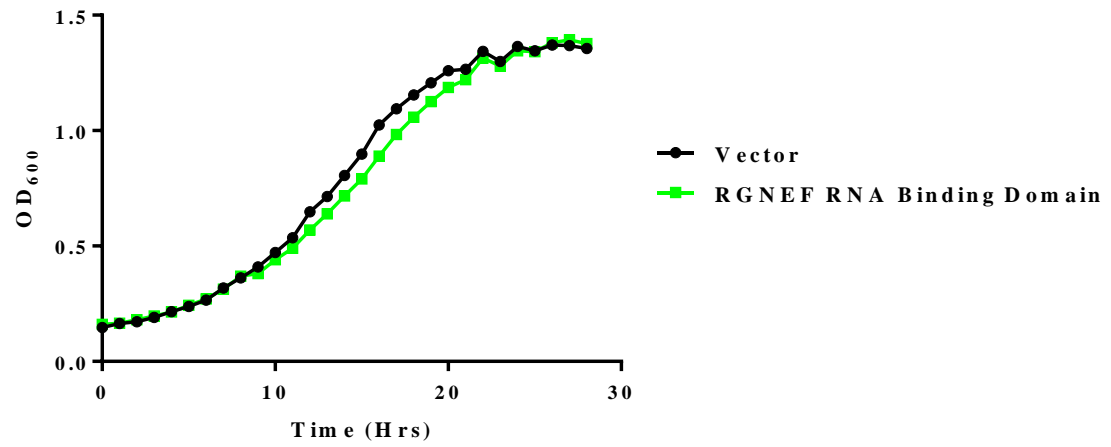
Supplement to Figure 3-10



Supplement to Figure 3-13



Supplement to Figure 3-17

Appendix 5. Growth curve of non-toxic protein expression in yeast.

Curriculum Vitae
Alex McCarton

Formal Education

September 2014 – Present

Western University

London, Ontario, Canada
Masters of Science, Biochemistry
Supervisors: Dr. Gary S. Shaw,
Dr. Martin L. Duennwald,
Dr. Jane R. Rylett

September 2010 – May 2014

Western University

London, Ontario, Canada
Bachelor of Medical Science, Honors Specialization
in Biochemistry
Recognized on Dean's Honor List
Supervisors: Dr. Gary S. Shaw
Dr. Martin L. Duennwald

Presentations

Oral Presentations

May 2014

4th Year Undergraduate Thesis Talk

London, Ontario, Canada
*Detecting parkin substrates and other interacting
proteins through split-ubiquitin reconstitution*

Poster Presentations

April 2015

London Health Research Day Poster Presentation

London, Ontario, Canada
*Employing a Yeast Model to Study the Basic
Genetic and Functional Basis of Parkin Dysfunction
in Parkinson's Disease*

January 2014/2015

Harold B. Stuart Lecture Day Poster Presentation

London, Ontario, Canada

Employing a Yeast Model to Study the Basic Genetic and Functional Basis of Parkin Dysfunction in Parkinson's Disease (2015)

Detecting Parkin Substrates by Split-Ubiquitin Reconstitution through Protein-Protein Interactions (2014)

Awards and Accomplishments

September 2014 – Present

Western Graduate Research Scholarship (WGRS)

Recurring bursary granted over 6 terms of graduate studies based on entrance marks.

April 2015

London Health Research Day Top 80 Poster Presenter

London, Ontario, Canada

Employing a Yeast Model to Study the Basic Genetic and Functional Basis of Parkin Dysfunction in Parkinson's Disease (2015)

Relevant Employment

September 2015 – December 2015

Biochemistry Teaching Assistant

Western University,

London, Ontario, Canada

Biochemistry 4450: Molecular Genetics of Cancer

May 2013 – August 2013

Biochemistry Summer Research Student

Western University

London, Ontario, Canada

Supervisor: Dr. Gary S. Shaw